

6. TITANIUM

Mary A. Jamieson^{*}, Nick Serpone [1]^{*}, and Ezio Pelizzetti[#]

^{*}Department of Chemistry, Concordia University, 1455 de Maisonneuve
 Blvd. West, Montreal, Quebec, Canada, H3G 1M8

[#]Istituto di Chimica Analitica, Università di Torino, 10126 Torino, Italia

CONTENTS

Introduction.....	176
6.1 Titanium carbides	177
6.2 Titanium silicides	178
6.3 Titanium nitrides	178
6.4 Titanium phosphides and phosphates	180
6.5 Titanium nitrates	181
6.6 Titanium oxides	181
a. Oxide films on Ti surfaces	181
b. Titanium oxides, except TiO ₂	182
c. TiO ₂	183
(i) Preparation, characterization and structure	183
(ii) TiO ₂ as a catalyst, catalyst support and photosensitizer..	189
(iii) Electrodes and electrochemistry	196
(iv) Applications	203
d. Mixed metal oxide systems	204
(i) SrTiO ₃	204
(ii) A _x Ti _y O _z	205
e. Vanadium/titanium oxide catalysts	208
f. Titanium electrodes	210
6.7 Titanium sulfides and sulfates	212
6.8 Titanium halides	216
a. Fluorides	216
b. Chlorides	218
c. Chlorides as catalysts	221
(i) TiCl ₃	221
(ii) TiCl ₄	222
d. Bromides and iodides	224
6.9 Titanium hydrides	226
6.10 Coordination complexes of titanium	230
a. Cyclopentadienyl complexes	230

(i) Preparation, characterization and structure	230
(ii) Reactions	242
(iii) Catalysis	246
b. Other coordination complexes of titanium	248
(i) Preparation, characterization and structure	248
(ii) Reactions	254
6.11 Miscellaneous	260
a. Electrochemistry	260
6.12 Acknowledgements.....	261
6.13 References	262

INTRODUCTION

This paper reviews as extensively as possible the advances made in titanium chemistry during the 1983 calendar year. It covers material in the major chemical and non-chemical journals, as well as the foreign, less-known journals for the period covered by Chemical Abstracts from Volume 97, number 21 to Volume 99, number 24. Contrary to our previous articles, this article is arranged according to species bonded to titanium. The solid-state physics of titanium is treated only as it pertains to the more relevant areas included herein.

General reviews of the chemistry of titanium have appeared which cover 1980[2], 1981[3] and 1982[4]. The transition metal chemistry of titanium has been reviewed by Newberry [5] and Whitehead [6]. Some brief reviews of organometallic complexes of titanium have appeared. These include reviews on compounds containing an alkoxy group which coordinates intramolecularly to Ti [7], studies on bis(cyclopentadienyl)bis(aryloxy)- and bis(aryl)titanium complexes [8], the synthetic applications of bis(η -cyclopentadienyl)titanium complexes [9], and the complexing of the cyclopentadiene-methylacrylate-titanium tetrachloride system in the solid phase [10]. Several reviews on various aspects of titanium oxides have also appeared, including the solar energy utilization and photoelectric processes of TiO_2 [11], the properties and use of titanium oxides [12], the design of catalyst-support systems [13], the application of DTA to reactivity measurements of TiO_2 [14], and the soft chemistry in NaTiO_2 sheet oxides [15]. It will become obvious that the bulk of the published work involves titanium oxide species, which serve primarily as electrodes, catalysts, and catalyst support systems.

6.1 TITANIUM CARBIDES

Titanium carbide foils have been prepared via reactions of TiCl_4 with H_2 and graphite substrates. These foils have microstructures composed of grains with dislocations measured for various samples [16]. Various techniques have been employed to ascertain the physical and chemical properties of titanium carbides, including the calorimetric determination of the heat of combustion of $\text{TiC}_{0.993}$ [17], the corrosion resistance of hot-pressed TiC in alkaline media [18], and the dependence of the constant components of the potential of TiC on the frequency in alkaline media. In the latter study, three combined processes occur on the TiC surface at a predetermined polarization regime: formation of titanium hydrides in the cathode half-period, formation of titanium oxides in the anodic half-period, and dissolution of titanium in the solution [19]. Additionally, the effects of pressure and temperature on the lattice parameters of TiC_xO_y ($x + y = 0.61 - 1.18$) have been investigated [20].

The nature of an interatomic interaction in refractory titanium carbides and nitrides was studied employing x-ray emission and photoelectron spectroscopy [21]. The heteroepitaxial growth of refractory titanium carbides and nitrides on specific faces of tungsten and molybdenum have provided orientation and mismatch parameter data [22]. X-ray spectra of the TiC-TiN solid solution system reveal separate partially overlapping bands, genetically bound with the 2s- and 2p-states of C and N and the 3d- and 4s-states of Ti [23].

Thin films of titanium carbides, -nitrides and -carbonitrides can be prepared by reactive rf-sputtering of a titanium-target in a N_2 and/or CH_4 atmosphere. The optical properties and spectral selectivity of these films were characterized by AES (atomic emission spectroscopy) and x-ray diffraction techniques, and interpreted in terms of distribution of states [24]. The optical properties of titanium carbonitrides and -nitrides for solar absorbers have been obtained. The data were analysed by the Drude-Lorentz model of the dielectric function and interpreted in terms of a simple semirigid bands model for the electronic structure [25]. The temperature dependence for the enthalpy of cubic titanium carbonitrides with composition $\text{TiC}_{0.555}\text{N}_{0.55}$, $\text{TiC}_{0.35}\text{N}_{0.62}$ and $\text{TiC}_{0.20}\text{N}_{0.78}$ at 400-1500K was determined, and theoretical expressions were derived for the temperature-composition dependences of the enthalpy, heat capacity and entropy at 298-1500K [26].

The catalytic oxidation of hydrogen on various titanium carbides, nitride and hydride species has revealed that the metallic nature of the bonds formed is the factor which affects the catalytic activity of the compounds employed [27]. The production of titanium powder via electrolysis of titanium oxycarbonitrides has been cited [28].

Band structure calculations on ZrC reveal that the degree of ionicity of the Zr-C bond is greater than that of the Ti-C bond in TiC. It was also reported that the formation of solid solutions in TiC-ZrC, TiN-ZrC and ZrC-ZrN systems (in contrast to TiC-TiN, TiN-ZrN and TiC-ZrN systems) is accompanied by significant band structure deformation which should prevent the formation of solid solutions without sublattice vacancies [29].

6.2 TITANIUM SILICIDES

The formation of TiSi_2 was followed by employing radioactive ^{31}Si (half-life 2.62 hr) to measure the activity profile. In contrast to the silicide Co_2Si wherein Co is the diffusing species, disilicide formation (i.e., TiSi_2) occurs via Si substitutional (vacancy) diffusion with a high self-diffusion coefficient [30]. The oxidation of TiSi_2 thin films on polysilicon was studied by Rutherford backscattering spectroscopy. At 973K in a wet oxygen atmosphere, a titanium oxide layer forms and Si is simultaneously rejected to greater depths. At 1373K, a metal-free SiO_2 layer forms, which would require use of the entire available polysilicon as well as reduction of TiSi_2 . These behavioral extremes are discussed [31] in terms of results obtained for TiSi_2 and other silicides and from known thermodynamic properties of the TiO_2 - SiO_2 system.

The structure of TiMn(Fe)Si_2 is characterized by an octahedral environment of the Mn(Fe) atom, and has been compared with other silicides, including ZrFeSi_2 , ZrMnSi_2 , HfFeSi_2 , and HfMnSi_2 [32].

6.3 TITANIUM NITRIDES

Films of TiN have been prepared by the implantation of N_2^+ ions in titanium layers deposited on silicon single crystals. The films thus prepared possess low electric resistivity and moderately good optical properties compared to films prepared by evaporation or sputtering techniques. Furthermore, exposure of these films to heat ($\leq 973\text{K}$) in vacuum or in a hydrogen atmosphere results in enhanced overall film characteristics, suggesting the application of TiN as a transparent conductive material in photovoltaics [33]. The compounds TiN_x and TiClN , along with $\text{TiCl}_4 \cdot 5\text{NH}_3$ and NH_4Cl , are produced from the reaction of gaseous TiCl_4 with NH_3 . The N/Ti atomic ratio, x , of TiN_x varies with temperature: 1.21 (973K), 1.16 (1073K), 1.13 (1173K) and 1.10 (1273K); the lattice constants of TiN_x have been reported [34].

The vacancy effects in TiN_x ($0.5 \leq x \leq 1$) were characterized by x-ray photoelectron spectroscopy [35]. X-ray emission spectra of titanium in

$\text{TiN}_{0.8}$ and $\text{TiN}_{0.8}\text{H}_x$ reveal the location of H atoms in tetrahedral cells of the $\text{TiN}_{0.8}$ lattice in the vicinity of nitrogen-deficient titanium octahedrons [36]. The reflectivity of TiN was measured in the spectral range 0.1 - 6.2 eV [37], and partial thermodynamic characteristics of the Ti-N system were obtained by evaporation equilibrium in the homogeneous region at 1500-2500K. Activities of Ti and N are expressed as a function of temperature and composition; the effect of composition on the entropy and energy of vacancy formation was also evaluated [38].

The electrophoretic behavior of TiN has been studied [39]. At pH 4.5, the isoelectric point is a value which coincides with that of TiO_2 , and the electrokinetic potential remains stable. However, at pH 4.6-6.0, the electrokinetic potential increases, the phenomenon is explained in terms of alkaline surface hydration. A study of the oxidation behavior of reactively sputtered TiN at 698-1073K in wet and dry oxidizing ambient reveals the formation of a single-oxide phase, rutile TiO_2 . The oxidation process is thermally activated, and its rate is higher in a wet than in a dry ambient. The parabolic time dependence of oxide growth was attributed to a transport-controlled process which is limited by the diffusivity of the oxidant in the oxide [40]. The anodic behavior of TiN in organic electrolytes has been reported [41]. In solutions of LiClO_4 in methanol, TiN is stable at <0.5V and >1.0V, and anodic dissolution and solvent decomposition occur simultaneously. In solutions of LiClO_4 in acetonitrile, a protective film forms on the electrode surface, probably due to water present in the system. X-ray diffraction was employed to ascertain the effect of oxygen addition on the lattice parameter of TiN samples prepared by reactive sintering of plasma-deposited TiN films in air. The lattice parameter was observed to decrease initially due to direct substitution of oxygen for nitrogen, then increase and finally decrease with increasing oxygen addition [42].

Several theoretical studies of titanium nitrides have been reported. An improved LCAO interpolation scheme was employed to determine the densities of states (DOS) and partial densities from self-consistent APW band structure calculations for TiN. A LCAO charge analysis for all valence states and for the individual valence bands was also made [43]. The DOS can be divided into local partial contributions to characterize the bonding in TiN and TiC. Further information is obtained from a decomposition of the metal d DOS into t_{2g} and e_g symmetry components. The partial local DOS were compared with the LCAO counterpart to render the nature of the chemical bonding [44].

The Compton profile of TiN was measured using 59.54 keV gamma rays, and found to be in reasonable agreement with theoretical estimates based on valence-electron configurations given by band-structure calculations. The bonding in TiN is very similar to that in TiC [45]. Calculations of the

transmittance and reflectance between 0.35 and 10 μm of semitransparent TiN films reveal that the films can be utilized as transparent heat-mirrors, as they exhibit considerably higher emittance than the noble metals and comparable or higher visible transmittance [46].

The charge distributions in TiB (B = N, C, O) have been determined by electronic structure calculations on TiB_6 octahedral clusters by the SCF- X_α method. The band gap, ΔE , values increase with increasing bond polarity of the compounds ($\Delta E(\text{TiC}) < \text{TiN} < \text{TiO}$) [47].

The electronic structure of $\text{NTi}_6\text{N}_{12}$ and Ti_6N_{12} clusters was calculated by the SCF- X_α scattered-wave method, and the bonding discussed in terms of energy and spatial distributions of valence electrons [48].

6.4 TITANIUM PHOSPHIDES AND PHOSPHATES

The crystal structure of the titanium copper phosphide TiCu_2P reveals it to be tetragonal and belonging to the Cu_2Sb structure family [49].

Titanium orthophosphate, TiPO_4 , can be synthesized from TiO_2 and $(\text{NH}_4)_2\text{HPO}_4$ at 1223K in an argon atmosphere with various oxygen partial pressures. Lattice constants were reported: TiPO_4 has a nearly temperature-independent magnetic susceptibility over a wide range of temperatures. This is suggestive of the existence of $\text{Ti}^{3+}\text{--Ti}^{3+}$ homopolar bonds, though part of the bonds are broken by defects and, subsequently, isolated Ti^{3+} ions are produced in the structure. At low temperatures, $\text{Ti}^{4+}\text{--}\square\text{--Ti}^{4+}$ clusters exist and cause a sharp decrease in the magnetic susceptibility. The temperature dependence of the EPR spectrum and magnetic susceptibility of TiPO_4 indicate a gradual breakdown of $\text{Ti}^{3+}\text{--Ti}^{3+}$ bonding [50].

Reaction of aqueous TiCl_4 with H_3PO_4 or H_3AsO_4 (1:1 molar ratio) in a sealed quartz ampule at 523K and 40 atm has produced $\text{Ti}(\text{OH})\text{PO}_4$ and $\text{Ti}(\text{OH})\text{AsO}_4$, respectively. Infrared spectroscopy, x-ray diffractometry and chemical analyses revealed the structures of the isostructural $\text{Ti}(\text{OH})\text{PO}_4$ and corresponding arsenate species [51].

The structure of $\text{Ti}(\text{HPO}_4)_2 \cdot x\text{H}_2\text{O}$ has been investigated by x-ray diffraction, density measurements and bond length and angle considerations. Subsequent to an investigation of the thermal behavior of $\alpha\text{-Ti}(\text{HPO}_4)_2 \cdot \text{H}_2\text{O}$, a new phase, $\gamma\text{-Ti}(\text{HPO}_4)_2 \cdot 2\text{H}_2\text{O}$, was isolated. The structure arises from the packing of layers of α - and γ -type, identical to those in the starting materials and held together by P-O-P bridges [52].

Reactions between TiP_2O_7 and CaCO_3 (10-90 mole %) were investigated by Inoue *et al.* [53]. The products, analyzed by x-ray diffractometry, include $\text{CaTi}_4(\text{PO}_4)_6$, $\beta\text{-Ca}_2\text{P}_2\text{O}_7$, TiO_2 (rutile and anatase), $5\text{TiO}_2 \cdot 2\text{P}_2\text{O}_5$, α - and β -

$\text{Ca}_3(\text{PO}_4)_2$, CaTiO_3 and $\text{Ca}_{10}(\text{PO}_4)_6(\text{OH})_{2-2x}\text{X}^0$.

The preparation and structure determination (^{183}W nmr) of single isomers of $\text{Ti}_2\text{W}_{10}\text{PO}_{40}^{7-}$ and $[\text{CpFe}(\text{CO})_2\text{Sn}]_2\text{W}_{10}\text{PO}_{38}^{5-}$ have been carried out.

$\text{Ti}_2\text{W}_{10}\text{PO}_{40}^{7-}$ forms isolable complexes with divalent Mn, Fe, Co, Ni, Cu and Zn [54].

6.5 TITANIUM NITRATES

Mechanistic and preparative studies of titanium(IV) nitrates have been reviewed by Garner and Joule [55]. As well, techniques for handling anhydrous $\text{Ti}(\text{NO}_3)_4$ were described. Gas-phase XPS (x-ray photoelectron spectroscopy) of $\text{Ti}(\text{NO}_3)_4$ have been reported and discussed in terms of molecular charge distributions. The inability to observe measurable band splitting between the $1s$ ionization energies of the chemically distinct oxygen atoms was suggested, from *ab initio* calculations on $\text{Cu}(\text{NO}_3)_2$, to result from differential orbital relaxation occurring upon core electron ionization [56].

6.6 TITANIUM OXIDES

a. Oxide Films on Ti Surfaces

Several studies on the nature of the oxide films formed on titanium surfaces in various media have been reported. Anodic polarization curves of mechanically polished titanium in a bath containing 0.05M $\text{Na}_2\text{B}_4\text{O}_7$ /0.05M KI/starch/agar-agar were plotted to ascertain the electronic conditions (homogeneous or heterogeneous) so as to explain possible defects in the oxide film [57]. An electrochemical characterization of the anodically formed oxide layers on titanium in HClO_4 has also been reported [58].

The structure of the oxide films and corrosion-induced behavior of titanium in HNO_3 solutions [59], and the prevention of titanium corrosion by cathodic leakage currents in chloride media [60] have been investigated.

The photoelectrochemical oxidation of titanium anodes (1.2-1.8V) and exposure to light ($\leq 0.16 \text{ W/cm}^2$) leads to the formation of both dissolved and solid-phase corrosion products. The solid-phase products consist of finely divided TiO_2 (anatase and rutile) possessing somewhat less bound water than the usual films. Increasing the potential or the exposure to light increases the rate of oxide formation [61].

The dissolution of native oxides on titanium was studied at 298-1273K to determine their role in the pyrotechnic reaction of Ti with KClO_4 . Auger electron spectroscopy data revealed a sharp increase in oxide solubility at 623K; this was explained in terms of the presence of free Ti at >623K [62].

b. Titanium Oxides, Except TiO_2

The phase transformation of evaporated $\alpha\text{-TiO}_{0.5}$ films to a transition structure was monitored by in situ heating in an electron microscope. Single crystals of $\delta\text{-TiO}_{0.5}$ precipitate in the film during the phase transformation, as verified by x-ray diffraction studies [63]. Electron microscopy, combined with optical diffraction, was also utilized to investigate the structure of the film formed by evaporating $\text{TiO}_{0.8}$. The amorphous-like film presumably contains microcrystallites of both the α - and TiO phases [64]. Similar experiments were carried out on $\text{TiO}_{1.0}$ and $\text{TiO}_{1.28}$ on NaCl substrates [65].

The electronic structures of TiO_x ($0.75 \leq x \leq 1.05$) were determined using cluster quantum mechanics, taking into account the vacancy concentration and ordering. Molecular-orbital energy-level schemes were also discussed [66]. The Fermi surface of TiO was calculated within the Green function method via the use of corrected x-ray spectral data. With respect to the bottom of the conduction band, the Fermi energy is 0.243 Rydberg for TiO [67]. A partial vibrational analysis of the $\text{f}^1\text{d} \rightarrow \text{a}^1\text{d}$ transition in TiO and the $\text{A} \rightarrow \text{X}$ transition in TiO_2 has been performed by Devore [68]. Vibrational and molecular constants were determined.

A series of (complete active space)-SCF calculations have been employed to describe the lowest states of TiO , which was described as having polarized double bonds involving the Ti-3d orbitals. The nature of the excited states was also discussed [69].

Selective interactions between Ti atoms and water molecules were observed in XPS studies [70] of polycrystalline FeTi surfaces under ultrahigh vacuum (2×10^{-10} torr). TiO becomes the dominant surface species, as inferred from the $\text{Ti}(2p_{3/2})$ and $\text{O}(1s)$ chemical shifts.

The thermodynamics of evaporation and stationary states (congruent states) have been investigated for the $\text{TiO}_3\text{-TiO}_2$ system in molybdenum cells. The results suggest a shift of the effusion flow component toward a reducing component, either by crucible reaction or by establishing a diffusion process [71].

The x-ray crystal structure of $\gamma\text{-Ti}_3\text{O}_5$ at 297K reveals it to be monoclinic and to be derived from the rutile structure (r) by crystallographic shear $(1\bar{2}1)r$. The structure is shown in Figure 1 [72]. Magnetic susceptibility measurements have been performed on solid solutions of vanadium-doped Ti_3O_5 , $\text{Ti}_{3-x}\text{V}_x\text{O}_5$ ($0 < x < 0.20$). The effect of the vanadium on the temperature of the semiconductor-metal phase transition in Ti_3O_5 was established, as was the valence state of vanadium [73].

An analysis of the EPR spectrum of single-crystal Ti_6O_{11} suggests the presence of Ti_2^{7+} ion pairs at temperatures below 147K. The spin count

to either formation of anatase pockets in the film or to the incomplete oxidation of Ti during anodization [78].

The effect of oxygen partial pressure on the deposition rate, crystal structure, and optical absorption of thin-film TiO_x prepared via reactive sputtering of a Ti target has been examined [79]. A glow discharge was employed to enhance reaction rates between TiCl_4 and O_2 to deposit thin TiO_2 films. Structural, optical, electronic and photoelectrochemical properties of the films were studied as functions of deposition parameters [80]. Thick-film TiO_2 anodes for use in photoelectrochemical solar cells were prepared from TiO_2 powders of both anatase and rutile structures, combined with varying amounts of a glass binder and dispersed in a liquid organic vehicle [81]. Semiconducting n- TiO_2 films on Ti foils were formed by controlled thermal oxidation, anodic oxidation with facultative subsequent reduction with hydrogen and by vapor deposition. The samples were compared with respect to their photochemical and photophysical behavior, their electrochemical and photoelectrochemical properties, and their surface structure and chemical composition. The optimal photoanodes were the n- TiO_2 layers prepared via controlled thermal oxidation [82].

An electron diffraction structure determination of amorphous TiO_2 films prepared by pyrolysis has been done for which a new algorithm was proposed for the radial distribution function and electron density. The films were found to retain the short-range order present in crystalline TiO_2 [83]. An analysis of ellipsometric measurements on anodic TiO_2 films of varying thickness was employed to obtain the optical indexes of the films [84]. A similar investigation showed that the optical indexes decrease with increasing film thickness, assuming constant values for sufficiently thick films [85]. Thin films of TiO_2 , prepared via reactive evaporation of TiO in an oxygen atmosphere were characterized by breakdown thresholds of ca. 4 MW-cm^{-2} when irradiated by 1-ms pulses of a $\lambda = 1.06 \mu\text{m}$ laser radiation. The breakdown thresholds were not dependent on substrate type, but decreased on increasing the substrate surface temperature during film deposition. The results obtained were discussed in terms of the effect of a nonstoichiometry of the films on the laser beam strength [86].

The changes observed in the surface potential of thin mica-supported TiO_2 films were lower than those calculated theoretically, indicated that a large portion of the induced charges was captured by the surface states. Electrical conductivity measurements revealed a slight Fermi level shift in the electrical field. These two effects have been suggested to be responsible for the absence of the field effect on the catalytic activity of TiO_2 in the oxidation of CO and the decomposition of NO on TiO_2 [87]. A hydrolytic film of TiO_2 was chosen to measure the bulk concentrations of ionized donors from 5×10^{19} (373-723K)

to $5 \times 10^{17} \text{ cm}^{-3}$ (973K) [88].

Auger spectroscopic measurements of the Ti $L_{2,3}V$ line shape were obtained for TiO , Ti_2O_3 , TiO_2 (anatase and rutile), for reactive sputter-deposited TiO_2 , and for chromic acid-anodized Ti-6Al-4V. The relation between the peak positions at ca. 417-420 eV and 411-415 eV was found to be a sensitive indicator of the average surface stoichiometry. A significant amount of reduction was observed for amorphous TiO_2 thin films, though none was observed for sputtered-induced reduction of crystalline TiO , Ti_2O_3 or TiO_2 . This effect has been attributed to the decreased thermodynamic stability of the amorphous films [89].

Hydrated TiO_2 was precipitated by mixing a titanium sulfate solution (containing TiO_2) with an alkaline solution and then hydrolyzing in hot water. The hydrolysis rate was determined by measuring unreacted TiO_2 by volumetric analysis; the hydrated TiO_2 diameter was determined by x-ray diffraction, and a mechanism for TiO_2 hydrolysis and hydrated TiO_2 crystal growth proposed [90]. Infrared and nmr spectroscopies, DTA, thermogravimetry and x-ray diffraction methods were used to study the films and precipitates of $\text{TiO}_2 \cdot n\text{H}_2\text{O}$, obtained by homogeneous precipitation in the presence of urea. On a quartz support, the film exists in the rutile form; on SiO_2 , it exists as a mixture of rutile and some anatase. The study explained the lack of pH effect of preparation on the sorption properties of $\text{TiO}_2 \cdot n\text{H}_2\text{O}$ [91]. The effect of added urea on the crystal and pore structures of hydrated TiO_2 (HTiO) was investigated using x-ray diffraction, electron microscopy and N_2 adsorption-desorption at 77K [92].

An investigation of the polarized oxygen K_α spectra of TiO_2 (rutile) reveals that in comparison to unpolarized spectra of polycrystalline samples, the polarized valence band spectra provide additional symmetry and bonding character information. The polarized spectra indicated the existence of bonding valence states with participation of oxygen $2p$ and titanium $4p$ -like orbitals. The highest occupied valence states were identified as nonbonding oxygen $2p$ states [93]. An Auger electron spectroscopic study of $\text{TiO}_2(110)$ surfaces revealed near-stoichiometry and the interatomic Auger transition [$L(\text{Ti}) M(\text{Ti}) V(\text{O})$] for annealed surfaces, and both inter- and intra-atomic Auger processes for ion-bombarded surfaces [94]. Rigid lattice proton nmr spectroscopy was employed to study the superficial constitutive water of TiO_2 (anatase, rutile, amorphous) [95]. A direct electronic recombination process was observed upon $3p$ excitation of Ti and TiO_2 . In the latter, the oxide valence-band emission was enhanced at the $3p$ resonance energy, the first observation of interatomic resonant photoemission in an oxide [96].

The optical absorption spectra and ESCA of pure TiO_2 , reduced TiO_2 , and $\text{V}_x\text{Ti}_{1-x}\text{O}_2$ have been recorded by Sakata [97]. In reduced TiO_2 , the Ti ion takes the variable valence states Ti^{4+} , Ti^{3+} and Ti^{2+} , and they form a broad donor

band which overlaps with the conduction band originating from Ti $4s$ levels, $3d-4s$ mixing results in a large change of the conductivity of TiO_2 from insulator to metal depending on the degree of reduction. The electronic structure of the ideal (110) surface of TiO_2 (rutile) was studied, and results presented in terms of surface bound states, surface resonances, and wave vector resolved densities of states. For $TiO_2(110)$, there were no occupied surface states in the gap region, in agreement with UPS measurements on defectless $TiO_2(110)$ surfaces [98]. Sushko *et al.* [99] have seen that in the presence of H_2O , the rutile-anatase phase transition temperature for TiO_2 is lower than in vacuum. Additionally, the lower temperature modifications of TiO_2 are stabilized by amorphous SiO_2 as a result of Si-O-Ti bond formation. TiO_2 is completely soluble in SiO_2 at $[TiO_2] < 5\%$.

The reactions of Nb_2O_5 , TiO_2 , ZrO_2 and C at 1000-4000K in argon and 9.81×10^{-2} MPa were modeled by calculating the formation of the ideal pseudobinary solid solutions of NbC-TiC and NbC-ZrC. These calculations are in good agreement with chemical and x-ray phase analyses for the reaction products of Nb_2O_5 , TiO_2 and ZrO_2 with carbon black in an argon-hydrogen plasma in a plasma-arc apparatus at 3000K [100]. From an EPR study of molybdenum ions impregnated on polycrystalline TiO_2 , it would appear that some of the Mo ions are stabilized as Mo^{5+} pairs in the bulk oxide after reduction treatment in CO or H_2 [101]. The electronegativity of surface energy levels produced via reduction of Ag^+ , $PdCl_4^{2-}$ and $PtCl_4^{2-}$ on TiO_2 films has been determined to investigate the effect these deposited ions have on electrocatalytic properties [102]. Similar studies of copper deposition on TiO_2 indicate the appearance of deeper surface states, compared with Ag-, Pd- or Pt-deposited TiO_2 [103]. An investigation of the codeposition of TiO_2 (anatase) with copper (from an acidic $CuSO_4$ bath) yielded the effects of cathode current density dispersoid, bath loading, Cl^- concentration and cesium and thallium ion addition on the codeposition process. A codeposition mechanism based on a two-step adsorption process has been proposed [104].

Valigi and Gazzoli [105] have reviewed the effects of incorporation and reducibility of Mn^{4+} , Sn^{4+} , Zr^{4+} , Ru^{4+} , Ir^{4+} and Mo^{4+} in solid solutions of TiO_2 (rutile). ESR spectroscopy was employed to study the nature of the Mo surface species on Mo-containing TiO_2 catalysts in the presence and absence of ethanol. Reduction by ethanol yields Mo^{5+} [106]. Studies on mixed ^{95}Mo -enriched Mo/ TiO_2 systems revealed the existence of different types of Mo^{5+} ions [107]. Electron-spin-echo measurements were made on the phase memory decay of V^{4+} in TiO_2 at liquid-helium temperatures [108]. A rectangular pulse technique coupled with various physicochemical measurements were used to determine the structures of vanadium oxide (V_2O_5) catalysts supported on TiO_2

(anatase, rutile, anatase-rutile mixture). Infrared and UV-visible spectral data suggest that the coordination of oxygens around vanadium ions is nearly the same for supported and unsupported catalyst systems [109]. V_2O_5/TiO_2 catalysts have been prepared by mixing TiO_2 with vanadium oxalate, followed by thermal decomposition of the oxalate [110].

The deposition of an Al_2O_3 or $Al_2O_3-SiO_2$ coating on TiO_2 (rutile) was satisfactorily achieved in an aqueous precipitation system [111]. Secondary-ion mass spectra of powders extracted during the process are consistent with an independent coating mechanism. EPR spectra were suggestive of the presence of paramagnetic ions coprecipitated at trace levels. The direct adsorption phenomenon of aluminum and pyrophosphate ions at a TiO_2 surface was examined by ^{27}Al and ^{31}P nmr spectroscopy; they reveal a cooperative interaction between the ions and colloidal particles together with a desorption of bound species with increasing pH [112].

The systems $zRuO_x-TiO_2$ ($z = 0.006-0.007$) and $zIrO_x-TiO_2$ ($z = 0.003-0.025$) have been prepared by impregnating TiO_2 with standardized $RuCl_3$ or $IrCl_3$ solutions, drying the slurry at 383K, grinding, heating in air at 873K, and regrinding and reheating at 1273K in air. X-ray diffraction and thermogravimetry were employed to determine the formation and stability of solid solutions in hydrogen [113]. A simple procedure outlining the modification of TiO_2 powder by the adsorption of $RuCl_3$ from isopropanol solution has been described. Heating the chloride-coated powder in air at 69K results in the formation of a RuO_2 -modified TiO_2 surface [114]. Microscopic and x-ray phase analyses of the eutectic composition $Fe + 5TiO_2$ reveals crystallization in the form $FeO \cdot 2TiO_2 \cdot Ti_3O_5$ (Fe anosovite) on rapid cooling [115]. The slow uptake of hydrogen (adsorption) by TiO_2 -supported Ni, NiFe, and Pt samples has been studied at room temperature following reduction at 770K [116].

Platinum supported on TiO_2 , TiO and Ti_2O_3 in various forms was investigated by various physical and chemical methods. Limited hydrogen uptake occurs on hydrogen-pretreated samples, as well as fast H-D exchange for H_2-D_2 mixtures on all samples. The TiO_2 -Pt interaction effect was interpreted in terms of a bulk oxide reduction model, in which bulk conduction band electrons readily tunnel through a thin TiO_2 layer at the surface to reach Pt particles, where they are trapped and furnish a negatively-charged Pt particle with good capacity for dissociating H_2 but weak binding of atoms [117]. An electron microscopic study of Pt dispersed on TiO_2 and TiO shows the presence of bulk Ti_9O_{17} crystallites and polyhedral Pt particles on prerduced TiO_2 samples. On extensive reoxidation, Ti_9O_{17} is removed and the Pt particles are hemispherical [118].

Core level electron binding energies were determined by XPS for Rh and Pt supported on Group IIIB-VB oxides after low and high temperature reductions.

For 2%Rh/TiO₂, a small reversible chemical shift was observed for the Rh 3d_{5/2} peak, indicative of some electron transfer from Ti³⁺ to Rh [119]. The kinetics of reduction of TiO₂ in Rh/TiO₂ catalysts was studied at 710-790K using a titration method. The results agree well with the model of circular sources of diffusion. The relatively high activation energy (25-28 kcal-mole⁻¹) suggests a transfer process with successive steps of formation and rupture of chemical bonds. In accordance with the model, the reduction rate was proportional to the interfacial perimeter of the metal crystallites [120]. An ESR and nmr spectroscopic examination of the reduction of Rh/TiO₂ at 298K showed facile reduction for this system with no appreciable reduction on TiO₂ alone being observed [121]. Renasco and Haller [122] have developed a simple model for the different kinds of interactions that occur following low- and high-temperature reduction of Rh/TiO₂ catalysts. The model proposes a delocalized transfer of charge from Rh to TiO₂ after low-temperature reduction, and a localized (chemical bonding) transfer of charge from support to Rh after a high-temperature reduction [122]. Other ESR spectroscopic studies of the reduction of TiO₂ and Rh/TiO₂ catalysts have appeared [123].

A nuclear analysis was performed to prove the existence of at least two forms of hydrogen incorporated with TiO₂ layers [124]. Simple molecules (e.g., H₂O, MeOH, Me₂CO, C₆H₆) can be adsorbed and condensed as a film on polycrystalline TiO₂ (anatase) to test the usefulness of SIMS (secondary-ion mass spectrometry) as a probe during reaction. The spectra exhibit characteristic quasimolecular ions, and differences between strongly and weakly associated molecules [125]. The adsorption of acetic and stearic acids onto TiO₂ has been studied. Chemisorption occurs on coordinately unsaturated Ti ions and on surface OH groups; physical adsorption on the acid-modified surface occurs on oxygen atoms and on OH groups of both the solid surface and the carboxylic acid linked to it. Methanol and water dislodge chemisorbed acetic acid with formation of surface MeO and OH groups, while neither methanol nor water dislodges stearic acid [126]. Carbon monoxide adsorption onto reduced and oxidized Pt/TiO₂ has been studied by FTIR. On reduced samples, two linear CO species are observed, assigned to adsorption on Pt close-packed (terrace) sites and on Pt open (step) sites; bridged CO species also occur. On oxidized Pt/TiO₂ samples, some Pt atoms are covered with oxygen atoms and the density of step sites is enhanced. Two kinds of linear and a bridged CO species were formed [127, 128].

Schumacher and coworkers [129] have investigated the influence of illumination on the flat band potential (V_{fb}) of the contact TiO₂/MeCN. They found that on addition of H₂O or illumination with band gap light, the value of V_{fb} is significantly affected (up to 2V) compared to V_{fb} obtained from capacitance/potential determinations on unilluminated electrodes. However,

V_{fb} values obtained from capacitance measurements on preilluminated electrodes agree well with data from photocurrent measurements. The results were discussed in terms of alterations of the inner Helmholtz plane [129]. Sub-band-gap electroreflectance spectroscopy was employed to detect intrinsic surface states of the unsolvated surface at the TiO_2 /aqueous/electrolyte interface. The energy of these states was located at 1.3eV below the conduction band and can only be detected in the weak accumulation mode [130]. Donor-like surface states at the TiO_2/H_2O interface have been detected by measuring capacitance under UV illumination. The surface states are located 0.65eV below the bottom of the conduction band of TiO_2 . Additionally, the density of the surface states increases on increasing the light intensity [131].

A generalized model, accounting for the structural influence of the solid-solid interface on thermodynamic and kinetic properties of phases in contact, has been suggested to account for the anatase-rutile transition activated by $V_2MoO_{7.5}$, MoO_3 , and $\alpha-VPO_4$ under the same conditions observed for the V_2O_5 -activated transition [132]. Richardson [133] has performed a molecular dynamics study of radiation damage in TiO_2 (rutile).

(ii). TiO_2 As a Catalyst, Catalyst Support and Photosensitizer

Several hydrogenation reactions are known to be catalysed by metal-loaded TiO_2 catalysts, M/TiO_2 , ($M = Pt, Rh, Co, Ni$). An XPS study of Rh/TiO_2 hydrogenolysis catalysts revealed a shift of -0.7 ± 0.1 eV between low-temperature-reduced and high-temperature-reduced rhodium. Cycling between 773K reduction, 673K oxidation and 573K reduction reduced this shift to -0.2 ± 0.1 eV. It was suggested that the increased XPS shift might reflect increased dispersion of Rh and a corresponding increase in catalytic activity [134]. Ethane, butane and cyclohexane hydrogenolysis reactions were also studied as a function of dispersion on Rh/TiO_2 catalysts. The results obtained suggest a charge transfer to the metal after high-temperature reduction where the degree of destabilization of the intermediate varies with the kind of bond to the Rh surfaces [135]. The catalytic properties of Pt/TiO_2 have been compared to those of Pt/CeO_2 for the hydrogenation of benzene [136]. The hydrogenolyses of ethane, hexane and CO were carried out in the presence of nickel catalysts supported on TiO_2 and SiO_2 , prepared by wet impregnation. Monolayer coverage was indicated from hydrogen adsorption isotherms, and it was observed that Ni/TiO_2 catalysts exhibit normal hydrogen chemisorption properties after reduction at 723K, though adsorption was suppressed after thermal treatment at 923K [137]. The rate of propene hydrogenation over a Co/TiO_2 catalyst (prepared by an alkoxide technique) was significantly enhanced upon catalyst reduction by hydrogen at 973K. When the Co/TiO_2 catalyst was prepared via

impregnation, however, no rate enhancement was observed at any reduction temperature [138]. The hydrogenation of crotonaldehyde is catalysed by ruthenium-palladium catalysts supported on TiO_2 . In 96% ethanol and in water, the reaction proceeds with H_2 addition at the C=C double bond; in 0.1N KOH, the addition of H_2 occurs nonselectively [139].

A significant amount of work on the hydrogenation of carbon monoxide catalyzed by M/ TiO_2 systems (M = Ni, Rh, Pt, Pd) has appeared this year. In addition to the SMSI (strong metal-support interaction) phenomenon exhibited by Ni catalysts supported on TiO_2 , SiO_2 and ZrO_2 , low-temperature catalyst reduction leads to another metal-support interaction for the $\text{CO} + \text{H}_2$ reaction. An interpretation of this latter interaction was proposed, based on the presence of unreduced Ni species [140]. An infrared spectroscopic study of the hydrogenation of CO over Rh/X (X = TiO_2 , Al_2O_3 , SiO_2) catalysts was performed for various Rh weight %. A support effect was evident for Rh/ TiO_2 , which was more active for the $\text{CO} + \text{H}_2$ reaction than were Rh/ Al_2O_3 or Rh/ SiO_2 [141]. Another study compared the catalytic properties of Rh supported on TiO_2 , SiO_2 , Al_2O_3 and MgO [142]. The presence of TiO_2 favored alkene and long-chain hydrocarbon production, and was attributed to a strong Rh- TiO_2 interaction which results in higher surface mobility of adsorbed carbidic intermediates and lower rates of alkene hydrogenation. The Rh/ TiO_2 catalyst also exhibited low hydrogenation activity [142]. Conesa and coworkers [143] have discussed the reactivity of CO with a TiO_2 -supported rhodium catalyst. Infrared spectroscopy was employed to characterize adsorbed CO species on Pt/X (X = TiO_2 , Al_2O_3 , SiO_2 - Al_2O_3 , SiO_2) under steady-state reaction conditions in the presence of H_2 and also under equilibrium adsorption conditions in the presence of helium. The Pt/ TiO_2 catalyst was found to have the highest activity, though it showed almost no IR-detectable CO during reaction. The study inferred that only a very small fraction of Pt atoms constitutes the active sites. The activity of the Pt/ TiO_2 catalyst was attributed to a weakened CO-metal bond resulting in more competitive H_2 chemisorption and higher surface concentration of hydrogen under reaction conditions [144]. Another IR study of adsorbed CO on Pt/ TiO_2 after hydrogen treatment at various temperatures revealed a gradual blue shift in the strong band for adsorbed CO and a corresponding change in conductivity when the system was allowed to stand. It was proposed that the blue shift arises from the interaction of CO with H_2 , which is provided by the TiO_2 support. Thus, there exists a general phenomenon of hydrogen back-spillover for the Pt/ TiO_2 system [145]. A model for CO methanation over Pt/ TiO_2 has been proposed, invoking hydrogen-assisted CO bond rupture as the rate-determining step [146]. The effects of oxygen pretreatment on the activity and selectivity of the $\text{CO} + \text{H}_2$ reaction over Na-doped and nondoped Pd/ TiO_2 catalysts were investigated. Oxygen pretreatment followed by low-temperature reduction

resulted in a large enhancement of MeOH and C₂ hydrocarbon product formation [147].

The Fischer-Tropsch catalysts α -Fe₂O₃, or α -Fe₂O₃ containing ~1% oxides of Al, Mo or Ru, were dispersed on TiO₂, SiO₂, SnO₂ and Al₂O₃ via impregnation, vacuum drying and heating. These catalysts were tested in a differential reactor with 9:1 H₂-CO at 1 atm and 523K. The reducible supports have similar dispersing effects to the refractory supports, unless the activation involves precursor reduction, in which case the support is partially reduced and the formation of an alloy suppresses catalytic activity [148]. Hydrogenation of CO₂ over unsupported Ni and over Ni supported on TiO₂, SiO₂ and Al₂O₃ has been examined. The data reveal that the CO₂/H adsorption ratio increases in the order Ni/SiO₂ < Ni/Al₂O₃ < Ni/TiO₂; that is, with increasing metal-support interaction [149]. Molecular oxygen was observed to oxidize CO at 290K over CoTPP/TiO₂ (TPP = tetraphenylporphyrin) at a rate of 5.3×10^{-3} mmol/g_{cat}-min, which is comparable to that of a common Hopcalite. Thus, an effective activation of CO on the partially reduced Co ion of the supported complex to attract an oxygen atom from weakly adsorbed molecular oxygen is revealed [150].

Catalysis of the Water Gas Shift Reaction (WGS) over Pt/TiO₂ has been observed [151]. The enhanced activity observed upon hydrogen reduction at 773K of Pt/TiO₂ was attributed to the presence of a greater number of basic OH groups on the Pt/TiO₂ surface. It was suggested that the Ti atom containing the basic hydroxyl group might be the site for the activation of H₂O in the WGS [151]. Similar observations were made for the photocatalytic activity of Pt/TiO₂ in the WGS [152].

The reduction of NO with NH₃ over iron oxide/titanium oxide catalysts was studied with a flow reactor between 573-723K. The catalytic activity was found to depend on the method of catalyst preparation [153]. Nb₂O₅ supported on TiO₂ also catalyses the reduction of NO with NH₃ at temperatures above 723K [154]. The catalytic reduction and decomposition of NO and N₂O over CoTPP/TiO₂ were studied kinetically and mechanistically at 323-423K. The kinetics suggest that the surface reaction between NO, adsorbed strongly on Co, and hydrogen, adsorbed dissociatively on the porphyrin ring, is the rate-determining step [155]. When evacuated at 473K, the CoTPP/TiO₂ catalyst exhibits enhanced activity, likely due to the increased capacity for hydrogen adsorption and further CO and NO activation [156].

The catalytic isomerization of 2-pinene to camphene and tricyclene over TiO₂, Fe₂O₃ or ZrO₂ is promoted in the presence of (NH₄)₂SO₄. The promoting effect was attributed to the formation of alum-type sulfates on the catalyst surface [157]. The dehydration of α -phenylethyl alcohol, PhCH(OH)Me, over a TiO₂ catalyst was investigated by CNDO/2 calculations and chemical adsorption analysis. The electron density calculation on water and PhCH(OH)Me in

combination with a two-site adsorption model favored a concerted two-center reaction mechanism with Ti as the Lewis acid center and O as the Lewis base center [158]. Infrared spectroscopy was employed to study formate formation when oxidized TiO_2 surfaces were exposed to HCO at 373K [159]. The synthesis of furfural (82-86% yield) from pentosan-containing raw materials in the presence of TiO_2 dissolved in 3-5% H_2SO_4 has been reported [160]. A microcalorimetric technique was used to determine the differential adsorption heats of C_2H_4 , C_3H_8 and CO on oxide catalysts containing Ti^{4+} , Co^{2+} , Ni^{2+} , Ag^+ and Cu^+ cations [161].

The ammonia synthesis reaction is catalysed by Fe/TiO_2 catalysts prepared via thermal decomposition of $\text{Fe}(\text{CO})_5$ [162]. The hydration of MeCH=CH_2 to Me_2CHOH , and its dehydrogenation to Me_2CO , over $\text{TiO}_2\text{-MoO}_x$ as a function of catalytic preparation method has been examined, as well as the isomerization of pulsed cyclopropane [163]. The activity of a reduced state $\text{Co-MoO}_3/\text{TiO}_2$ catalyst for the hydrodenitrogenation of pyridine is observed to be higher than that of the same catalyst in the sulfided state. In the reduced catalysts, both the conversion and the nitrogenation of pyridine increased with increasing Co content [164].

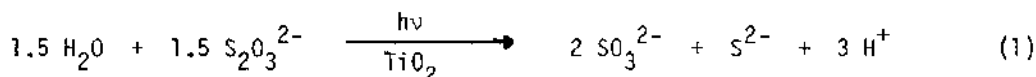
The $\text{Fe}^{2+}/\text{Fe}^{3+}$ redox system was investigated on passive Ti with gold deposits ($0 < \theta_{\text{Au}} < 1$). Typical diode characteristics were observed with thick films at high overvoltages: a) large cathodic and small anodic transfer coefficients, b) currents increasing with θ_{Au} and independent of concentration of redox system. A rate-determining tunnel process from the conduction band of $\text{TiO}_2(\text{Au})$ to that of $\text{Au}(\text{TiO}_2)$ was employed to explain the influence of temperature and of density on current. At small Au coverage and low overpotential, the influence of diffusion-limited processes at film defects dominates the system [165]. Ruthenium dioxide deposited on TiO_2 particles catalyses vigorous reduction of BrO_3^- ions to Br_2 (or Br^-) by H_2O , and simultaneous generation of stoichiometric amounts of oxygen. The O_2 evolved originates from H_2O , not BrO_3^- [166]. The oxidation of methanol is catalysed by a solid solution consisting essentially of VO_2 in TiO_2 , with a composition $\text{Ti}_{0.96}\text{V}_{0.04}\text{O}_2$. The increased catalytic activity and higher selectivity for formaldehyde formation observed for this system, compared to V_2O_4 or a mixture of VO_2 , V_2O_5 and TiO_2 , was attributed to the V-O bond polarity in the catalysts [167].

Thermodesorption techniques have been utilized to examine the nature of the hydrogen species bound to Rh/TiO_2 catalyst systems. Temperature-programmed desorption nmr studies revealed the presence of three irreversibly bound hydrogen species, two assigned to species produced when Rh metal is present on the surface and one to surface hydroxyl groups [168]. Other thermodesorption

studies have shown that the Rh/TiO₂ solid holds high amounts of hydrogen, particularly when it is reduced at elevated temperatures (773K). It was also suggested that residual hydrogen is not the cause of the unusual chemisorptive properties of the SMSI catalysts [169].

Catalytic systems involving TiO₂ have also been used in photocatalytic systems. In dilute aqueous solution, CCl₄, CHCl₃ and CH₂Cl₂ are completely mineralized to CO₂ and HCl in the presence of the heterogeneous photocatalyst TiO₂. The relative rate constants are in the approximate ratio of 29(CHCl₃): 9(CH₂Cl₂): 1(CCl₄). Chloride ions and product protons inhibit the degradation rate [170]. The photocatalytic decomposition of glucose over TiO₂ or reduced Nb₂O₅ was studied in the presence and absence of added NaOH. The extent of decomposition depends on the glucose concentration and on the nature of the catalyst [171]. The photocatalytic isomerization of butenes over TiO₂ or ZnO has also been examined. With TiO₂, 2-butene is more reactive than 1-butene; this results from a stronger interaction of the C=C double bond of 2-butene with UV-irradiated TiO₂. By contrast, with ZnO, 1-butene is more reactive than 2-butene, the photoenhancement being attributed to photoformed O⁻ hole centers [172]. Augugliaro and coworkers [173, 174] have studied the photoassisted formation of NH₃ over various Fe-doped TiO₂ catalysts supported on γ-Al₂O₃ under near-UV irradiation. A reaction mechanism was proposed [174] for which the photogeneration of electron-hole pairs and their separation were considered to be the rate-determining steps of the overall reaction.

The presence of TiO₂(anatase) enhances (≈ 40%) the photolytic reduction rate in dilute sulfuric acid solutions of Ce⁴⁺ and Tl⁺ ions [175]. The photochemical reduction of carbonate (CO₃²⁻) [176] and thiosulfate (S₂O₃²⁻) [177] ions is also catalysed by TiO₂. When CO₃²⁻ is used to intercept the photogenerated hole on TiO₂, the intermediate species ·OC(O)O⁻ is produced and undergoes secondary surface reactions to yield HCHO. The quantum yield of formation of HCHO is 4 × 10⁻³, but extended irradiation results in loss of HCHO [176]. The illumination of S₂O₃²⁻ leads to the production of S²⁻ and SO₃²⁻ (reaction 1). The reaction is accompanied by a hole transfer to S₂O₃²⁻



to produce S₄O₆²⁻, which undergoes disproportionation in alkaline solution [177]. γ-irradiation of carbon dioxide in aqueous solution in the presence of TiO₂ results in the formation of oxalic acid, formaldehyde and traces of formic acid. The rate of reduction depends on the reactant concentration, pH, and the introduction of different additives (e.g., phosphomolybdates, phosphotungstates, etc.) [178].

Sulfur can be oxidized directly to SO_4^{2-} on a TiO_2 (anatase) photocatalyst in a suspension into which oxygen is bubbled. The oxidation process was assigned to the electron and hole produced by light of <400 nm, although sulfur itself photoreacted in light of ≤ 300 nm. H_2S was produced simultaneously in H_2O . A sunlight illumination test revealed direct production of H_2SO_4 [179]. Liquid 2-propanol undergoes photocatalytic (366-nm irradiation) oxidation over TiO_2 (rutile and anatase) to yield propanone. The estimated activation energies ($31\text{--}91 \text{ kJ}\cdot\text{mole}^{-1}$) were ascribed to the solid-state properties of the catalysts rather than to the radical oxidative mechanism of 2-propanol [180]. Various semiconductor powders (TiO_2 , ZrO_2 , CeO_2) were shown to enhance the oxidation of oxalic acid under UV illumination in the presence of oxygen. The oxidation rate was enhanced in the presence of TiO_2 , Fe_2O_3 and WO_3 under visible-light illumination. TiO_2 was found to be the most active species. A mechanism was proposed which involves attack by atomic oxygen on the C-C bond of adsorbed HC_2O_4^- ions, for which atomic oxygen was activated by photoproduct holes [181].

The photooxidation of heptane, catalysed by TiO_2 , proceeds via peroxide formation, the decomposition of which gave isomeric heptanols and heptanones. This was used as a convenient model for processes occurring in pigmented regions for low-density polyethylene [182]. The relative rates of the TiO_2 -catalysed photochemical oxidative cleavage of the olefins $p\text{-RC}_6\text{H}_4\text{CPh=CH}_2$ ($\text{R} = \text{H, OMe, Me, Cl, NO}_2$) to the corresponding benzophenones gave rise to an LFER with $\rho^+ = -0.56$. The low ρ^+ value reflects near diffusion-controlled electron transfer from an adsorbed olefin to the photogenerated hole at the TiO_2 surface, followed by slower electron transfer equilibration of the competing olefin with this photogenerated radical cation [183].

The activities of TiO_2 powders loaded with various transition metal borides, nitrides, phosphides and carbides have been examined for photocatalytic hydrogen evolution from aqueous methanol solutions. It was found that the tungsten carbide loaded catalyst WC/TiO_2 had the highest activity of those studied; however, this was $<1/4$ of the activity of that for a Pt black/ TiO_2 catalyst [184]. Borgarello and Pelizzetti [185] have investigated the photocatalytic hydrogen production from aliphatic alcohols over semiconductor particles (TiO_2 , ZnO , SnO_2) loaded with redox catalysts. Hydrogen was observed to evolve at a sustained rate from primary and secondary alcohols, with the corresponding aldehyde (or ketone) being the other major product. The effects of different TiO_2 preparation methods, loading, and the presence of oxygen and surfactants were also determined.

The photolysis of water vapor on the surface of titanium-coated polycrystalline n- TiO_2 at 653K yields a quantum conversion efficiency of 2% for

hydrogen production, as measured for ultra-band-gap excitation of TiO_2 . These experiments indicate the catalytic nature of the reaction with respect to the active material and also suggest an important role for the Ti metal [186]. Titanium dioxide (TiO_2) has been studied extensively in recent years as a basic material for the direct conversion of water to hydrogen and oxygen by solar energy. The mechanism and the experimental technique of the light-induced cleavage of H_2O on catalyst (RuO_2 , Pt)- and photosensitizer-containing TiO_2 have been summarized by Hauffe [187]. The design, preparation and characterization of $\text{RuO}_2/\text{TiO}_2$ catalytic surfaces for the photooxidation of H_2O have been reported [188]. The catalyst $\text{RuO}_2 \cdot x\text{H}_2\text{O}$ was found to be active in dark and light-induced sacrificial systems mediating O_2 evolution in solution. Electron microscopic measurements on the $\text{RuO}_2/\text{TiO}_2$ surface showed that the active catalytic species consists of islands of $\text{RuO}_2 \cdot x\text{H}_2\text{O}$, present as agglomerates of 10-20 nm interspersed with TiO_2 particles of 200-nm diameter [188]. A disk prepared from mixtures of $\text{RuO}_2/\text{TiO}_2$ with the application of a thin (~ 9 nm) Pt film has been employed in experiments on the UV-light irradiation of H_2O . Yields of O_2 and H_2 were observed to be much greater than those observed in the absence of Pt, or compressed disks of TiO_2 or TiO_2 coated with a thin Pt film [189]. Additionally, diamagnetic metalloporphyrins have been examined as candidates to reduce electron acceptors, while macroreticular-supported viologens or photoelectrochemical cells were investigated to improve stability of relays in hydrogen evolution systems, and the efficiency of RuO_2 catalysts supported on TiO_2 have been tested [190]. It appears that complexes such as $\text{Ru}(\text{bpy})_3\text{Cl}_3$ ($\text{bpy} = 2,2'$ -bipyridine) and methyl viologen promote hydrogen evolution from aqueous suspensions of Pt/ TiO_2 , illuminated with a high-pressure Hg lamp. In the Pt/ TiO_2 -Rh($\text{bpy})_3\text{Cl}_3$ system, the hydrogen produced originates from H_2O photolysis [191]. The catalytic behavior of Pt/ TiO_2 for H_2O photolysis was examined in the presence of CO. Upon CO introduction, a large increase in hydrogen evolution was observed, and a stoichiometric ratio of H_2 and CO_2 was obtained. These results suggest that the H_2 and O_2 generated originated from the photolysis of H_2O . It was also found that a catalyst prepared from anatase and treated with hydrogen at 973K was more effective than those pretreated at 773K and 1123K [192].

The formation of H_2 by the action of H_2O on SMSI (strong metal-support interaction) catalysts (e.g., Rh/ TiO_2 , Pt/ TiO_2 , Ni/ TiO_2) has been examined using a pulsed chromatographic system. The results were interpreted in terms of the reaction of H_2O with anionic vacancies created during the high-temperature hydrogen treatment of the catalyst [193].

The activities of various metal/ TiO_2 catalysts, with or without pretreatment with air or hydrogen, have been compared for the photocatalytic (UV-irradiation) hydroxylation of C_6H_6 and the dehydrogenation of 2-propanol

[194]. The photocatalytic reduction (86%) of dichromate ($\text{Cr}_2\text{O}_7^{2-}$) in acid solutions occurs in the presence of a catalyst containing TiO_2 (99.7), platinum black (0.2), and Cr_2O_3 (0.1%) [195].

Electron transfer from the UV-illuminated support (TiO_2) to the metal (Pt) was performed on powdered samples of Pt/ TiO_2 (anatase), containing 0.05–10% Pt and homodispersed particles was investigated by photoconductivity methods [196]. Increasing the Pt content above 4% and attenuation of the UV light flux resulted in a decreased photoconductance of TiO_2 at equilibrium under vacuum. The results were explained in terms of electron transfer from TiO_2 to Pt. In the presence of H_2 , the Pt deposits decreased the resistance of TiO_2 , owing to the migration of adsorbed H atoms from Pt to TiO_2 to form OH^- ions and to release electrons [196]. The effectiveness of powdered semiconductor materials, namely Pt/ TiO_2 , in photolysing candidate redox reactions was examined. Differential pulse polarography was used to determine the extent of the photocatalysed oxidation of cyanide [197]. At pH 4.5, the photooxidation of glucose occurs in aqueous solutions containing suspended platinized TiO_2 (anatase) powder. The resulting gaseous products were H_2 and CO_2 in an inert atmosphere, and CO_2 in an oxygen atmosphere. Rates for hydrogen evolution were found to decrease with time. Isotopic experiments incorporating D_2O supported the occurrence of conventional hydrogen evolution without glucose involvement [198]. A quantitative determination of the products in the gaseous phase formed in the photocatalytic decomposition of acetic acid/acetate mixtures on Pt/ TiO_2 has appeared; the species in solution were determined qualitatively. The relative yield of ethane/methane was high at high decomposition rates, and the CO_2 yield usually exceeded that of the methyl radical consumed in the formation of methane and ethane. Excess CO_2 production may be attributed, at least in part, to the oxidation of the $\text{CH}_3\text{CH}_2\text{OH}$ and CH_3COH produced in solution [199].

Solids containing Fe^{3+} ions in the TiO_2 lattice are catalytically active for the photoproduction (near-UV irradiation) of NH_3 , while solids containing the Fe_2TiO_5 phase appear to be inactive in this reaction [200].

(iii). Electrodes and Electrochemistry

A time-resolved coulostatic flash technique has been used to study the photoelectrochemical behavior of single-crystal n- TiO_2 electrodes in acetonitrile, in native and chemically-modified forms. A two-component response (≤ 10 ns) was ascribed to electron-hole pair separation in the space charge layer. The slower response (within 5 μs) presumably involves redox-system responsive double layer effects and/or heterogeneous electron transfer at the electrode/electrolyte interface [201]. The current-voltage characteristics of

metal/TiO₂(rutile) and electrolyte/TiO₂(rutile) barriers have been studied [202]. The following observations were made: a) the current through the electrolyte/TiO₂(rutile) barrier is limited by the charge transfer rate; b) there is an insulating rutile layer between the surface and the semiconducting (reduced) rutile which plays an important role in the charge transfer when the barrier serves as an electrochemical solar cell. These observations, along with a UPS study of the rutile surface, indicate that the states in the forbidden gap of semiconducting rutile aid the charge transfer process [202]. Hypotheses have been postulated regarding the origin and nature of the surface states present at the TiO₂(rutile) bandgap. These hypotheses were based on cyclic potentiodynamic and capacitance measurements, as well as from energy band diagrams, using this TiO₂ electrode in a photocell containing a Pt counter electrode and an SCE reference electrode in 1M Na₂SO₄ [203].

Various structural and photochemical properties of different TiO₂ samples have been determined. For example, Williams [204] has studied the properties of plasma deposited TiO₂; the photoelectrochemical behavior of mechanically polished TiO₂(rutile) single-crystal electrodes during surface etching in acid solution was also studied [205]. In the latter investigation, changes were found in the shape of the photocurrent-voltage curve and an increase in limiting photocurrent observed. The results were interpreted in terms of a model in which it is assumed that a damaged surface layer, containing a large number of recombination centers, is gradually removed by the photoelectrochemical etching process [205]. A thermodynamic and photoelectrochemical investigation of the TiO₂ electrode in fluoride-containing solutions shows an increased solubility of TiO₂ in these solutions over a narrow range of solution pH near 3.2. This is an important observation with regard to choosing optimum conditions for photoetching TiO₂ electrodes [206]. Some striking aging effects occur in TiO₂ single-crystal photoanodes which are subjected to polishing and heating to 973K in hydrogen, and exposed in the dark to alkaline solutions [207]. Photoelectrochemical conversion by polycrystalline TiO₂ electrodes is observed to be affected by applied voltage, oxidized TiO₂ thickness, and temperature and concentration of the photoelectrochemical cell [208]. A cathodic pretreatment of thermic TiO₂ apparently increases the photoresponse of TiO₂ under UV illumination in chloride ion media. The duration of pretreatment and the nature of the acidic medium used affect the photocurrent increase [209]. The applicability to an analysis of the photoelectrochemical process on TiO₂ has been verified with equations relating the photocurrent quantum yield to the potential drop in the space-charge layer of the semiconductor [210]. By measuring the potential of the photocurrent onset (referred to as flatband), it was possible to determine the exchange or reference current density of

photoelectrochemical processes with minority carriers on semiconductor electrodes (TiO_2 , GaP, GaAs, InP, Fe_2O_3) [211].

A study of the field effect on the catalytic activity of thin TiO_2 or ZnO films, supported on Pyrex glass, reveals a reversible reaction of Na atoms with TiO_2 (or ZnO) upon application of an external electric field [212]. Electrochemical methods were employed to effect an electrophoretic codeposition of dimethylaminoethyl methacrylate-ethyl acrylate-methyl methacrylate copolymer with TiO_2 , $\alpha\text{-Fe}_2\text{O}_3$ or Al_2O_3 powders. The data demonstrate that the powders are adsorbed by the copolymer and possess the same electrophoretic mobility and coagulation behavior as the copolymer at the cathode surface [213].

Photo- and electro-luminescence spectra of an n-type TiO_2 electrode in aqueous solutions have been recorded as functions of the electrode potential and the solution pH, together with the current-potential curves. The photoluminescence spectra exhibit a relatively sharp band at 1.47eV which, from photoluminescence quenching experiments, was thought to arise from an oxidative surface species, $X_{1.47}$, acting as an intermediate in the photooxidation reaction of water. The $X_{1.47}$ species was assigned to a kind of $\text{OH}\cdot$ radical surface adduct, based on a comparison of electroluminescence spectra in H_2O_2 and $\text{S}_2\text{O}_8^{2-}$ solutions [214]. The illumination of a TiO_2 anode at 0.5V (vs $\text{Ag}/0.1\text{M AgNO}_3$) in acetonitrile containing an aromatic olefin causes a photocurrent flow and photocatalysed oxygenation of the olefin. The olefin oxidation reaction is initiated by electron transfer from the olefin to the positive hole of the excited semiconductor, followed by a radical chain reaction to yield oxygenated products. The photocurrent increases with decreasing oxidation potential of the reactant olefin [215].

Kiwi [216] has observed a pronounced magnetic field effect on a wide variety of reactions under UV and visible light illumination leading to hydrogen formation from water. This effect obtains for the heterogeneous catalytic systems a) $\text{TiO}_2/\text{RuO}_2/\text{Pt}$, b) $\text{Ru}(\text{bpy})_3^{2+}/\text{TiO}_2/\text{RuO}_2/\text{Pt}/\text{EDTA}$, and c) $\text{CdS}/\text{RuO}_2/\text{Pt}$.

The application of a moderate magnetic field leads to a variation of the fraction of radicals that interact with a heterogeneous catalyst. Also, the chemical reaction rate depends on the strength of a steady magnetic field, but is observed only under certain conditions. The deposition of RuO_2 on a single-crystal TiO_2 electrode yields a marked decrease in anodic photocurrent at potentials more positive than -0.1V vs SCE, and a considerable increase in cathodic photocurrent results at -0.3 to -0.5V in aqueous solution. RuO_2 deposited on TiO_2 plays the role of a catalyst for reductive hydrogen evolution, although it serves as a catalyst for oxygen evolution especially when strong oxidizing agents (e.g., Ag^+ , $\text{S}_2\text{O}_3^{2-}$) are present in solution or TiO_2 is not excited. The deposition of RuO_2 and/or Pt on TiO_2 accelerates the

photocatalytic hydrogen evolution from an ethanol/water (1:1) mixture [217]. The photoelectrochemical properties of thin films of RuO_2 deposited on single-crystal TiO_2 were determined. The electrodes, prepared by rf reactive sputtering, exhibit low overvoltages compared to those prepared via RuCl_3 pyrolysis [218]. The corrosion products accumulating in the electrolyte and the dissolution rate of ruthenium from the active coating of a $\text{RuO}_2/\text{TiO}_2$ anode (up to high positive potentials) in aqueous and alcoholic H_2SO_4 and perchlorate solutions were analyzed radiometrically [219].

An electron beam modification of titanium-ruthenium oxide anodes was attempted in an effort to increase service life. Catalytically active layers of mixed oxides of titanium and ruthenium were obtained by baking (673-773K) the oxychloride of ruthenium and the chloride of titanium applied to the surface of a titanium substrate. The electron beam treatment affords localization of the increased temperature in the catalyst surface layer over a short time. However, no significant increase in stability appears evident for the electrodes prepared in this manner as compared to those prepared by a heat treatment method [220]. Optical, x-ray, electron spectroscopy and measurements of electrophysical principles were examined of some characteristics of the electronic structure of an active coating of titanium oxide-ruthenium oxide anodes, solid solutions of $\text{Ru}_x\text{Ti}_{1-x}\text{O}_2$. At $x < 0.25$, lengthy clusters exist which have metallic properties; at $x > 0.25$, the clusters unite into an infinite cluster [221].

Andreev and Kazarinov [222] have reviewed the adsorption properties of $\text{RuO}_2/\text{TiO}_2$ electrodes. They have also reported the use of a technique involving radioactive indicators to study the adsorption of organic compounds on $\text{RuO}_2/\text{TiO}_2$ and Pt/TiO_2 electrodes at high potentials [223].

The use of $\text{RuO}_2/\text{TiO}_2$ anodes in electrolytic processes is limited to the potential range $E \leq 1.4\text{--}1.6\text{V}$ in aqueous solutions. Upon polarization to higher E values, a rapid potential growth with respect to time occurs, along with shutting off of the electrode, an increase in the dissolution rate of ruthenium, and complete destruction of the active material. Polarization of $\text{RuO}_2/\text{TiO}_2$ anodes was also carried out in methanol, aqueous methanol solutions of acetic acid and monoesters of dicarboxylic acids [224]. The principal electrochemical characteristics of $\text{RuO}_2/\text{TiO}_2$ anodes are the evolution potential of chlorine during operating current density values $\leq 1 \text{ A}\cdot\text{cm}^{-2}$, and wear resistance. A method has been proposed by Ignat'ev and Parshikov [225] for experimentally determining the correction to the ohmic resistance in studies of the electrochemical kinetics in an electrolyte (e.g., NaCl) without substantial complications arising from the instrument.

The preparation and characterization of a new electrode, $\text{Ti}/\text{PtO}_x\cdot\text{TiO}_2$, has

been reported. Its electrochemical behavior in dilute HCl was studied as a function of the relative compositions of both oxides, which were thermally deposited at various temperatures. A maximum catalytic activity obtains for chlorine evolution at a $\text{PtO}_x/\text{TiO}_2$ ratio of 10:1 [226]. A series of platinized TiO_2 (Pt/TiO_2) film electrodes were prepared and examined for use in light-induced reactions. The chemical shift of the Pt electron binding energy has been related to the electron transfer to the Pt atom and the possible effect on the catalytic properties of the Pt/TiO_2 electrodes [227]. TiO_2 , Pt/TiO_2 , and Pt/Pt anodes were investigated in acidic and basic electrolyte solutions in the presence of ethanol. For macroscopic Pt/TiO_2 anodes, the oxidation of EtOH to MeCHO and further oxidation to AcOH was predominantly catalytic, rather than photocatalytic; catalysis was accomplished in the dark with a bias voltage of $\sim 0.6\text{V}$. Cyclic voltammetric studies have suggested that oxidation of AcOH requires the production of the highly reactive $\text{OH}\cdot$ species. Both catalytic and photocatalytic processes occur simultaneously at illuminated Pt/TiO_2 anodes [228]. The decrease in cathodic overvoltages by platinization of TiO_2 single crystals was investigated for the dark reductions of Ce^{4+} , Fe^{3+} , oxygen and H^+ as a function of the thickness of the Pt overlayers both for a well-etched TiO_2 substrate and for a mechanically damaged one. The observed improvements upon platinization apparently occur in two modes: a) one mode is related to the high electrocatalytic activities of Pt and is observed for reduction of oxygen and evolution of hydrogen when the TiO_2 electrodes are loaded with a 3 Å-thick Pt layer; b) the other mode results from enhancement of probabilities of electron exchange between the electrode and electrolyte species caused by platinization. This latter mode is observed for the reductions of Ce^{4+} , Fe^{3+} and oxygen when etched TiO_2 is loaded with a Pt layer thickness of > 100 Å or the damaged TiO_2 loaded with a greater than 10 Å-thick Pt layer. Action spectra of anodic photocurrents were suggestive of new electronic levels being created by platinization [229]. Variations of the photocatalytic hydrogen production from primary aliphatic alcohols (e.g., MeOH, PrOH) as a function of the Pt content (0.05-10%) of the Pt/TiO_2 catalysts were investigated by Pichat and coworkers [230]. The maximum reaction rate was tentatively attributed to an optimum attraction of the free TiO_2 electrons by the Pt crystallites, which corresponds to an optimum ratio of the acidic and basic sites involved in the abstraction of H atoms from the alcohol on TiO_2 . At 313K (the temperature of the maximum reaction rate), the reaction of photogenerated holes with adsorbed alkoxide ions was thought to be rate-determining. At lower temperatures, the rate of hydrogen desorption seems to play an important role [230].

The electrochemical behavior of TiO_2 electrodes with silver and palladium particles deposited on their surfaces has been characterized. Two different

deposition methods were employed: a) photocatalytic, and b) cathodic polarization of the electrode in a solution containing Ag^+ or PdCl_4^{2-} . For the anodic oxidation of HCHO , the effectiveness of the photocatalytic preparative method was somewhat higher than on TiO_2 electrodes with cathodically deposited metal particles. The metal particles deposited by different methods contacting portions of the TiO_2 surface have different structures of the space-charge region as well as significantly different areas of contact of $\text{TiO}_2/\text{metal}$ [231]. Silver particles deposited on the TiO_2 film electrodes were employed for the anodic oxidation of the reducing agents HCHO , BH_4^- , and H_2PO_2^- [232]. The effect of TiO_2 surface modification by silver particle deposition on the nature of the change in potential of the TiO_2 electrode during exposure to light, and on the relaxation of the photopotential of the electrodes after the light was shut off, was investigated. The observed differences in the behavior of modified and non-modified electrodes was related to the differences in the structure of the oxide film electrode, as well as to the direct participation of Ag microelectrodes, included in the TiO_2 film electrodes [233]. The $\text{TiO}_2(\text{Ag})-\text{Ag}^+$ half cell can be photochemically charged via irradiation of the TiO_2 surface with sunlight. Electrical energy was extracted from the half cell by connection through the load with a suitable half cell which has an electrode potential more positive than Ag/Ag^+ [234].

The cathodic reduction of metal ions (PdCl_2 , H_2PtCl_4 , $\text{Pb}(\text{OAc})_2$ and the sulfates of Cu, Ag, Sn, Cd, Ni) on TiO_2 film electrodes was characterized by Strel'tsov and coworkers [235]. Photocurrent-potential curves in aqueous solutions were obtained for a TiO_2 electrode coated with a thin gold or palladium film. When the metal-coated TiO_2 electrode is illuminated under anodic potentials, the potential of the metal film shifts toward the positive until it reaches the oxygen evolution potential at the metal, with little change in the surface band energies of the TiO_2 electrode. This would imply that the height of the Schottky barrier at the metal/ TiO_2 contact is considerably increased by illumination, and the photovoltage obtained is much larger than expected from the barrier height in the dark [236]. TiO_2 -Ni composite electrodes, prepared by the dispersion plating method, were compared with single-crystal TiO_2 electrodes prepared in propylene carbonate solution. The composite electrodes exhibit a higher photopotential and a nonlinear Mott-Schottky plot, in comparison to the TiO_2 electrodes [237].

A mechanism for the sensitization of single-crystal TiO_2 photoanodes by cation doping (Cr, Mn, Ga) has been proposed by Kovach et al. [238]. The mechanism was based on the determination of the efficiencies of photo-electrochemical cells containing these photoanodes. Studies were carried out with sintered disks of pure Fe_2O_3 and Fe_2O_3 doped with TiO_2 , SnO_2 , ZrO_2 and

Ta_2O_5 for the photoassisted electrolysis of water. The flatband potential, the saturation current and the minority charge carrier diffusion length are higher for TiO_2 -doped Fe_2O_3 samples than for other doped specimens. The results were interpreted in terms of depletion layer theory [239]. Characteristics of a $\text{TiO}_2/\text{PbO}_2$ anode with a titanium base were examined as a potential anode for the electrochemical purification of drinking water and wastewater. Compared with a RuO_2 anode, the $\text{TiO}_2/\text{PbO}_2$ anode allows for the use of a higher current density, which can lead to an increase in the productivity of the equipment [240]. Optically transparent layers of TiO_2 and SnO_2 were deposited on Vycor glass plates via chemical vapor deposition using $\text{Ti}(\text{PrO}^i)_4$ and SnCl_4 . The TiO_2 -covered plates were vacuum heated to convert the oxide layer into a semiconductor material. The TiO_2 layer alone is highly resistant to the passage of electricity, and thus the SnO_2 -covered plates were employed for electrochemical studies. Additionally, the SnO_2 -covered plates showed no photoanodic current upon UV illumination, though TiO_2 on SnO_2 -covered plates exhibits significant photoanodic current. The coulombic efficiency for the formation of persulfate is about three-fold higher for TiO_2 on SnO_2 -covered plates than for plates with SnO_2 alone. The efficiency increases slightly upon illumination, for TiO_2 on SnO_2 -covered plates [241].

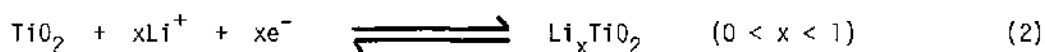
Using a number of methods, the characteristics of the formation, phase composition, anodic behavior and photoelectrochemical activity (under chlorine evolution conditions) have been studied for pyrolytic film coatings of Co_3O_4 on titanium, $\text{Ti}/\text{TiO}_x/\text{Co}_3\text{O}_4$ [242]. Vasilevskaya and coworkers [243] have reported on the photopotential relaxation and photoimaging memory effect in a $\text{Ti}/\text{SiO}_2/\text{TiO}_2$ film system. The presence of a SiO_2 layer (5 μm) separating the TiO_2 film and the titanium support results in a decreased photopotential and a slower potential relaxation process.

The photoelectrochromic characteristics of thin Prussian blue films on both single-crystal and polycrystalline TiO_2 electrodes have been described. The Prussian blue films were galvanostatically deposited under cathodic conditions in a 0.02M FeCl_3 /0.02M $\text{K}_3\text{Fe}(\text{CN})_6$ solution, rinsed with distilled water and placed in 1M KCl (Ph 3.45) where all electrochemical measurements were conducted [244]. The TiO_2 and SnO_2 semiconductor electrodes have been covalently modified via attachment of functionalized olefins and arenes by surface silanation or by a cyanuric chloride linkage. Photocurrent measurements and time-resolved laser coulometric monitoring were employed to elucidate the mechanism of charge injection on these modified surfaces [245].

(iv). Applications

Titanium dioxide is employed in a wide variety of industrial applications, including its use as a dielectric coating, as an electrode in an electrochromic display, in photoimaging, pyrotechnics, pigments and in the catalysis of hydrodesulfurization.

The temperature dependence of laser strength of TiO_2 dielectric coatings in various gases was measured to determine the effect of water molecule adsorption at $\lambda = 1.06 \mu$ [246]. An electrochromic display incorporating a TiO_2 (anatase)- In_2O_3 -coated glass electrode was examined. Upon application of negative and positive voltage bias to the electrode, the coloration and bleaching phenomena were alternately observed by the electrochemical reversible reaction (2) [247].



The photographic activity of TiO_2 -based photosensitive materials relative to physical development with Cu-based physical developers was dependent on the preparative conditions of the samples and the developer composition. A maximum photosensitivity for TiO_2 -based layers was attained using a copper physical developer containing ascorbic acid as the reducing agent [248]. The introduction of Pd^{2+} into a TiO_2 -based photoimaging layer leads to an observed increase in layer-sensitivity [249]. Photoimaging properties of Pd-containing TiO_2 layers under nickel development depend on Pd concentration, TiO_2 preparation conditions, and developer composition [250]. Additionally, the role of silver ions adsorbed onto the TiO_2 layers has been examined [251].

Thin films of TiO_2 serve as adhesion promoters for photoresists [252]. TiO_2 films grown on Ti foils anodically under galvanostatic conditions in saturated aqueous solutions of ammoniumtetraborate were studied by Auger electron spectroscopy in an effort to understand the ignition mechanism of pyrotechnics containing Ti or TiH_x [253]. EPR spectra of TiO_2 pigments reveal five types of paramagnetic centers [254].

The effects on the catalytic activity of a TiO_2 -promoted hydrodesulfurization catalyst ($\text{Co-Mo}/\gamma\text{-Al}_2\text{O}_3$) were determined for hydrotreating of gas oil-range distillates [255]. Anatase, present in ash from bituminous coal, appears to have a poisoning effect on the Co-Mo catalyst for the liquefaction of coal [256].

d. Mixed Metal Oxide Systems

(i). SrTiO_3

Strontium titanate is produced at 1473K upon heating an equimolar mixture of $\text{SrC}_2\text{O}_4 \cdot n\text{H}_2\text{O}$ and TiO_2 in an inert gas [257]. The progressive reduction of Mn-doped SrTiO_3 has been monitored by EPR, revealing the conversion of Mn^{4+} to Mn^{2+} and Mn^{2+} to $\text{Mn}^{2+}-V_O$ by oxygen-vacancy capture [258].

A study of the electronic characteristics and photoelectrochemical activity of extrinsic ceramic SrTiO_3 and TiO_2 has appeared [259]. Salvador and Gutierrez [260] have studied the electroreduction of dissolved and/or photogenerated oxygen and H_2O_2 at the polycrystalline n- SrTiO_3 -electrolyte interface. Both reactions occur at potentials positive of the flatband potential. Oxygen is mainly reduced to water in a four-electron reaction, while H_2O_2 is strongly adsorbed. Evidence that H_2O_2 is photogenerated in an intermediate step of the water splitting reaction was given [260]. Strontium titanate has been used successfully in photocatalytic systems for the decomposition of water, most often mixed with some other component. The photodecomposition ($\lambda > 300 \text{ nm}$) of $\text{S}_2\text{O}_8^{2-}$ to SO_4^{2-} with concomitant oxidation of H_2O to O_2 over n- SrTiO_3 powder mixed with LaCrO_3 has been shown to proceed more rapidly than either the photochemical decomposition of $\text{S}_2\text{O}_8^{2-}$ in water or the thermal reaction with or without the SrTiO_3 - LaCrO_3 powders under the same conditions [261]. The rate of the photocatalytic decomposition of liquid water on NiO- SrTiO_3 catalysts increases considerably when an improvement in pretreatment conditions and the use of a concentrated NaOH solution are employed [262]. Rhodium-loaded SrTiO_3 catalysts have been prepared by thermal deposition and studied by XPS to characterize the surface deposits. The Rh/ SrTiO_3 system was employed in the photochemical decomposition of H_2O as a catalyst [263].

The effect of various dopants on the behavior of single-crystal SrTiO_3 electrodes in a photoelectrochemical cell for water decomposition has been studied. The electrode surface was doped with $\text{Sr}_3\text{MnNb}_2\text{O}_9$ ($\text{M}^{2+} = \text{Mn, Fe, Co, Ni}$) and LaMO_3 ($\text{M}^{3+} = \text{V, Cr, Mn, Fe, Co, Rh}$). The results were compared with those for the sensitization of single-crystal SrTiO_3 photoanodes homogeneously doped with LaCrO_3 or Cr, Mn, Fe, Co, Ni, Nb, Mo, Ta and W oxides. Response to visible light is greatest for Cr^{3+} , decreasing in the sequence Co^{2+} , Ni^{2+} , Mn^{2+} , Rh^{3+} . The dopant ions V^{3+} , Mn^{3+} , Fe^{2+} , Fe^{3+} , Co^{3+} and the Nb, Mo, Ta and W oxides reveal a very small, if any, photosensitization [264]. An improved performance in the photooxidation of H_2O has been observed using a Cr-doped SrTiO_3 photoanode coated with RuO_2 . The results were interpreted in terms of a two-interface model [265]. Various properties of the electrical contacts between catalytically active metals (e.g., Pt, Rh, Ru) and semiconductors (e.g.,

SrTiO_3 , TiO_2) have been measured in air and in hydrogen to ascertain their behavior in water photolysis systems. Barrier heights at the Schottky junctions were determined, and provide an explanation for hydrogen evolution [266].

The reduction of CO_2 to give HCOOH , HCHO , CH_3OH , CH_3COH and EtOH has been investigated under electrolytic as well as photoassisted conditions. Cyclic voltammograms were recorded in the dark under cathodic polarization at crystalline $n\text{-SrTiO}_3$, $n\text{-SrTiO}_3/\text{TiO}_2/\text{RuO}_2$, $n\text{-SrTiO}_3/\text{TiO}_2/\text{PtO}_2$ and $n\text{-SrTiO}_3/\text{TiO}_2/\text{Rh}_2\text{O}_3$ electrodes in various electrolytic media. This study demonstrates the possible competition between the reduction of H_2O and the reduction of either CO_2 or HCOOH [267]. The photoassisted reduction of CO_2 has been carried out in the presence of SrTiO_3 powder, surface treated with various transition metal oxide additives [268, 269] or doped with LaCrO_3 [269]. Low optical to chemical conversion efficiencies (ca. 0.03%) were due to the reoxidation of the reduction products into CO_2 . Furthermore, it was established that the apparent reduction of CO_2 preceding the hydrogen evolution is due to pH effects at the electrode-solution interface, with water reduction being more favorable than CO_2 reduction [269].

(ii). $\text{A}_x\text{Ti}_y\text{O}_z$

Topotactic insertion of lithium into TiO_2 (anatase) results in the formation of Li_xTiO_2 with the maximum stoichiometry at $x = 0.7$. The system is two-phase in the region $0 \leq x \leq 0.5$. The spinel LiTi_2O_4 was prepared thermally from $\text{Li}_{0.5}\text{TiO}_2$, and further uptake of Li yields $\text{Li}_2\text{Ti}_2\text{O}_4$ [270].

Sodium-ordered Na_xTiO_2 is transformed into its disordered form via a new ordered form, though it may transform directly into the disordered form in the vicinity of domain boundaries [271]. New phases with the formula Na_xTiO_2 have been obtained from electrochemical de-intercalation of sodium from the lamellar oxide NaTiO_2 [272]. $\text{Na}_2\text{Ti}_3\text{O}_7$ and $\text{K}_2\text{Ti}_4\text{O}_9$ form layered lattices of titanium-oxygen octahedra, in which the interlayered regions are occupied by the alkali metals. In HCl solutions, exchange of the alkali metals for protons results in the production of $\text{H}_2\text{Ti}_3\text{O}_7$ and $\text{H}_2\text{Ti}_4\text{O}_9 \cdot \text{H}_2\text{O}$. The dehydration of $\text{H}_2\text{Ti}_4\text{O}_9 \cdot \text{H}_2\text{O}$ yields $\text{H}_2\text{Ti}_8\text{O}_{17}$ with a channel-type framework [273].

The incorporation and reducibility of Ni^{2+} in the MgTiO_3 ilmenite-type structure to form $\text{Ni}_x\text{Mg}_{1-x}\text{TiO}_3$ ($x \leq 0.20$) was studied employing x-ray diffraction, reflectance and ESR spectroscopy, magnetic susceptibility and thermogravimetric analyses. The incorporation of Ni^{2+} causes a small decrease in the MgTiO_3 unit cell volume. Segregation of metallic nickel and TiO_2 occurs upon reduction of Ni^{2+} in hydrogen (973K) in $\text{Ni}_x\text{Mg}_{1-x}\text{TiO}_3$ solid solutions. At

higher temperatures, MgTi_2O_5 forms via reaction of TiO_2 with MgTiO_3 [274]. A Raman spectroscopic study of single crystals of the one-dimensional superionic conductors $\text{K}_{1.6}\text{Mg}_{0.8}\text{Ti}_{7.2}\text{O}_{16}$ and $\text{K}_{1.6}\text{Al}_{1.6}\text{Ti}_{6.4}\text{O}_6$ reveals similar features for the two compounds [275]. The orthorhombic $\text{KTi}_6\text{Nb}_5\text{O}_{25}$ has been shown (by x-ray diffraction) to be a member of a chemically twinned rutile series $(\text{AM}_3\text{O}_9)(\text{M}_2\text{O}_4)_n$ as is $\text{KTi}_2\text{Ta}_5\text{O}_{17}$ [276]. The structure of the rhombohedral compound $\text{Ca}_2\text{Zn}_4\text{Ti}_{16}\text{O}_{38}$ has been determined crystallographically, and shown to be isostructural with crichtonite-group minerals ($\text{AM}_{21}\text{O}_{38}$). That is, the structure is based on a nine-layer ('hhc') close-packed anion framework [277]. The A_xNbO_3 ($\text{A} = \text{Ca}, \text{Sr}, \text{Eu}$) and A_xTiO_3 ($\text{A} = \text{K}, \text{Rb}, \text{Cs}, \text{La}, \text{Ce}, \text{Md}, \text{Sm}$) bronzes have been prepared, and their crystal structures, and electronic and magnetic properties determined [278].

The doping of VO_2 with Ti leads to the appearance of a new phase (M2). Changes in electrical resistance, entropy, x-ray reflection and magnetic susceptibility at the transition were measured [279]. Quaternary phase diagrams have been constructed and confirmed by chemical analyses for the systems A-Fe-Ti-O ($\text{A} = \text{Mn}, \text{Co}$) [280]. X-ray diffraction and Moessbauer spectroscopy show the behavior of monoclinic Fe_2TiO_5 and hollandite-type $\text{K}_{1.45}\text{Fe}_{1.45}\text{Ti}_{6.55}\text{O}_{16}$ in a flux environment ($\text{K}_2\text{O}, \text{V}_2\text{O}_5, \text{SiO}_2$) [281]. When a suspension of $\text{Fe}(\text{OH})_2$ containing a metal ion A (e.g., $\text{Ti}^{4+}, \text{Cr}^{3+}, \text{Zn}^{2+}$) is oxidized by air (or NO_3^-) at pH 7-12 and 338 or 353K, a ferrite compound which contains A at the lattice point is obtained. Almost all Ti^{4+} and Zn^{2+} in the reaction suspension are incorporated into the ferrite [282].

Phase equilibria and thermodynamic behavior in Ti-Ni and Ti-Ni-O systems have been investigated [283]. Specifically, the isothermal section of the Ti-Ni-O system at 1200K was examined in the region between Ni(Ti) solid solution and the binary oxides of Ti. An infrared spectroscopic study of non-stoichiometric Ti-doped $\text{Co}_{3-x}\text{O}_4$ pyrolytic films reveals the dopant to be localized predominantly in interstitial positions of the octahedral sublattice where the intrinsic structural defects and cationic vacancies are also localized. For $\lesssim 3\%$ (at.) Ti, a $\text{Co}_{3-x}\text{O}_4$ - TiO_2 solid solution is observed [284].

Vanadium(V) ions have been incorporated into the octahedral sites of the cubic perovskite $\text{Sr}_{0.75}\text{Ti}_{0.25}\text{V}_{0.5}\text{O}_3$ by heating stoichiometric amounts of TiO_2 , NH_4VO_3 and $\text{Sr}(\text{OH})_2$ [285]. A chemical-transport reaction technique was used to prepare good-quality single crystals of $\text{Nb}_x\text{Ti}_{1-x}\text{O}_2$ ($0 \leq x \leq 0.005$) with a rutile-type structure [286]. A Raman spectroscopic study of TiNb_2O_7 , prepared by a liquid mix method, is in good agreement with previous x-ray and neutron diffraction results. An octahedral coordination for both Ti and Nb, and the presence of NbO_4 tetrahedra in small concentrations, was proposed [287]. A photoelectrochemical study of the ceramic alloys $(\text{Ti}, \text{Nb})\text{O}_2$ and $(\text{Ti}, \text{V})\text{O}_2$ has

revealed an n-type electrical conductivity for the entire composition range. Energy gaps, flatband potentials, quantum efficiencies and photocurrents were also determined [288]. The syntheses and infrared spectra of ATiNbO_6 ($A = \text{Y, Ce}$), $\text{A}'\text{Nb}_2\text{O}_6$ ($A' = \text{Ca, Pb}$), ANbO_4 , $\text{A}''\text{TiO}_3$ ($A'' = \text{Mg, Zn, Pb}$) and ThTi_2O_6 have been reported by Shabalín [289]. The preparation involves calcination of the coprecipitated metal hydroxides. The infrared spectra reveal definite configurations and definite position of the valence vibrations maxima, which can be related to the valence of the element and their coordination in the compound.

High resolution electron microscopy revealed the structural images of crystallized BaTiO_3 thin films prepared by vacuum deposition on NaCl cleavage faces. The comparison of experimental images with those computed by multislice methods provided direct information on atomic arrangement, and showed the possibility of finding atomic displacement in ferroelectric BaTiO_3 [290]. A study of the mechanism of carbon monoxide oxidation over BaTiO_3 has been reported by Rozentuller *et al.* [291]. Barium titanate insulating layers have been successfully incorporated into ZnS:Mn a.c. thin-film electroluminescent devices. The advantages of using BaTiO_3 (vs Al_2O_3) include reduced operating voltage and the consequent larger safety margin between operating voltage and device breakdown voltage [292]. The first stacking polytype with a rhombohedral 21-layer structure, $\text{Ba}_7\text{Nb}_4\text{Ti}_2\text{O}_{21}$, has been synthesized by heating (1473K) a $\text{BaCO}_3\text{-Nb}_2\text{O}_5\text{-TiO}_2$ mixture in air [293]. The solid solution perovskites $\text{BaSn}_{1-x}\text{M}_x\text{O}_3$ ($M = \text{Ti, Zr, Hf}$) were prepared via solid state reaction at 1573-1673K. The compounds were characterized by x-ray diffractometry at room temperature [294].

An examination of the infrared and Raman spectra of polycrystalline TiTa_2O_7 at room temperature revealed no systematic coincidences in frequency, indicative that TiTa_2O_7 crystallizes with an inversion of symmetry. High-frequency Raman bands were assigned to corner- and edge-shared octahedra, while the band at 1020 cm^{-1} was ascribed to the presence of a short cation-oxygen distance [295]. Electrical resistivity and magnetic susceptibility measurements reveal the collective behavior of the Ti^{3+} d electrons in $\text{Ln}_{(2/3+x)}\text{TiO}_{3+y}$ ($\text{Ln} = \text{La, Ce, Sm, Nd}$; $0 \leq x \leq 1/3$) [296]. X-ray diffraction, thermography, crystalloptical and chemical analysis methods were used to characterize the crystallization of rare earth element titanates in $\text{K}_2\text{O-Nd}_2\text{O}_3(\text{Yb}_2\text{O}_3)\text{-TiO}_2\text{-H}_2\text{O}$ at 553K. The Nd_2O_3 system contains $\text{Nd}_2\text{Ti}_2\text{O}_7$ and $0.5\text{ K}_2\text{O}\cdot\text{Nd}_2\text{O}_3\cdot 3\text{TiO}_2$, while the Yb_2O_3 system contains $\text{Yb}_2\text{O}_3\cdot\text{TiO}_2\cdot n\text{H}_2\text{O}$, $\text{Yb}_2\text{Ti}_2\text{O}_7$ and $\text{K}_2\text{Ti}_6\text{O}_{13}$ [297, 298].

The initial oxidation product of LnTiO_3 ($\text{Ln} = \text{Sm, Eu, Gd}$) in air at 673-873K is x-ray amorphous $\text{Ln}_2\text{Ti}_2\text{O}_7$. At 873-973K amorphous $\text{Ln}_2\text{Ti}_2\text{O}_7$ crystallizes

with the metastable monoclinic $\text{Ca}_2\text{Nb}_2\text{O}_7$ -type structure. At 973-1123K, $\text{Gd}_2\text{Ti}_2\text{O}_7$ exists as perovskite-type and cubic-pyrochlore-type phases. At >1123K, $\text{Ln}_2\text{Ti}_2\text{O}_7$ exists irreversibly in the pyrochlore phase [299]. The $\text{Ln}_2\text{Ti}_2\text{O}_7$ (Ln = Pr - Lu) dititanates are prepared using a hydrothermal technique and characterized by x-ray diffraction. For $\text{Ln}_2\text{Ti}_2\text{O}_7$ (Ln = Sm, Eu, Gd) prepared in this manner, a perovskite structure is indicated; whereas a pyrochlore structure is assigned to those prepared by the solid-state method [300].

Various compounds with formulae $\text{LaCo}_{1-x}\text{Ti}_x\text{O}_3$ and $\text{La}_{1-x}\text{Sr}_x\text{Co}_{1-x}\text{Ti}_x\text{O}_3$ have been prepared and their electron transport and magnetic behavior investigated. Itinerant electron ferromagnetism is not observed, unlike what is observed in $\text{La}_{1-x}\text{Sr}_x\text{CoO}_3$. Electron transport is discussed in view of the presence of different Co valence states and changes in crystal field splitting [301].

Sidorova and coworkers [302, 303] have prepared and examined various compounds in the $\text{SrO-Ln}_2\text{O}_3\text{-TiO}_2$ system. The compounds, including $\text{SrLn}_2\text{Ti}_3\text{O}_{10}$ (Ln = La, Pr, Nd) and $\text{SrLn}_2\text{Ti}_4\text{O}_{12}$, were characterized by x-ray diffraction and infrared spectroscopy [302]. Infrared and Raman spectroscopy were also used to examine the compounds $\text{SrLa}_2\text{Ti}_2\text{O}_8$, $\text{SrLn}_2\text{Ti}_3\text{O}_{10}$ and $\text{Sr}_{0.5}\text{LnTiO}_6$ (Ln = La, Pr, Nd). All three compounds are characterized by the presence of a titanium polyhedron with coordination numbers of 4 and 6, while the rare earth elements and Sr have coordinated polyhedra with coordination numbers of 8-12 [303]. The lattice parameters of the compounds A_2MgTiO_6 (A = La, Nd, Sm - Yb) have been determined [304].

Diffuse reflectance measurements were obtained to determine the influence of MnO_2 and La_2O_3 addition on the band structure of polycrystalline PbTiO_3 and PbZrO_3 solid solutions [305]. The new layered-type compounds $\text{PbBi}_2\text{TiTaO}_8\text{F}$, $\text{PbBi}_2\text{TiNbO}_8\text{F}$, $\text{Bi}_5\text{Ti}_2\text{WO}_{14}\text{F}$ and $\text{Bi}_7\text{Ti}_5\text{O}_{20}\text{F}$ have been synthesized and identified by x-ray diffractometry [306]. The intergrowths and defect structures in the perovskite $\text{Bi}_9\text{Ti}_3\text{Fe}_5\text{O}_{27}$ were revealed by high-resolution electron microscopy, and the chemical implications of these observations discussed by Smith and Hutchison [307]. Dilatometric and x-ray structural studies of the binary sections $\text{BiVO}_4\text{-TiO}_2$, $\text{Bi}_4\text{Ti}_3\text{O}_{12}\text{-V}_2\text{O}_5$, $\text{Bi}_4\text{Ti}_3\text{O}_{12}\text{-BiVO}_4$, $\text{BiVO}_4\text{-Bi}_2\text{Ti}_4\text{O}_{11}$, and $\text{BiVO}_4\text{-Bi}_8\text{TiO}_{14}$ revealed the existence of $\text{Bi}_3\text{V}_5\text{TiO}_{34}$ and limited solid solutions based on BiVO_4 [308].

e. Vanadium/Titanium oxide Catalysts

A recent EXAFS study of $\text{V}_2\text{O}_5\text{-TiO}_2$ catalysts has suggested a model for these catalysts which consists of molecular species with two double-bond and two single-bond oxygen ligands bound to the TiO_2 support surface. The structure observed is not similar to that of V_2O_5 . With the extremely high degree of

disorder present, it would seem clear that any importance of crystal epitaxy need not be considered when constructing a structural model [309].

Several investigations have been carried out for the oxidation of *o*-xylene catalyzed by vanadium/titanium oxide catalysts. Bond and Konig [310] have shown that hydroxyl groups on the surface of TiO_2 (anatase) react with VOCl_3 vapor at room temperature to yield a partial monolayer of a vanadium species which, after heating to 670K, is active for the oxidation of *o*-xylene. A model was proposed [310] for which chemisorbed oxygen atoms doubly bonded to V^{5+} ions are the oxidizing species. If, from a single methyl group at an uncovered site, *o*-xylene adsorbs by dissociation of a hydrogen atom, further oxidation to phthalic anhydride proceeds smoothly. Studies of the dependence of catalytic activity on the surface layer composition [311, 312], calcination temperatures [312] and the addition of promoters [313] in the oxidation of *o*-xylene have revealed that : a) a decisive role is played by the content and reactivity of V_2O_5 ; b) optimum activity is achieved at <773K and V_2O_5 concentrations at the contact mass vary from 5-25 mole percent; and that c) the addition of alkali metal oxides or TeO_2 stabilize the oxidized form of V and lower the surface acidity. A study of the comparative reactivity of some *p*-derivatives of toluene (*p*- $\text{MeC}_6\text{H}_4\text{R}$; R = H, Me, CMe_3 , F, Cl) under oxidative ammonolysis conditions on a V_2O_5 - TiO_2 catalyst has shown that the compounds for which R = Me, CMe_3 , F, Cl are all more reactive than *p*- $\text{MeC}_6\text{H}_4(\text{H})$, and the main product observed is the benzonitrile derivative [314].

The V_2O_5 - TiO_2 catalyst has been shown to be active for the reduction of NO with NH_3 . The changes in oxidation state by the reaction of vanadium supported on TiO_2 and TiO_2 -coated SiO_2 were followed by ESR techniques. The V^{5+} is reduced by NO- NH_3 to V^{4+} , which is reoxidized by oxygen to V^{5+} [315]. Fujimoto and Shikada [316] have regenerated (70-90%) V_2O_5 - TiO_2 catalysts for NO reduction which had been poisoned by potassium salts. The method involves catalyst calcination in air to oxidize all the vanadium species to V^{5+} , followed by treatment with a $\text{Na}_2\text{SO}_4/(\text{NH}_4)_2\text{SO}_4$ solution to remove 97-98% of the potassium salts. The V_2O_5 - TiO_2 catalyst was prepared with hydroxylates from titanium tetra-*tert*-amyloxyde and vanadium tetra-*tert*-amyloxyde solutions (89 ppm - 10% V_2O_5). The activity of the thus-prepared catalyst has been examined for the NO- NH_3 - O_2 reaction [317]. Over 90% (at 623K) NO_x reduction by NH_3 over a V_2O_5 - TiO_2 catalyst was observed in flue gases containing high SO_x concentrations from an oil-fired boiler of a pilot plant [318].

A study of the oxidation of ethanol over a V_2O_5 - TiO_2 catalyst has revealed a dependence of MeCHO formation on the V/Ti ratio, indicative of the active dehydrogenation phase being amorphous V_2O_5 [319]. The turnover frequency for V_2O_5 - TiO_2 (anatase) was larger than that for V_2O_5 - TiO_2 (rutile) or unsupported

V_2O_5 in the oxidation of ethylene [320]. Infrared spectroscopy monitored the adsorption of ammonia and pyridine on V-Ti oxide catalysts for which the vanadium content varied between 2 and 5 weight percent. Results indicated that the catalyst exhibited both Brønsted and Lewis acidities [321]. Haase and coworkers [322] have investigated the formation of an active component layer in coated catalysts. The coatings were prepared using a concentrated vanadium oxalate solution and different amounts of acetic, oxalic and citric acid, different alcohols, detergents and polymeric substances. On the surface of V_2O_5 - TiO_2 layers, the coatings caused the formation of differently shaped V_2O_5 crystals.

f. Titanium Electrodes

The electrochemical reduction of HNO_3 using Ti and graphite electrodes has been achieved [323]; the current-potential and current-time curves and mass spectroscopic product analysis were also obtained. Catalysis by Cu^{2+} , Ag^+ or Pb^{2+} deposited at the base electrode was also discussed. An electrochemical study on the prevention of bacterial attachment in seawater was carried out on Ti metal and SnO_2 -coated glass in the potential range 0.2 to -0.6V (vs NHE). Application of steady-state potentials decreased bacterial concentrations on the cathode and anode by ca. 100-300 fold. The effect of potential on bacteria supposedly arises because of in situ electrochemical reduction of O_2 to H_2O_2 and OH^- [324]. The effect of anode material (Ti vs Ti-Ru alloy) on the electrochemical oxidation of iodide ions was examined and polarization curves constructed with Pt and graphite anodes as well [325]. The Ti is passivated by anodic currents [325]. The electrochemical oxidation of ferrocyanide ions on a passive Ti anode was examined. The characteristics of the kinetics of the redox reaction are the higher anodic current and its strong dependence on the prior treatment method of the electrode. The peculiarities in the kinetics were related to the change in the mechanism of electron transfer through the oxide film formed by mechanically polishing the Ti surface [326].

The kinetics of the active anodic dissolution of titanium in strongly acidic chloride solutions (HCl) was performed at 353K. The structure-sensitive method of photoelectric polarization and ESCA have characterized the state of the rotating disk electrode surface, prepared from VT-1-0Ti [327]. Corrosion tests have been carried out on a rotating disk electrode made of VT1-0 [329]. Riskin and coworkers [329] have also examined crevice corrosion of titanium in sulfate-chloride media in the presence of an anodic current.

Effects of various technological factors on the formation of porous titanium electrodes for electrophoresis have been studied as well as the amount

of pore-former (NH_4HCO_3) used and the effect of sintering [330].

Anodes of Ti and TiO_2 have been tested for recovery of metals and oxides to determine any technical or economical advantages they might possess [331]. Possible improvements in hydrogen production and storage using Ti electrodes were undertaken by modifying the electrode with chromium; an increased spectral response was obtained though the overall efficiency decreased [332]. Platinized titanium anodes are superior to samples of dimensionally stable anodes (DSA) prepared in the same way in electroflotation processes. This could be attributed to the inability of the DSA to support the inversions of polarity as well as do the platinized titanium samples [333]. Electrochemical photocells, composed of CdSe thin-film deposition on Ti (also Cr, Mo, SnO_2 , glass C, graphite) as the anode and a Pt cathode, have been reported and the current-voltage relations, output power efficiency, open circuit voltage, and short-circuit current measured [334]. Polyphthalocyanine coatings on Ti obtained by *in situ* synthesis with 1,2,4,5-tetracyanobenzene. The surfaces were characterized by UV and IR spectroscopy and SEM. The stabilization of these materials as electrodes in different electrolytes reveals a high faradaic activity and anodic photocurrents upon visible-light irradiation [335].

Several titanium-supported metal oxide electrodes have been prepared and their behavior investigated. The anodic behavior of a titanium substrate in various acidic manganese(II) solutions was investigated to determine the most suitable electrolyte for obtaining a MnO_2/Ti electrode [336]. An experimental analysis of the Br/Br^- redox reaction in a porous back-fed RuO_2 -coated Ti electrode has been done, and a mathematical model of the steady-state process proposed. The resulting design equation reveals that the back-fed electrode could reduce the loss of Br across the separator and the ohmic loss in a Zn/Br battery [337]. The study of corrosion characteristics of RuO_2 -coated Ti electrodes under anodic conditions in organic solvents reveals rapid dissolution of the Ti support through pores and cracks in the active oxide coating, eventually resulting in complete detachment of the surface layer. Particular emphasis on this system in methanolic solutions is described [338]. RuO_2 -coated Ti anodes have been utilized in oxygen evolution and oxide dissolution in acidic and basic media. The anode service life is affected by oxide annealing time, annealing temperature, current density for oxygen evolution, oxide loading solution temperature and pH. A common intermediate, a surface-bonded oxyruthenium complex, was proposed for both oxide dissolution and oxygen evolution reactions [339]. Potentiodynamic data was obtained for Ti anodes coated with $\text{RuO}_2 + \text{TiO}_2 + \text{SnO}_2$ mixtures, and compared with results using electrodes coated with $\text{RuO}_2 + \text{TiO}_2$ or pure RuO_2 [340]. The effect of Sb-doped SnO_2 intermediate layer on the anodic characteristics of Ti-supported PbO_2

electrodes has been studied. X-ray diffraction results reveal the intermeidate layer contains $\text{SnO}_2\text{-SbO}_x$ solid solution, and small amounts of Ti_4Sb , Ti_3Sb , Ti_3Sn , SbO and $\text{Ti}_{1.2}\text{O}$. An electronic model for the electrode was proposed, and factors for surface resitivity reduction discussed [341].

Optimal conditions for the formation and behavior of $\text{Ti-Co}_3\text{O}_4$ anodes under conditions of chlorine evolution have been determined [342, 343].

6.7 TITANIUM SULFIDES AND SULFATES

The phase relation from $\text{TiS}_{1.38}$ through $\text{TiS}_{1.96}$ at 1173K was studied employing the thermobalance method under controlled sulfur pressure. Four phases were found to exist: a) Ti_2S_3 (4H) with a short-range ordering of titanium vacancies; b) superstructure of Ti_2S_3 (4H) due to the ordering of titanium vacancies; c) Ti_2S_3 ; and d) TiS_2 (2H) [344].

The relativistic corrections to the 'p-d' gaps of Ti-TiS_2 and TiSe_2 were calculated using self-consistent nonmuffin-tin OPW band structure results [345]. Also, the heat capacities of TiS_2 from 5.87 to 300.7K were measured by adiabatic calorimetry [346]. Auger and ESCA spectroscopy revealed the stoichiometry of TiS_2 single crystals grown by the iodine vapor transport method. Analyses varied from $\text{Ti}_{0.87}\text{S}_2$ at the surface to $\text{Ti}_{1.28}\text{S}_2$ at depths of ca. 1000 nm [347]. Electron and x-ray diffractometric methods were used to investigate polytypic $\text{Ti}_{1+x}\text{S}_2$ ($x=0.25\text{-}0.33$) with ordered titanium atoms and vacancies [348].

Titanium disulfide has been prepared, and chemically and structurally analysed. Thermogravimetric analysis of TiS_2 reveals two to four distinct steps for the phases derived [349]. A pulsed proton nmr study of titanium-rich $\text{Ti}_{1+x}\text{S}_2\cdot\text{NH}_3$ reveals that the diffusion of intercalated NH_3 is not dependent on the presence of titanium interstitials, although these do significantly reduce the rate of NH_3 uptake [350].

The discharge characteristics of the TiS_2 cathode in organic solvents and their 1:1 mixtures containing LiClO_4 , LiBF_4 or LiPF_6 at 298K have been studied by Matsuda et al. [351]. It was found that the discharge capacities were large in a mixture of THF and γ -butyrolactone containing LiClO_4 or in a mixture of THF and propylene carbonate containing LiBF_4 . A rechargeable solid-electrolyte cell has been developed using a copper ion conductor of rubidium copper iodide chloride ($\text{Rb}_4\text{Cu}_{16}\text{I}_{7-6}\text{Cl}_{13+6}$) and a TiS_2 cathode. At 298K, the open-circuit voltage was 0.59V, the cell yielded a current of several tens of μA without polarization, and the cell could be submitted to ≥ 100 charge-discharge cycles without showing appreciable deterioration [352].

The x-ray photoelectron spectra of TiS_3 with a one-dimensional structure

were interpreted in terms of $\text{Ti}^{4+}(\text{S}_2)^{2-}\text{S}^{2-}$ with pairs of sulfur atoms (S_2) and isolated sulfur atoms. The binding energies of the S_2 pairs is 1.4eV higher than that of the isolated S atoms, which is consistent with the larger negative charge of the isolated atoms. A molecular orbital scheme for the S_2 pairs was used to describe the structure of the valence band of TiS_3 [353]. Infrared reflectivity measurements of quasi-one-dimensional TiS_3 with light polarizations both perpendicular and parallel to the chains reveal that most of the infrared-active phonons predicted by group theory are observed; the reflectivity measurements were compared with Raman measurements [354]. TiS_3 single crystals grown by chemical vapor transport have been characterized by x-ray diffraction and electronic transport property measurements. The photoelectrochemical behavior in various media is reported, along with a photocorrosion mechanism. The mechanisms were discussed in terms of the existence of S_2 dimers and S^{2-} ions [355].

Several investigations of intercalated titanium sulfide compounds, incorporating lithium, sodium, vanadium, chromium, silver, copper, zinc and thallium, have been reported. Jacobsen *et al.* [356] have offered a model for the electrostatic interactions between Li^+ ions and the conducting electrons in the layered compound Li_xTiS_2 . The Li^+ ions presumably intercalate in the van der Waal's gap and are treated as point charges in the dielectric. The strong deviations from ideality observed during intercalation of Li^+ in Li_xTiS_2 were ascribed to electrostatic forces screened by the conduction electrons [356]. An x-ray diffraction investigation of Li_xTiS_2 reveals a three-fold superlattice structure in the region where $x = 0.33$ [357].

Titanium-sulfur compounds have been prepared electrochemically on titanium plates to be used as a cathodic active material for a lithium battery. The active compounds are formed via anodic oxidation of a titanium plate in molten $\text{Na}_2\text{S} \cdot 9\text{H}_2\text{O}$ at 353K. Charge-discharge behavior was studied [358]. The galvanostatic cycling of Li-TiS₂ batteries in 1M LiAsF₆/propylene carbonate/ acetonitrile, in 1M LiClO₄/propylene carbonate has been reported. The battery performed best in LiAsF₆/propylene carbonate/acetonitrile electrolyte with respect to charge-discharge ratio, active material utilization, and cycle life [359]. Improved cathode utilization (e.g., TiS_2 , CuS , Cu_2S , etc.) is afforded employing 1M LiAsF₆ in 50%(vol) propylene carbonate/acetonitrile in primary lithium batteries. It was suggested that the lower viscosity and lower molar volume of the acetonitrile and incorporation of solvated Li^+ into the cathodic material as part of the cathodic process are responsible for the improved behavior of this system vs LiAsF₆ in propylene carbonate electrolyte solutions [360].

A report on the thermodynamic and structural character of Li_xTiS_2 has

appeared [361]. Also, entropy measurements [$\delta V/\delta T_x$, V = emf, T = temperature] on $\text{Li-Li}_x\text{TiS}_2$ electrochemical cells were utilized to obtain information on the entropy of Li_xTiS_2 [362].

A mean-field approximation has been applied to a triangular-lattice gas model with three different site energies randomly distributed and nearest-neighbor pairwise repulsion, to represent intercalated lithium in $\text{Li}_x\text{Ta}_y\text{Ti}_{1-y}\text{S}_2$. This model appears applicable for alloys where experimental results indicate a disordered distribution of lithium atoms [363]. The $\text{Li}_x\text{Ta}_y\text{Ti}_{1-y}\text{S}_2$ system has been studied as a potential rechargeable battery in terms of interactions between lithium atoms and the applicability of a lattice gas model to the problem of the ordering of these atoms [364].

Charge and discharge properties of Li-TiS_2 and Na-TiS_2 intercalation batteries in relation to the structural changes of TiS_2 have been reported by Kikkawa and Koizumi [365].

Na_xTiL_2 ($0 < x \leq 1$; $L = \text{S, Se}$) were prepared by intercalation of sodium into TiL_2 in liquid ammonia, as well as by direct combination of the elements. X-ray diffractometry characterized the second-stage intercalate ($x \sim 0.3$) structure [366]. The magnetic properties of the insulating $\text{Na}_x\text{Cr}_x\text{Ti}_{1-x}\text{S}_2$ system were investigated by susceptibility and magnetization measurements down to 4.2K and by EPR techniques to 77K. Geometrical considerations were used as the basis for the ferro-antiferromagnetic transition [367].

Powder samples of V_xTiS_2 ($0 \leq x \leq 0.33$) have been prepared and characterized [368]. Presumably, the vanadium atoms are randomly distributed in layers which are empty at $x = 0$, while the magnetic susceptibility follows the Curie-Weiss law at 10-300K. For $x < 0.2$, the magnetic moment on every vanadium atom is ca. $0.6\mu\text{B}$. Angular-resolved photoemission spectroscopic results on the electronic structure of $\text{V}_x\text{Ti}_{1-x}\text{S}_2$ ($0 \leq x \leq 0.2$) revealed the existence of a localized impurity band, ascribed to excess Ti and/or V impurities [369]. Results of near-normal incidence reflectivity measurements on $\text{V}_x\text{Ti}_{1-x}\text{S}_2$ ($0 \leq x \leq 0.3$) have been discussed in terms of a dielectric function containing contributions from the valence electrons, the phonon, and the free carriers [370]. The phase relations of the $\text{V}_{1-x}\text{Ti}_x\text{S}_{1.57}$ system have been elucidated from x-ray diffraction results, while the site distribution of Ti and V atoms in the structure were clarified through an nmr absorption study. The two apparently closely related properties were discussed in terms of the metal-metal interaction of the face-shared octahedra in the metal-deficient distorted NiAs structure [371].

Stage II samples of Ag_xTiS_2 have been prepared via electrointercalation of silver into TiS_2 ; the silver atoms undergo an order-disorder transition at $T_c = 265\text{K}$. Raman spectra were recorded and discussed [372]. The room-temperature

transmission spectrum of Ag_xTiS_2 was measured at 1.3-2.8 eV for various x values. A rigid band model, wherein charge transfer from the silver cation to the lowest d conduction band of the host macroanion, was proposed to explain the spectral changes observed [373]. An x-ray diffraction study of the basal ('ab') plane and the short-range order diffuse scattering from intercalated silver atoms in disordered state-II $\text{Ag}_{0.18}\text{TiS}_2$ reveals that the silver ions in the intercalated plane occupy the octahedral sites, as well as a two-dimensional disordered structure [374]. An experiment has been reported which presumably makes it possible to distinguish between the intrinsic and extrinsic contributions to the plasmon structure of the core lines in the x-ray photoelectron spectrum of $\text{TiS}_2\text{-Ag}$ [375].

The electrochemical synthesis of Cu_xTiS_2 has been reported [376], and intercalation electrodes (such as Cu_xTiS_2) have been studied for potential use in the storage of electrical energy generated by photoelectrochemical solar cells [377].

The magnetic susceptibilities of the solid solution $\text{Cr}_{1-x}\text{Ti}_x\text{S}$ ($0.10 \leq x \leq 0.60$) [378], and a new phase, $\text{Zn}_2\text{Ti}_{18}\text{S}_{32}$, prepared from titanium metal, ZnS and titanium sulfide at 1473K [379] have been reported.

The x-ray crystal structure of TiTi_5Se_8 has revealed this selenide compound to be monoclinic, space group C2/m [380]. A structural study of iron intercalated titanium diselenides has also appeared in the literature [381].

The nature of complex forms of titanium(IV) which exist in concentrated sulfuric acid solutions has been studied [382]. In sulfate solutions free of ClO_4^- , the polymerization of titanium(IV) has been investigated potentiometrically in pure sulfuric acid solutions over a broad range of acid concentrations. In solutions of 3-8M H_2SO_4 , binuclear titanium(IV) complexes are formed at comparatively low concentrations of titanium(IV) [383].

The thermal decomposition of $\text{TiO}(\text{SO}_4) \cdot \text{H}_2\text{O}$ in air and in argon was studied by DTA and thermogravimetry (TG). The TG curves are similar in both atmospheres, indicating that air does not affect the decomposition [384]. The study of the impurity segregation of Nb, Fe and La during the solution crystallization of $(\text{NH}_4)_2\text{TiO}(\text{SO}_4)_2 \cdot \text{H}_2\text{O}$ from aqueous sulfuric acid revealed that the total amount of trapped impurities is dependent on the initial degree of supersaturation and the rate of crystallization [385]. The reduction of titanium(IV) in $(\text{NH}_4)_2\text{TiO}(\text{SO}_4)_2 \cdot \text{H}_2\text{O}$ solutions by zinc and aluminum was investigated in terms of reaction conditions (temperature, length of heating, nature of reducing agent) [380]. The reaction of water vapor and the vapor of 50-80% aqueous H_2SO_4 with $\text{CaTi}(\text{SO}_4)_3(\text{s})$ was studied tensimetrically. The hydration reaction (3) presumably occurs via a step-like mechanism involving the gradual formation of TiOSO_4 , then $\text{TiOSO}_4 \cdot \text{H}_2\text{O}$ and $\text{TiOSO}_4 \cdot 2\text{H}_2\text{O}$. Such a



mechanism can elucidate the sulfation of sphene [387].

Infrared spectroscopy and chemical analyses were used to follow the extraction of titanium by bis(2-ethylhexyl)phosphate. At low H_2SO_4 concentrations, titanium is extracted as a chelate compound, not containing SO_4^{2-} [388].

6.8 TITANIUM HALIDES

a. Fluorides

The emission spectra during thermoluminescence have been recorded for various $\text{LiF}:\text{Ti}$ and $\text{LiF}:\text{Mg}:\text{Ti}$ specimens. The results suggest that the luminescence center is a defect complex of titanium modified in the Mg-doped crystals by magnesium in various forms. Red emission is observed in the Mg-doped crystals. The dependence of the thermoluminescence peaks on dose and linear energy transfer appear to support the suggestion that the higher temperature peaks are complexes which trap more than one charge [389].

The thermodynamic properties of crystalline TiF_3 have been determined by emf measurements with a solid electrolyte cell consisting of Ti , $\text{TiF}/\text{CaF}_2/\text{Al}$, AlF_3 at 800-900K. The results were compared to data obtained by other methods [390]. The processes that occur during reduction of different valency forms of titanium and the anodic oxidation of titanium in chloride-fluoride melts were studied in order to better understand the conditions of formation of titanium(II) fluorides [391].

The crystal structure determination of the peroxofluoro complex $\text{K}_2\text{Ti}(\text{O}_2)_4 \cdot \text{H}_2\text{O}$ has revealed the complex to be monoclinic, with isolated $\text{di}(\mu\text{-fluoro})\text{-bridge}[\text{Ti}_2(\text{O}_2)_2\text{F}_8]^{4-}$ anions interconnected by hydrogen-bonded water molecules forming infinite chains [392].

Using a multipulsed nmr technique, the isotopic average chemical shift of ^{19}F was measured in hexafluoro complexes of titanium, germanium, tin and silicon [393]. The temperature dependence of the structural transformation rate in $\text{NiTiF}_6 \cdot 6\text{H}_2\text{O}$ was measured by monitoring the ESR line of Ni^{2+} from the trigonal phase. The dependence of the rate appropriate to the first thermal cycle is indicative of the presence of a second transition with a critical temperature $T_c = 126.0 \pm 0.5\text{K}$. This second transition was suggested [394] as being associated with an additional distortion of the $(\text{TiF}_6)^{2-}$ ion known to occur in this temperature range. The Raman spectra of $\text{ZnTiF}_6 \cdot 6\text{H}_2\text{O}$ and $\text{MnTiF}_6 \cdot 6\text{H}_2\text{O}$ as single crystals in different polarizations and in solution has allowed the determination of mode frequencies [395]. Deuterium-2 nmr was

employed to determine the quadrupole coupling constants and the direction cosines of the principal axes of the electric field gradient tensors of the deuterons in $\text{CoTiF}_6 \cdot 6\text{D}_2\text{O}$ and $\text{ZnTiF}_6 \cdot 6\text{D}_2\text{O}$ single crystals at 300K. Temperature dependence studies (185-300K) revealed structural phase transitions in both complexes, at ca. 225K in $\text{CoTiF}_6 \cdot 6\text{D}_2\text{O}$ and 230K in $\text{ZnTiF}_6 \cdot 6\text{D}_2\text{O}$ [396]. Infrared spectroscopy has been used to study the phase transitions in $\text{ZnTiF}_6 \cdot 6\text{H}_2\text{O}$ and $\text{MnTiF}_6 \cdot 6\text{H}_2\text{O}$. The librational modes of the water molecule change significantly around the transition temperature [397].

BaF_2 , TiO_2 and BaTiF_6 react at 773-973K for 14-20 hr. under argon to give $\text{Ba}_3\text{Ti}_2\text{F}_{12}\text{O}_2$. X-ray diffraction studies showed the orthorhombic structure of $\text{Ba}_3\text{Ti}_2\text{F}_{10}\text{O}_2$ (Figure 2) [398]. The thermal decomposition of Na_2TiF_6 in air,

hkl	$10^3 \sin^2 \theta_{\text{calc}}$	$10^3 \sin^2 \theta_{\text{obs}}$	I_{obs}	I_{calc}	hkl	$10^3 \sin^2 \theta_{\text{calc}}$	$10^3 \sin^2 \theta_{\text{obs}}$	I_{obs}	I_{calc}
110	11.42	—	—	0.2	123	85.66	85.73	1	0.9
101	11.87	11.85	1	0.6	400	89.14	89.20	1	0.4
111	12.15	12.13	1	0.2	040	93.57	93.65	1	0.3
111	17.72	17.70	1	0.5	410	94.89	95.00	3	2.3
200	22.28	—	—	0.2	322	98.73	98.94	1	0.7
020	23.39	23.34	2	1.5	140	99.14	99.20	8	9.0
002	25.20	25.17	1	0.3	232	100.11	100.21	1	1.0
210	26.13	—	—	0.3	004	100.79	100.87	11	13.3
120	28.06	28.03	4	3.6	111	101.28	101.32	7	6.9
211	31.43	—	—	0.0	223	102.37	102.50	2	2.1
101	33.23	—	—	0.0	330	102.77	—	—	0.6
112	36.82	36.80	16	17.3	111	105.44	105.21	5	3.7
200	45.88	45.87	19	20.6	303	106.83	—	—	0.2
012	47.48	47.48	26	33.7	331	108.07	—	—	3.4
022	48.59	48.60	12	19.9	033	108.32	108.10	7	0.1
221	51.58	52.01	10	14.8	111	112.30	112.29	8	5.4
212	53.33	53.37	12	22.8	420	112.53	—	—	1.4
122	54.16	54.18	16	23.2	313	112.68	—	—	6.1
110	55.99	56.04	16	15.4	102	114.33	114.44	2	1.5
201	56.41	56.52	1	0.5	133	114.90	114.97	2	1.8
120	58.20	58.22	21	26.0	240	115.45	115.83	1	0.6
011	58.93	—	—	0.1	042	118.77	118.78	3	2.8
101	62.26	62.29	30	7.1	421	118.83	—	—	0.0
011	62.29	—	—	16.7	412	120.18	120.25	8	7.2
012	62.54	62.58	1	4.3	241	122.15	122.23	2	1.3
101	64.50	64.50	10	8.8	204	123.07	—	—	0.0
113	68.11	68.12	5	4.4	024	124.18	—	—	1.0
222	70.87	—	—	0.0	142	124.34	124.34	7	4.6
120	73.53	73.66	4	3.2	332	127.97	127.99	30	22.1
230	74.92	75.03	1	0.0	214	128.92	128.95	5	3.9
121	78.83	—	—	0.2	124	129.75	129.80	12	9.2
212	81.18	81.31	1	1.3	323	130.22	—	—	0.2
241	81.22	—	—	0.2	233	131.61	131.74	1	1.4
102	83.40	83.50	4	2.9	422	137.73	137.76	15	9.3
213	84.82	—	—	0.1					

FIGURE 2 : Tabulation of observed and calculated crystal data for $\alpha\text{-Ba}_3\text{Ti}_2\text{F}_{10}\text{O}_2$ [398]. followed by vapor-phase hydrolysis of the resulting TiF_4 or TiOF_2 produces TiO_2 crystals. When heated in an electric furnace (1073-1373K) for 4 min-4 hr, a mixture of Na_2TiF_6 and TiO_2 gave Na_3TiOF_5 and TiF_4 at 1073K, and TiO_2 (rutile) above 1073K. At temperatures greater than 1173K, the rutile changes to $\text{Na}_2\text{Ti}_6\text{O}_{13}$ on reaction with a sodium compound formed from the decomposition of Na_3TiOF_5 [399].

The complex formation equilibrium between Ti(IV) and F ions were studied at 298K in 3M NaCl by measuring the free HF concentration in acidic solutions with an ion selective electrode. The data were interpreted by assuming the

formation of $\text{Ti}(\text{OH})_2\text{F}^+$, TiF_4 and HTiF_6^- with given equilibrium constants [400]. Magnetic susceptibility, thermal analysis, x-ray powder diffraction, and IR and Raman spectral measurements were employed to characterize $\text{N}_2\text{H}_5\text{Zn}[\text{TiF}_6] \cdot 5\text{H}_2\text{O}$ which was isolated from the $\text{H}_2\text{TiF}_6/\text{N}_2\text{H}_5\text{F}_2/\text{Zn}/\text{H}_2\text{O}$ system [401].

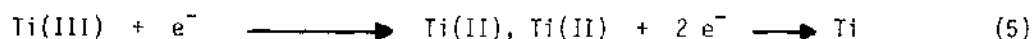
b. Chlorides

A modification of the Born-Mayer equation (without compressibility term) has led to the suggestion that a polynomial of the type in equation (4) be used

$$U_L = U_{\text{ELEC}}[k - 0.3729x + 0.0695x^2 + \dots] \quad (4)$$

to calculate the lattice energy of titanium monohalide crystals [402]. Results reveal a marked improvement over those reported previously. The violet emission bands of TiCl have been re-investigated by Devore [403], who has reassigned the 419-nm and 387-nm system to doublet-doublet transitions rather than quartet-quartet transitions. Additionally, vibrational frequencies for each state involved were established. New experimental data obtained from XPS has been shown [404] to be applicable to the ionicity concept in solid state chemistry. Applications presented included titanium halide compounds.

Vibrational and electrochemical studies have been performed for some titanium subchloride compounds. Infrared spectra of gaseous TiCl_4 , TiCl_3 , TiCl_2 and possibly TiCl were recorded using a microwave discharge through a TiCl_4 /argon mixture as the molecular source. The vibrational frequencies were located at 497 cm^{-1} for TiCl_3 , at 489 cm^{-1} for TiCl_2 , and at 450, 400 and 422 cm^{-1} for TiCl [405]. The electrochemical behavior of Ti(III) and Ti(II) in NaCl-KCl melts (993K) was investigated by linear sweep voltammetry and chronopotentiometry. Reaction (5) depicts the electrode reaction for the



cathodic reduction of Ti(III) . The diffusion coefficients are $(3.4 \pm 0.7) \times 10^{-5}$, $(4.1 \pm 0.6) \times 10^{-5}$, and $(9.2 \pm 0.5) \times 10^{-5} \text{ cm}^2\text{-s}^{-1}$ for Ti(IV) , Ti(III) and Ti(II) , respectively [406].

Analyses of the reflectance spectrum of $\alpha\text{-TiCl}_3$ and the absorption spectrum of $\beta\text{-TiCl}_3$ (1.8-10.4 eV) has shown that the low-energy peaks (2-4 eV) of both species may be assigned to localized interionic transitions between d states of neighboring titanium ions. The strong band above 4 eV was ascribed to charge-transfer and band-to-band transitions. The anion $3p$ -cation $4s$ interband gap was estimated to be ca. 7.3 eV for $\alpha\text{-TiCl}_3$ and 6.9 eV for $\beta\text{-TiCl}_3$ [407].

Fluorescence EXAFS measurements on MgCl_2 -supported TiCl_3 (8.0 wt. %) reveal a maximum of ca. 4 wt. % TiCl_3 interacts with MgCl_2 , leaving a residue of $\delta\text{-TiCl}_3$. It was also proposed that the Cl atoms likely interact with the coordinatively unsaturated Mg atoms at the fractured side planes of the MgCl_2 particles [408]. Kushner and coworkers [409] have observed the inactivation of hydroxamic acid siderophores when exposed to TiCl_3 . From comparative IR and nmr spectral analyses, the products of the reduction reaction were the corresponding amides. Ionization potentials (I_k) have been calculated for TiCl_4 using a) the CNDO-Koopmans theorem (KT) and b) CNDO-perturbative CI (PCI) methods. It was found that the I_k values calculated employing the PCI method agreed better with existing experimental data than values calculated using the KT method [410]. The molecular, Coriolis coupling and centrifugal distortion constants have been evaluated using kinetic constants for tetrahedral Group IV halides, and found to agree well with observed values [411]. High-resolution XPS of solid-state TiCl_4 has afforded an analysis of the core levels, their shape-up satellites and valence levels, as well as a comparison with gas-phase XPS data, UPS spectra and theoretical models from the literature [412]. Direct observation of $^{47,49}\text{Ti}$ resonances in a series of TiX_4 ($\text{X} = \text{Cl}, \text{Br}, \text{I}, \text{OPr}, \text{NEt}_2$), $(\text{Cp})_2\text{TiX}_2$ ($\text{Cp} = \text{cyclopentadienyl}$; $\text{X} = \text{F}, \text{Cl}, \text{Br}, \text{I}, \text{N}_3, \text{NCS}$) and TiX_6^{2-} ($\text{X} = \text{F}, \text{Br}$) complexes has been reported by Nao *et al.* [413]. A detailed study of TiCl_4 reveals the dominance of a quadrupolar relaxation mechanism. Correlation times calculated from the Gierer and Wirtz relation combined with observed Ti results afforded an estimation of the quadrupole coupling constants for $^{47,49}\text{Ti}$ nuclei to be 2.8 and 2.4 MHz, respectively. The $^{47,49}\text{Ti}$ nuclei appear to be as sensitive to changes of halide ligands in the Cp_2MX_2 series as the ^{91}Zr nucleus.

The electrochemical behavior of TiCl_4 in low-temperature organic melts (e.g., urea, ammonium sulfamate, ammonium formate, acetamide) was studied to determine the effect of decreasing temperature on titanium electroplating from melts [414]. Thermal analyses and an isothermal saturation method were used to study the $\text{TiCl}_4\text{-TiI}_4$ system at 203-423K. A phase diagram reveals that TiClI_3 , TiCl_2I_2 and TiCl_3I melt incongruently at 289, 275 and 259K, respectively, and the eutectic between TiCl_4 and TiCl_3I melts at 240K [415].

The chemical stability of the surface species formed from the reaction between silica gel and TiCl_4 has been examined. It was found that $\text{Et}_x\text{AlCl}_{3-x}$ ($x = 1, 2, 3$) is capable of dissolving large amounts of surface-anchored titanium, and a mechanism proposed for the substitution of the anchored Ti by Al [416]. The reaction between anhydrous TiCl_4 and pyrolytic graphite in the liquid or vapor phase (250-500K, 0.1-0.6 MPa Cl pressure) affords a graphite intercalation compound. After 120 hr., $\text{C}_{54}\text{Ti}_{1.0 \pm 0.1}\text{Cl}_{4.45 \pm 0.05}$ forms at 350-360K; and after 250 hr., $\text{C}_{63}\text{TiCl}_{4.41}$ forms at 364K. At higher temperatures,

$C_nTiCl_{4.45 \pm 0.05}$ ($n = 61, 84, 116, 177$) form. Various electrical properties of these compounds were determined [417]. Vibrational frequency correlations and neutron powder diffraction methods were used to characterize the crystal structure of α - $TiAl_2Cl_8$. As well, the IR spectra of α - and β - $TiAl_2Cl_8$ and $TiAl_2Cl_8 \cdot C_6H_6$ have been described [418]. The magnetic behavior of $Cs_3Ti_2Cl_9$ was investigated from the viewpoint of isolated binuclear $(Ti_2Cl_9)^{3-}$ units [419].

Thermochemical studies of the adducts formed between titanium subgroup tetrachlorides and thiourea (thio) have afforded the heats of formation of and the heats of solution of $MCl_4 \cdot \text{thio}$ and $MCl_4 \cdot 2\text{thio}$, as well as the heats of addition of thio to MCl_4 ($M = Ti, Zr, Hf$). The stability of the adducts follow the order $M: Ti > Hf > Zr$; and the heat of addition of thio to $MCl_4 \cdot \text{thio}$ is only 40-80 $\text{kJ} \cdot \text{mole}^{-1}$ [420, 421]. Infrared spectra of $MCl_4 \cdot n\text{thio}$ ($n = 1, 2$) reveal a dimeric structure with bridging Cl for $MCl_4 \cdot \text{thio}$, while $MCl_4 \cdot 2\text{thio}$ has a similar structure but the second thio molecule is hydrogen bonded [422, 423]. Similar adducts $MCl_4 \cdot nL$ have been prepared and characterized between $TiCl_4$ and L : acetoneethiosemicarbazone [424]; semicarbazide [425]; urea [426]; acid esters $C_4H_9SO_2OR$ ($R = \text{Me, Et, Pr}$), $R'SO_2OPr$ ($R' = \text{Pr, Bu}^i, \text{pentyl}$) or $C_6H_5SO_2OR''$ ($R'' = \text{Me, Et, Bu}$) [427]; dithiooxamides [428]; N -acetylsalicylamides [429]; phenazone and amidopyrine [430]; 1,2,4 λ^4 ,3,5-trithiadiazole, AsF_5 and SbF_5 [431]; and glycine [432].

Titanium tetrachloride reacts with $BuSO_2OR$ ($R = \text{Me, Et, Pr}$) and $PhSO_2OEt$ to give $[TiCl_3(O_3SBu)]_2$ and $[TiCl_3(O_3SPh)]_2$, respectively. Infrared and nmr spectral data were interpreted in terms of a bridging sulfonate ligand with coordination of two oxygen atoms to one Ti atom of the dimer and coordination of the third oxygen atom to the second Ti atom [433]. Near-stoichiometric barium titanyl oxalate tetrahydrate, $BaTiO(C_2O_4)_2 \cdot 4H_2O$, was prepared at $BaCl_2: TiCl_4$ and $H_2C_2O_4: TiCl_4$ mixing ratios of 1.05 and 2.20, respectively, at 343K; the product was identified by x-ray diffraction [434].

$TiCl_4$ and $MgCl_2$ react in dry $ClCH_2CO_2Et$ to yield the monoclinic complex $TiMgCl_5(O_2CCH_2Cl)(ClCH_2CO_2Et)_3$ depicted in Figure 3. An x-ray crystal structure, Figure 3, reveals that the complex consists of two chloride bridges and one $ClCH_2CO_2^-$ bridge. The Ti atom also coordinates three chloride ligands and the Mg atom coordinates three $ClCH_2CO_2Et$ groups through the carbonyl oxygen atom. Both Ti and Mg have an octahedral environment [435].

The physiochemical properties of the extraction system $TiCl_4$ -acetylacetone-1M HCl were investigated, and afforded calculation of the work of cohesion and adhesion and entropy and surface energy. Extraction coefficients and percent extraction as a function of Ti concentration in the system were also calculated [436]. Optical-absorption spectroscopic studies afforded the rate constants for the hydrogen photoreduction of gaseous $TiCl_4$, for which a photodissociation

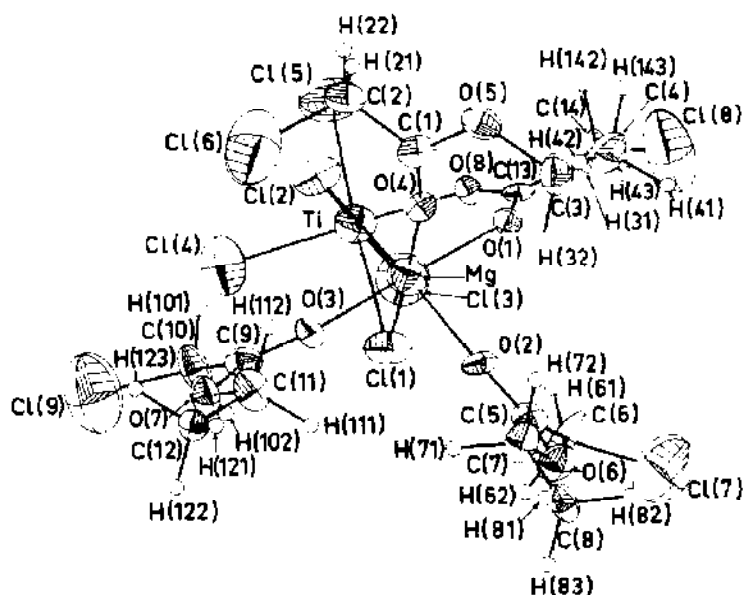


FIGURE 3 :: Structure of the $\text{TiMgCl}_5(\text{O}_2\text{CCH}_2\text{Cl}) \cdot (\text{ClCH}_2\text{CC}_2\text{C}_2\text{H}_5)_3$ adduct molecule, indicating 30% probability thermal vibration ellipsoids [435].

mechanism was given [437]. Liquid TiCl_4 has been studied as a fire-hazard-free practice bomb signal device. Upon use, the TiCl_4 is expelled from the bomb and immediately reacts with atmospheric moisture to form a dense white cloud [438]. The reaction of TiCl_4 and AlMe_3 with high-surface-area SiO_2 was studied using FTIR photoacoustic spectroscopy. The peak at 980 cm^{-1} was assigned to the strained, surface siloxane bridge in the dehydrated SiO_2 spectrum. Low-frequency peaks previously unassigned were assigned to various M-O and M-C stretching vibrations of the products of the surface reactions [439].

The orthorhombic oxychlorides $\text{Ln}_2\text{Ti}_2\text{O}_6\text{Cl}_x$ ($\text{Ln} = \text{La} - \text{Tm}$, $x \leq 1$) have been prepared via calcination of LnTiO_3 or $\text{Ln}_2\text{Ti}_2\text{O}_7$ in a chlorine atmosphere. Infrared spectroscopy and x-ray diffraction methods were used to characterize $\text{Ln}_2\text{Ti}_2\text{O}_6\text{Cl}$ [440].

c. Titanium Chlorides As Catalysts

(i) TiCl_3

The structure and properties of TiCl_3 as a catalyst were investigated by x-ray diffraction during its preparation via reduction of TiCl_4 by Et_2AlCl . The crystallite dimensions and phase compositions (α , β , δ , and γ) were determined [441].

The use of TiCl_3 as a catalyst has been incorporated into polymerization,

reductive elimination and pinacolic coupling reactions. Olefin polymerization catalysed by an unsupported titanium-magnesium (from reaction of MgCl_2 with TiCl_3) catalyst has been studied by NQR (nuclear quadrupole resonance) spectroscopy [442]. 2-Ene-1,4-diols undergo 1,4-reductive elimination on treatment with $\text{TiCl}_3\text{-LiAlH}_4$ to yield 1,3-dienes. For example, (E)- and (Z)- $\text{HOCRR}'\text{CH=CHCR}^2\text{R}^3\text{OH}$ [$\text{RR}' = \text{R}^2\text{R}^3 = (\text{CH}_2)_5$, $\text{R-R}^3 = \text{Me, Ph}$, $\text{R} = \text{R}^2 = \text{Ph}$, $\text{R}' = \text{R}^3 = \text{H}$] gave the 1,3-dienes $\text{RR}'\text{C=CHCH=CR}^2\text{R}^3$ in <83% yields [443]. Carbon dioxide is electrocatalytically reduced at pH 7 in the presence of TiCl_3 , pyrocatechol and Na_2MoO_4 at 1.55V (vs SCE) to produce $\text{CH}_4/\text{C}_2\text{H}_6/\text{C}_2\text{H}_4/\text{C}_6$ hydrocarbons in the ratio 4.2/0.45/0.16/0.12 [444]. Aromatic aldehydes and ketones undergo one-electron reductive coupling on treatment with aqueous TiCl_3 in basic media to give pinacols. Thus, PhCHO when treated with 15% aqueous TiCl_3 in alkaline MeOH gave a mixture of dl/meso- $[\text{PhCH(OH)}]_2$ and PhCH_2OH [445]. Aqueous TiCl_3 has been observed to promote the synthesis of substituted pyridyl glycols. As such, RCOR' ($\text{R} = 2,4\text{-pyridyl}$, $\text{R}' = \text{H, Me}$) reacts with R^2COR^3 [$\text{R}^2 = \text{R}^3 = \text{Me}$; $\text{R}^2\text{R}^3 = (\text{CH}_2)_4, (\text{CH}_2)_5$; $\text{R}^2 = \text{H}$, $\text{R}^3 = \text{Me, Et, Ph}$] to yield $\text{HOCRR}'\text{CR}^2\text{R}^3\text{OH}$ and $\text{HOCRR}'\text{CRR}'\text{OH}$ [446].

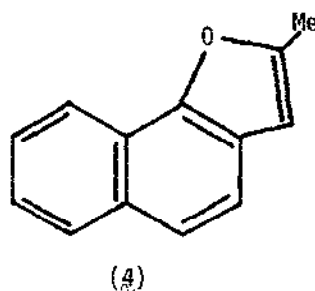
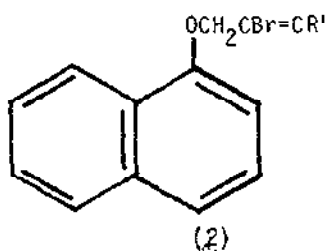
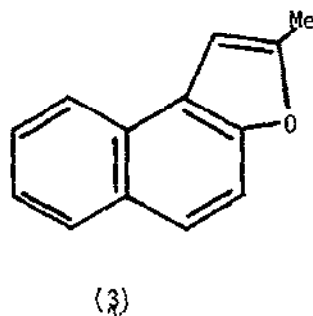
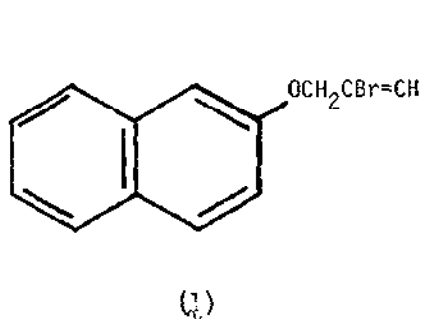
A Monte Carlo investigation of the adsorption of BeR_2 and R_2AlCl ($\text{R} =$ organic radical) on the surface of TiCl_3 crystals revealed that physical adsorption determines the quantitative composition of centers. In the subsequent stage of chemisorption, these centers may undergo rearrangement to stereospecific active polymerization centers [447].

(ii) TiCl_4

Titanium tetrachloride has been incorporated into reaction systems for catalysing debromination and hydrocyanation reactions, as well as in syntheses and polymerization.

The debromination of the vic-dibromides $\text{RCHBrCHBrR}'$ [$\text{R} = \text{H}$, $\text{R}' = n\text{-octyl}$, EtCOCH_2 , EtCH(OH)CH_2 ; $\text{R} = \text{Pr}$, $\text{R}' = \text{Bu}$; $\text{RR}' = (\text{CH}_2)_6$] with zinc and a catalytic amount of TiCl_4 in THF produced 82-91% $\text{RCH=CHR}'$ [448]. Ito and coworkers [449] have reported the conjugate hydrocyanation of α,β -unsaturated ketones via nucleophilic β -addition of Me_3CNC onto an enone activated by TiCl_4 , followed by β -elimination of the tert-butyl cation to give a β -cyanoketone. Thus, reaction of $\Delta^{4(10)}$ -octalin-3-one and 9-methyl- $\Delta^{4(10)}$ -octaline-3-one with $\text{TiCl}_4\text{-Me}_3\text{CNC}$ gave a 9:1 mixture of trans- and cis-10-cyano-octalin-3-one and a 7:3 mixture of trans- and cis-10-cyano-9-methyl-octalin-3-one, respectively. Trialkylboranes and lithium acetylides readily form trialkyl-(1-alkynyl)borates, which can subsequently react with orthoesters in the presence of TiCl_4 followed by $\text{H}_2\text{O}_2/\text{NaOH}$ oxidation to yield α,β -unsaturated carbonyl compounds. Reaction of

$\text{PhC}=\text{CBPr}_3\text{Li}$ with $\text{HC}(\text{OEt})_3$ in the presence of TiCl_4 , followed by oxidation with 70% H_2O_2 and 3M aqueous NaOH , afforded $\text{Pr}_2\text{C}=\text{CPhCHO}$ in 82% yield [450]. TiCl_4 promotes the rearrangement of naphthyl ethers. Specifically, the naphthyl ethers (1) and (2) ($\text{R}' = \text{H}, \text{Me}$) rearrange to give the naphthofurans (3) and (4), respectively [451]. Jenson [452] has reported on the quaternary systems



$\text{M}/\text{MCl}_4/\text{X}_8/\text{Al}_2\text{Cl}_6$, for which $\text{M} = \text{Ti}, \text{Zr}$ and $\text{X} = \text{S}_8, \text{Se}_8$.

An infrared spectral study of complex catalysts based on TiCl_4 and AlR_2Cl ($\text{R} = \text{Me}, \text{Et}$) immobilized on polymer supports has elucidated the structures of the active sites which catalyse olefin polymerization [453]. Several other catalyst systems incorporating an organoaluminum component and a titanium-halide containing component have been investigated for olefin polymerization. These include the polymerization of 1-olefins catalysed by a $\text{R}_n\text{AlX}_{3-n}$ ($\text{R} = \text{C}_{1-6}$ alkyl; $\text{X} = \text{Cl}, \text{Br}$; $\text{N} = 1, 2$)/methylallyl halide/ TiCl_4 system [454], the copolymerization of butadiene with isoprene in the presence of 1:0.1:2 $\text{VOCl}_3/$

$\text{TiCl}_4/\text{Al}(\text{Bu}^i)_3$ [455], and the copolymerization of butadiene with propylene catalysed by the 1-phenylethanone/ $\text{TiCl}_4/\text{Al}(\text{Bu}^i)_3$ system [456]. The polymerization rate of isoprene on $\text{TiCl}_4/\text{AlR}_3$ /electron donor/unsaturated compound in isopentane or toluene depends on the nature of the solvent and the presence of an unsaturated compound [457]. A study of the polymerizations of ethylene, propylene, 1-hexene, and 1,3-butadiene over a SiO_2 -supported TiCl_4 catalyst using AlEt_2Cl or AlEt_3 as the reducing agent established a correlation between the oxidation states of titanium and the polymerization activities of the monomers [458]. Similar catalytic systems (i.e., $\text{TiCl}_4/\text{AlR}_n\text{X}_{3-n}$) have been used in the polymerization of α -olefins [459, 460], butadiene [461], and ethylene [462, 463].

A mathematical procedure to elucidate the lattice disorder by stacking faults in polycrystalline solids was employed to study samples of MgCl_2 activated by ball-milling for various times in the presence of TiCl_4 [464]. This chloride has also been observed to catalyse the polymerization of cyclopentadiene at 77-165K [465].

Chien and coworkers [466, 467, 468] have performed an extensive investigation of a magnesium chloride supported high-mileage catalyst system for the polymerization of propylene. The chemical composition of the catalyst was determined at every stage of its preparation [466], as well as the physical state [467]. The catalyst system involves the ball-milling of MgCl_2 in the presence of BzOEt , followed by reaction with *p*-cresol and AlEt_3 and final mixing with TiCl_4 .

d. Bromides and Iodides

Thermal and x-ray phase analysis data for the TiBr_4 - TiI_4 system were employed to construct a phase diagram. Continuous solid solutions are formed with a minimum melting point at ca. 305K and ca. 16 mole% TiI_4 . Also, it was established that the cubic lattice parameter depends on solid solution composition [469].

6.9 TITANIUM HYDRIDES

Multireference double excitation (MRD-CI) calculations were performed on the low-lying electronic energy levels of TiH to tentatively assign some spectral data. Also, the calculated dissociation energy of TiH agrees well with previously obtained data [470]. Calculations of the energy bands of model supercells where the hydrogen atoms occupy various tetrahedral sites of the face-centered cubic lattice were made for TiH_x , where $x = 0, 0.25, \dots, 1.75, 2$.

The Fermi level does not shift with respect to the d bands inasmuch as one new state is formed below the Fermi level per hydrogen atom. The tetragonal distortion of TiH_x with $1.8 < x < 2$ is presumably due to a Jahn-Teller effect as a sharp peak in the density of states at the Fermi level is present for TiH_2 and $TiH_{1.75}$, not clearly present for $TiH_{1.5}$ [471].

The phase transitions in TiH_2 were examined by nmr spectroscopy. At room temperature, the crystals are face-centered cubic; at 292K, the crystals transform to the tetragonal phase via reordering of the hydrogen atoms; at 310K the lattice distortions present appear indicative of a fluctuational structure [472]. Another nmr investigation of the structure of TiH_2 has been reported by Kudabaev et al. [473]. Nmr spectroscopy was employed to determine the temperature and concentration dependences of the spin-lattice relaxation time (T_1), the Knight shift (K), and lattice parameters of TiH_x and ZrH_x [474]. The low-frequency dependence of the spin-lattice relaxation rate of spin-1/2 nuclei moving by translational diffusion on a simple cubic lattice has been measured for H in γ - $TiH_{1.63}$ at 725K. The data fit the relationship in (6), that is

$$T_1^{-1}(\omega_0) = T_1^{-1}(0) - A\omega_0^{1/2} \quad (6)$$

expected for three-dimensional solids [475]. A helium-bath cryostat and a probe for nmr studies at 4.2K have been designed and tested for $TiH_{1.77}$ and Th_2H_5 [476].

The electrochemical formation of titanium hydride (TiH_x) has been studied as a function of current density and time. X-ray diffraction patterns revealed that a specific hydride is formed at each current density, independent of the duration of the formation process [477]. A report of hydrogen permeation through α -titanium and an electrolytically hydrided titanium has appeared, and it was found that the hydriding facilitates hydrogen permeation [478].

A comparison of the pyrotechnic properties of $TiH_x/KClO_4$ and $ZrH_x/KClO_4$ blends has been cited [479]. Also, the shock wave response of $TiH_x/KClO_4$ has been reported [480]. It was found that the resistance of TiH_2 powder, as well as ZrH_2 , toward high-temperature oxidation in air is not very high. At 523K, oxygen begins to permeate the TiH_2 lattice, accompanied by oxyhydride formation. The formation rate of TiO_2 was found to be limited by diffusion of oxygen through the TiO_2 layer, by gaseous products formed via interaction with hydrogen (<923K), and by the presence of H_2O [481].

Several intermetallic hydride compounds $M_2Ti_yH_x$ have been prepared and/or investigated. Laves phase $(Cl_5)Be_2Ti$ forms a hydride with approximate composition Be_2TiH_3 [482]. Co_2Ti reacts with hydrogen with combustion to yield $CoTi_2H_x$ ($x \leq 3$). When heated at 573-773K in argon or hydrogen, $CoTi_2H_3$ produces

CoTi_2 , CoTi and H_2 [483]. The hydrogenation kinetics of activated FeTi were examined via comparison of experimental data and theoretical results. The rate-controlling step is thought to be the chemisorption of hydrogen molecules on the metal surface up to a reacted fraction of ca. 0.4, involving the nucleation and growth of the hydride. As the reacted fraction increases (≥ 0.4), the rate-controlling step changes to hydrogen diffusion through the hydride phase [484]. Inelastic neutron scattering techniques were employed to measure the local hydrogen vibrations in FeTi_x , for $x = 0.6$ (α -phase), 0.94 (β_1 -phase), 1.4 (β_2 -phase), and 1.86 (γ -phase) [485]. The electronic structures of FeTiH and FeTiH_2 have been examined employing the APW method with warped-muffin tin corrections and the tight binding CPA methods [486, 487].

High-resolution Fourier transform proton nmr has been utilized to determine the hydrogen Knight shift (K_H) and the magnetic susceptibility (χ_m) of thin polycrystalline foils of $(\alpha, \alpha')\text{-Nb}_{1-y}\text{Ti}_y\text{H}_x$ ($0 \leq y \leq 0.5$; $0 \leq x \leq 1$). Both K_H and χ_m depend on the valence electron concentration, in agreement with APW band structure calculations and the application of the rigid band model [488]. High-resolution quasi-elastic neutron scattering examined hydrogen diffusion in the Laves phase $\text{Mn}_{1.8}\text{Ti}_{1.2}\text{H}_3$ at momentum transfers Q 0.17-1.95 \AA^{-1} at 100-375K. The dynamics of hydrogen diffusion on a microscopic scale are governed by the existence of energetically different interstitial sites and by blocking effects due to the high hydrogen concentration. This behavior was described in terms of three motional states where hydrogen atoms a) propagate over the energetically higher sites, b) are at rest in structural traps, and c) exhibit a rapid local motion [489]. The magnetic properties (by susceptibility, magnetization, and Moessbauer effect measurements) of the paramagnetic C14 Laves phase $\text{Ti}_{0.40}\text{Mn}_{0.52}$, the ψ phase $\text{Ti}_{0.46}\text{Mn}_{0.54}$, the ϕ phase $\text{Ti}_{0.48}\text{Mn}_{0.52}$ and their ferromagnetic hydrides have been studied by Hempelmann et al. [490]. The onset of ferromagnetism in the ternary hydrides is presumably due to the volume expansion which causes a narrowing of the d bands and thus increases the density of states at the Fermi level upon hydrogenation.

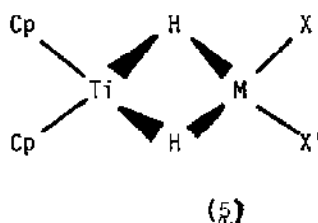
Proton nmr spectroscopy was used to study the behavior of hydrogen in $\text{V}_{0.40}\text{Ti}_{0.60}\text{H}_{0.90}$, $\text{V}_{0.60}\text{Ti}_{0.40}\text{H}_{0.79}$ and $\text{V}_{0.80}\text{Ti}_{0.20}\text{H}_{0.77}$ at 125-425K. A phase separation was observed, with the β - and γ -phases predominating [491]. The electronic structures of TiH_x and $\text{V}_y\text{Ti}_{1-y}\text{H}_x$ were elucidated from positron annihilation results, based on s- and d-like electron number changes. The author's [492] interpretation appears consistent with results from band structure calculations.

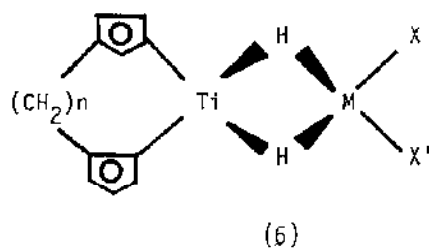
The proton line shapes, spin-lattice and rotating-frame relaxation times, and Knight shifts were determined for crystalline $\text{CuTiH}_{0.94}$, $\text{CuTi}_2\text{H}_{1.9}$ and

$\text{CuTi}_2\text{H}_{2.63}$, and amorphous $\alpha\text{-CuTiH}_{1.4}$. The line shape results presumably indicate that protons occupy Ti_4 interstitial sites in $\text{CuTiH}_{0.94}$ and $\text{CuTi}_2\text{H}_{1.9}$ while both Ti_4 and Cu_2Ti_4 sites are occupied in $\text{CuTi}_2\text{H}_{2.63}$. The proton second moment results imply octahedral and tetrahedral site occupancy in $\alpha\text{-CuTiH}_{1.4}$. The hydrogen diffusion behavior was also investigated [493]. In addition, activation energies for hydrogen diffusion and the densities of electronic states at the Fermi level were obtained for these compounds [494].

The electronic and magnetic behavior of the hexagonal (C14) and cubic (C15) allotropes of the $\text{Cr}_{1.8}\text{Ti-H}$ [495] and $\text{Cr}_{1.8+0.1}\text{Ti-H}_2$ [496] systems have been examined employing proton nmr and magnetic susceptibility measurements. For these systems there is an unusual increase in the density of states at the Fermi surface with increasing hydrogen/metal ratio, apparently due to changes in the d -electron states although a high concentration of s -electron states at the Fermi level is also present. Originally, an orthorhombic structure was assigned to the non-stoichiometric $\text{Cr}_{1.8}\text{TiH}_{3.6}$ compound. More recently, Johnson and coworkers [497] have suggested that this solid consists of two hydride phases, an α' Laves having a composition $\text{Cr}_{1.8}\text{TiH}_{2.8}$ and a face-centered cubic phase with a much higher hydrogen content, $\text{Cr}_{1.8}\text{TiH}_{5.3}$. The high hydrogen concentration phase possesses a disordered fluorite structure. Pressure-composition-temperature properties were determined for the system, and a reversed phase diagram proposed. The proton relaxation times, measured by ^1H nmr, of the low (α -phase) and intermediate (α' -phase) hydrogen concentrations in CO-stabilized Cr_2TiH_x with both hexagonal (C14) and cubic (C15) Laves structures have been determined. The results infer rapid proton diffusion for all phases at $>200\text{K}$, though large differences in diffusion activation energies were observed. This behavior is structure-sensitive and is associated with variations between interstitial site occupancies and diffusion pathways for the C14 and C15 structures [498].

Bulichev and coworkers [499] have examined the rate of homogeneous catalytic isomerization of α -alkenes by complexes (5) ($\text{M} = \text{B}, \text{Al}; \text{X}, \text{X}' = \text{H}, \text{halo}$) or (6) ($\text{M} = \text{B}, \text{Al}; \text{X}, \text{X}' = \text{H}, \text{halo}; n = 1-3$). Only (5) or (6) ($\text{M} = \text{Al}$)





having nonrigid ligand environments and containing Al-H bonds exhibit catalytic activity. The reaction presumably involves a) coordination of the alkene at the six-coordinate Al atom, followed by b) insertion of the alkene into the Al-H bond to yield a hydroalumination product; then, c) isomerization involves coordination of the parent alkene to the hydroaluminated product giving a six-membered transition state, which leads to d) β -elimination of the isomeric alkene and the original hydroaluminated intermediate species.

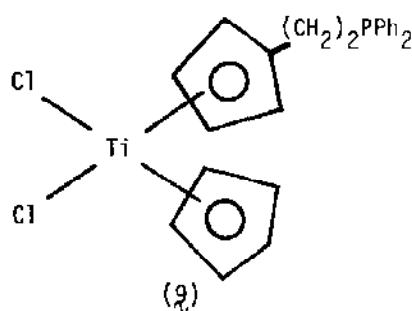
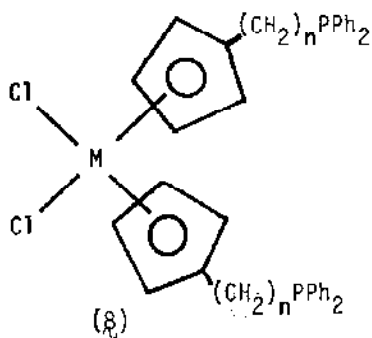
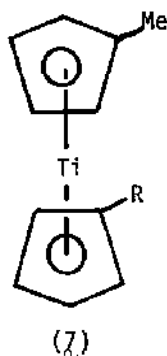
6.10 COORDINATION COMPLEXES OF TITANIUM

a. Cyclopentadienyl Complexes

(i). Preparation, Characterization and Structure

A low-temperature infrared spectral study of π -cyclopentadienyl derivatives of titanium has been reported in the Russian literature [500]. Manzer [501] has reported the 1:2 reaction of TiCl_3 with TiCp (Cp = cyclopentadienyl) in THF to give >94% yield of the titanium(III) complex Cp_2TiCl . Proton spin lattice relaxation times have been measured to determine the rotation barriers of the cyclopentadienyl ring in $(\eta^5\text{-2,4-cyclopentadien-1-yl})\text{trichloro titanium(IV)}$ (9.6 kJ-mole^{-1}) and $\text{di-}\eta^5\text{-2,4-cyclopentadien-1-yl titanium(IV) pentasulfide}$. In the latter complex, two Ti processes were observed, with barriers of 8.9 and 7.7 kJ-mole^{-1} proposed for the axial and equatorial ring, respectively [502]. A negative chemical ionization mass spectral investigation of organometallic complexes of titanocene with methane revealed the complementarity and specificity of this technique toward positive mass spectra by electron impact. Some chlorinated titanocene complexes exhibit an ion-molecule attachment peak corresponding to $[\text{M} + \text{Cl}]^+$ [503]. Titanocene cations have been generated in a novel gas-phase metal switching reaction between Ti^+ and a common metallocene (NiCp_2 or FeCp_2) [504].

The new 1,1'-ring-substituted titanocene dihalide complexes $(R_3EC_5H_4)_2TiX_2$ (R = alkyl; E = C, Si, Ge; X = halo, SCH) have been prepared by known synthetic methods [505]. Analytical results, chemical and physical properties and proton nmr spectral data were also reported. The highly reactive and pyrophoric titanium(II) complexes $Ti(CpMe)(CpR)$ (R = H, Me) (**7**) were synthesized via reduction of $Ti(Cl)_2(CpMe)(CpR)$ by potassium naphthalide in THF at $\sim 193K$ [506]. The crystal and molecular structures of $(\eta^5-EtC_5H_4)_2TiCl_2$ were determined by x-ray structure analysis, for which the Ti-Cl bond length is $2.370(2)$ Å [507]. Two complexes, $Cl_2Ti[(\eta^5-C_5H_4)(CH_2)_nPPH_2]_2$ (**8**) and $Cl_2CpTi[(\eta^5-C_5H_4)(CH_2)_2(PPH_2)]$ (**9**), were prepared in good yields from $TiCl_4$ or $CpTiCl_3$, respectively, and $Ph_2P(CH_2)_n(C_5H_4)Li$ (n = 0, 2). The complexes (**8**) and (**9**) undergo chemical reduction with aluminum, electrochemical reduction in a CO atmosphere, and reaction with transition metal carbonyls to give heterobimetallic complexes. The low-energy photoelectron spectra of Cp_2TiL_2



(L = CO, F, Cl, Br) have been studied by semiempirical MO calculations of the CNDO/INDO type in the framework of many-body perturbation theory (based on

Green's function formalism). The electronic structure of the dihalide complexes were rationalized on the basis of a MO model that accounts for the interaction strength between the cyclopentadienyl π orbitals and the halide lone-pair and σ combinations [509].

Reaction between $\text{Cp}_2\text{Ti}(\text{CO})_2$ and $[\text{CpMo}(\text{CO})_2]_2$ in THF gave $\text{Cp}_2\text{Ti}(\text{THF})\text{OCMo}(\text{CO})_2\text{Cp}$, which contains a μ_2 - η^1 metal carbonyl bridge between Ti and Mo [510]. Electronic and molecular structures were determined for the octahedral $\text{Cp}_6\text{M}_6(\mu_3\text{-A})_8$, trigonal-bipyramidal $\text{Cp}_5\text{M}_5(\mu_3\text{-A})_6$ and tetrahedral $\text{Cp}_4\text{M}_4(\mu_3\text{-A})_4$ clusters. EHMO calculations were performed in order to explain the structure and magnetic properties of $\text{Cp}_6\text{Ti}_6(\mu_3\text{O})_8$ [511]. Polymers have been synthesized from reaction (interfacial or aqueous solution polymerization) of Cp_2TiCl_2 and various xanthene dyes (e.g., erythrosin B, fluorescein, Bengal red, etc.). The polymers were found to be soluble in dipolar, aprotic solvents though not in aqueous or simple organic solvents. The polymers can be used as fluorescent dyes for paper and textiles, as dope dyes for plastics, and as pigments for latex paints [512].

The synthesis and an x-ray diffraction study of $(\eta\text{-C}_5\text{Me}_5)_2\text{Ti}(\eta\text{-C}_2\text{H}_4)$ (Figure 4) is reported by Cohen and coworkers [513]. The complex in Figure 4 participates in a wide variety of stoichiometric and catalytic reactions, including the catalytic conversion of C_2H_4 to butadiene and C_2H_6 , and the catalytic isomerization of alkenes which occurs via a lithium hydride intermediate species. The standard enthalpies of formation for the crystalline

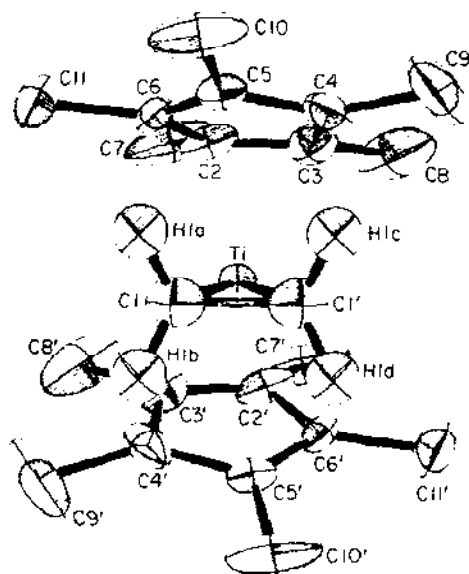
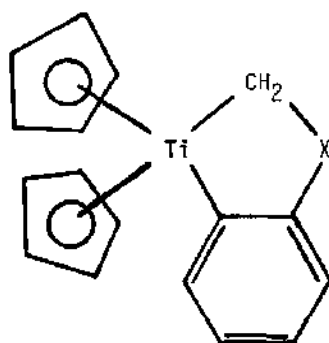


FIGURE 4: Structure of $(\eta\text{-C}_5\text{Me}_5)_2\text{Ti}(\eta\text{-C}_2\text{H}_4)$, revealing 50% thermal probability level [513].

complexes $(\eta^5\text{-C}_5\text{H}_5)_2\text{Ti}(\text{Ph})_2$ [$\Delta H_f^\circ = 294.4 \pm 8.8 \text{ kJ-mole}^{-1}$] and $(\eta^5\text{-C}_5\text{H}_5)_2\text{Ti}(\text{Fc})_2$ (Fc = ferrocenyl; $\Delta H_f^\circ = 520.4 \pm 12.0 \text{ kJ-mole}^{-1}$) were obtained by reaction-solution calorimetry [514]. Reaction between Cp_2TiCl_2 or $(\eta^5\text{-C}_5\text{H}_4\text{Me})_2\text{TiCl}_2$ and aryllithium compounds (aryl = substituted phenyl) produces $(\eta^5\text{-C}_5\text{H}_5)_2\text{Ti}(\text{aryl})_2$ and $(\eta^5\text{-C}_5\text{H}_4\text{Me})_2\text{Ti}(\text{aryl})_2$, respectively. The complexes are stable toward hydrolysis, and reaction with HX (X = Cl, Br, F), acetyl chloride or Br_2 gave the dihalide complexes [515].

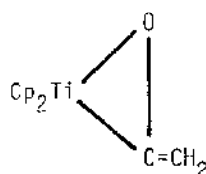
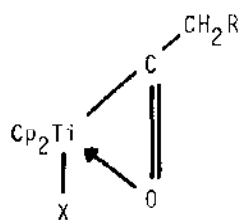
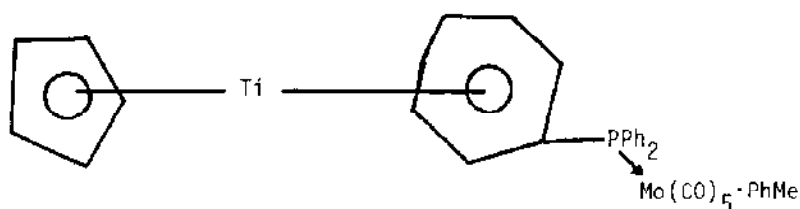
The sulfinyl carbanion $[\text{PhS}(\text{O})\text{CH}_2]^- \text{Li}^+$ reacts with $[\text{Cp}_2\text{TiCl}]_2$ and butyllithium to give a 31% yield of complex (10) (X = S), which on treatment with MeOSO_2F followed by NH_4BF_4 gave (10) with X = $\text{MeS}^+\text{BF}_4^-$ [516]. The addition



(10)

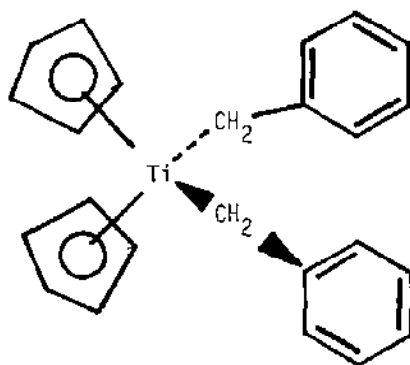
of butyllithium to $(\eta^5\text{-C}_5\text{H}_5)_2\text{Ti}(\eta^7\text{-C}_7\text{H}_7)$ and subsequent reaction with Ph_2PCl affords the titanium(II) phosphine complex $(\eta^5\text{-C}_5\text{H}_5)_2\text{Ti}(\eta^7\text{-C}_7\text{H}_6\text{PPh}_2)$, which exhibits coordinating capabilities. A carbonyl ligand is displaced from $\text{Ni}(\text{CO})_4$, $\text{Fe}(\text{CO})_5$ or $\text{Mo}(\text{CO})_6$ when reacted with the above phosphine complex to yield the bimetallic complexes $(\eta^5\text{-C}_5\text{H}_5)_2\text{Ti}(\eta^7\text{-C}_7\text{H}_6\text{PPh}_2\text{M}(\text{CO})_n)$ (M = Ni, Fe, Mo; n = 3, 4, 5, respectively) (e.g., (11)). The +2 oxidation state of titanium remains intact in complex (11). The crystal structure of complex (11) shows the Mo atom to be roughly in the C_7 -ring plane at a nonbinding distance of $5.442(2) \text{ \AA}$ from the Ti atom. The $\text{Ph}_2\text{PMo}(\text{CO})_5$ group causes a shortening of the Ti- C_5 ring distance and a lengthening of the Ti- C_7 ring distance. The coordination about Mo corresponds to an octahedron with a long Mo-P bond length and a short trans-Mo-C(5) bond distance [517].

Dehydrohalogenation of the haloacyl complex (12) (X = Cl, Br) with strong



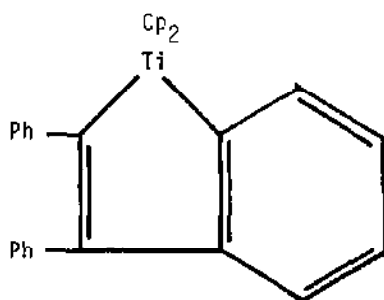
bulky bases produces the ketene complex (13) ($R = H$); the latter complex exists in two forms, which appear to be $\eta^2(C,O)$ bound but differ in their mode of aggregation. Both isomers react with ethylene and acetylene to form oxotitanacyclopentanes [518].

A theoretical study of the Tebbe reagent $Cp_2TiCH_2AlClMe_2$ was done by ab initio (STO-3G) calculations on the model complex $H_2TiCH_2AlClH_2$. The calculated structure of the model shows that Lewis acid $AlClH_2$ to be strongly bound to the titanium alkylidene [519]. The thermally stable metallacycle (14) has been obtained [520]. A novel route to the synthesis of titanaindene and titanacyclopentadiene complexes has been reported by Shur et al. [521]. The

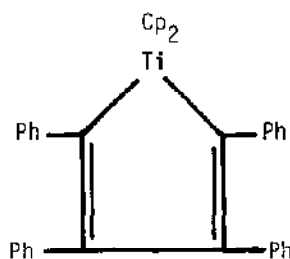


(14)

titanaindene complex (15) was prepared by direct reaction of tolan with Cp_2Ti and benzene, generated in the system $\text{Cp}_2\text{TiCl}_2 + \text{Mg} + o\text{-fluorobromobenzene}$ in THF. The treatment of Cp_2TiCl_2 with magnesium in THF containing tolan ($\text{Cp}_2\text{TiCl}_2/\text{Mg}/\text{Ph}_2\text{C}_2 \approx 1 : 1 : 2$) gave the titanacyclopentadiene complex (16) [521]



(15)



(16)

Cp_2TiL and TiL_3 ($\text{L} = \text{PhN}=\text{CPhCPh}=\text{NPh}$) have been prepared and characterized by nmr, infrared and electronic spectra, and magnetic moment measurements [522]. The photolysis of $\text{Cp}_2\text{Ti}(\text{C}^{18}\text{O})_2$ in hexane containing excess C^{16}O results in facile formation of $\text{Cp}_2\text{Ti}(\text{C}^{16}\text{O})_2$, revealing that the carbonyl ligands are photolabile. Photolysis of $\text{Cp}_2\text{Ti}(\text{CO})_2$ in hexane containing excess PF_3 gave 86% $\text{Cp}_2\text{Ti}(\text{PF}_3)_2$. $\text{Cp}_2\text{Ti}(\text{CO})(\text{PEt}_3)$ and $\text{Cp}_2\text{Ti}(\text{CO})(\text{PPh}_3)$ were also prepared. The phosphine ligands in these complexes are very labile in solution and react with

a variety of reagents (e.g., PF_3 , $\text{P}(\text{OPh})_3$, $\eta^2\text{-PhC}\equiv\text{CPh}$, $\eta^2\text{-C}_6\text{F}_5\text{C}\equiv\text{CC}_6\text{F}_5$). The crystal structures of $\text{Cp}_2\text{Ti}(\text{PF}_3)_2$ and $\text{Cp}_2\text{Ti}(\text{CO})(\text{PPh}_3)$ have been determined by x-ray diffraction, as depicted in Figures 5 and 6 [523].

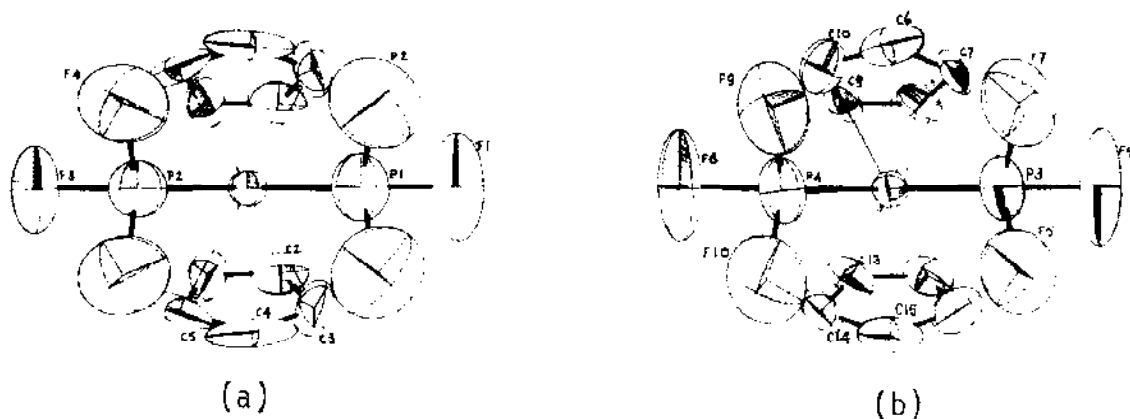


FIGURE 5: Structure of $\text{Cp}_2\text{Ti}(\text{PF}_3)_2$, depicting (a) one of the two independent molecules in the asymmetric unit, residing on a crystallographic mirror plane; and (b) a second molecule which possesses no crystallographically imposed symmetry [523].

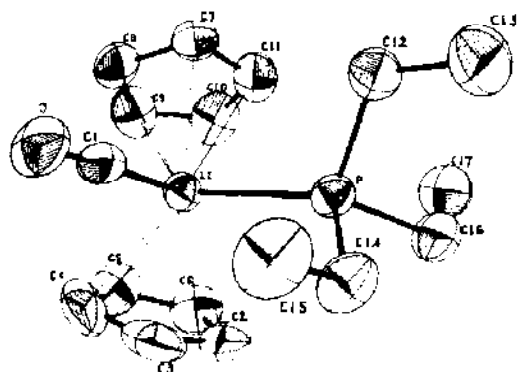


FIGURE 6: Molecular structure of $\text{Cp}_2\text{Ti}(\text{CO})(\text{PET}_3)$, with atoms represented by their 50% probability ellipsoids for thermal motion [523].

The crystal and molecular structure of $\text{Cp}_2\text{Ti}(2,4,6\text{-Cl}_3\text{OPh})_2$ has been reported [524]. The synthesis of $[\text{L}_2\text{Ti}(\text{phenoxy})_2(\text{amide})_2]$ ($\text{L} = \text{Cp}$, indenyl) occurs via reaction of bis(amide)-bis(polyhydricphenol)titanium(IV) complexes with cyclopentadiene or indene in THF/ROH. Upon heating, these complexes yield $\text{L}_2\text{Ti}(\text{phenoxy})_2$. The infrared and UV spectra of $[\text{L}_2\text{Ti}(\text{phenoxy})_2(\text{amide})_2]$ suggest π -electron delocalization from the Cp or indenyl rings to the phenoxy ring via the Ti d-orbitals [525].

Several complexes containing aryloxy ligands have been synthesized and characterized. Among them are $(\eta^5\text{-RC}_5\text{H}_4)_2\text{Ti}(\text{OR}')_2$ ($\text{R} = \text{Et}$, Pr ; $\text{R}' = \text{p-R}^2\text{C}_6\text{H}_4$, $2,4,6\text{-Cl}_3\text{C}_6\text{H}_2$; $\text{R}^2 = \text{H}$, Me , CMe_3 , Cl , Br , I), which were prepared via aryloxylation of $(\eta^5\text{-RC}_5\text{H}_4)_2\text{TiX}_2$ with phenols $\text{R}'\text{H}$. The relation between the nmr chemical shifts of $(\eta^5\text{-RC}_5\text{H}_4)_2\text{Ti}(\text{OR}')_2$ and the electronegativities of the atoms and steric hinderance have been discussed [526, 527]. The ^{13}C nmr chemical shifts of the Cp ring in $\text{Cp}_2\text{M}(\text{p-RC}_6\text{H}_4\text{O})_2$ ($\text{M} = \text{Ti}$, Zr , Hf ; $\text{R} = \text{H}$, MeO , Cl , Br , I) have been observed [528] to move upfield as the M varies from Ti to Hf. Furthermore, LFER are observed for the chemical shifts of the corresponding carbon atoms in the three series. Separation of several $\text{Cp}_2\text{Ti}(\text{aryloxy})_2$ complexes over silica gel has been accomplished by thin-layer chromatography [529].

The preparation, structure and properties of dicyclopentadienyloxalato-titanium(IV) and dicyclopentadienylbis(hydrogen maleato)titanium(IV) have been reported. Both complexes are monomeric, the oxalato ligand acting as a bidentate chelating ligand, and each of the hydrogen maleate groups is bonded via one oxygen atom to the titanium atom [530]. An x-ray analysis of $(\eta^5\text{-C}_5\text{H}_5)_2\text{Ti}(\text{OBz})_2$ reveals a distorted tetrahedral structure in which Ti is attached to two $\eta\text{-C}_5\text{H}_5$ groups and two monodentate benzoate ligands. The relatively short Ti-O bond lengths and the large Ti-O-C bond angles are suggestive of Ti achieving an effective 18-electron configuration via Ti-O π -bonding [531]. The synthesis and structure determination of $\text{Cp}_2\text{Ti}(\text{OBz})_2$ has been reported by Hoffman [532], along with a theoretical study of ligand-bridged transition metal dinuclear organometallic complexes.

The crystal structure of $(\pi\text{-C}_5\text{H}_5)\text{Ti}(\text{NO}_3)_3$ (Figure 7) indicates an approximate pentagonal-bipyramidal geometry with bidentate NO_3 ligands and the C_5H_5 in an axial position [533]. Some sulfanilates, metanilates and *o*-toluidine-sulfonates of titanium(IV) have been synthesized. Thus, the treatment of $(\eta^5\text{-C}_x\text{H}_y)_2\text{TiCl}_2$ ($\eta^5\text{-C}_x\text{H}_y$ = cyclopentadienyl, indenyl) with the appropriate acid yields $(\eta^5\text{C}_x\text{H}_y)_2\text{TiR}_2$ ($\text{R} = \text{O}_3\text{SC}_6\text{H}_4\text{NH}_2\text{-p}$, $\text{O}_3\text{SC}_6\text{H}_4\text{NH}_2\text{-m}$, $\text{O}_3\text{SC}_6\text{H}_4\text{Me}(\text{NH}_2)\text{-3,4}$) [534].

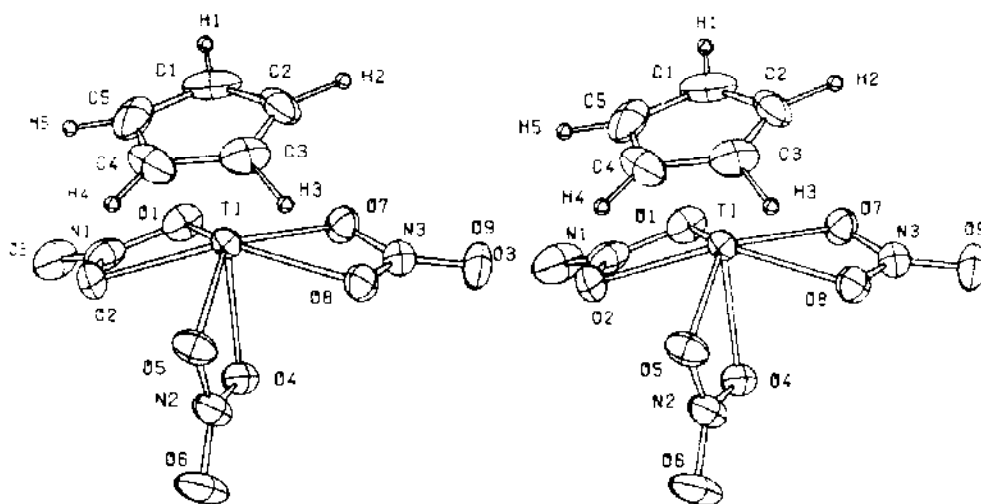


FIGURE 7: Structure of $(\pi\text{-C}_5\text{H}_5)\text{Ti}(\text{NO}_3)_3$, with atoms represented by their 30% thermal probability ellipsoids [533].

The crystal structures of $(\eta^5\text{-C}_5\text{H}_5)_2\text{Ti}(\text{O}_2\text{CC}_6\text{H}_5)_2$ (17), $(\eta^5\text{-C}_5\text{H}_5)_2\text{Ti}(\text{O}_2\text{CC}_5\text{H}_6\text{CO}_2)_2$ (18), and $(\eta^5\text{-C}_5\text{H}_5)_2\text{Ti}(\text{O}_2\text{CC}_4\text{H}_6\text{CO}_2)_2$ (19) have been determined, along with variable-temperature (3-12K, 298K) EPR spectral data which were interpreted in terms of the presence of intramolecular magnetic exchange interactions in the binuclear titanium(III) complexes [535]. The hydrolysis of $(\pi\text{-C}_5\text{H}_5)_2\text{TiCl}_2$ at $\text{pH} > 3.5$ yields the trinuclear complex $(\pi\text{-C}_5\text{H}_5)_2\text{TiCl-O-Ti}(\pi\text{-C}_5\text{H}_5)\text{Cl-O-TiCl}(\pi\text{-C}_5\text{H}_5)_2$ (Figure 8); it can be isolated in the crystalline state by treating $(\pi\text{-C}_5\text{H}_5)_2\text{TiCl}_2$ with Ag_2O and H_2O in CHCl_3 [536].

The preparation and characterization of thiol derivatives of bis(η^5 -methylcyclopentadienyl)titanium(IV) have been reported by Arora and

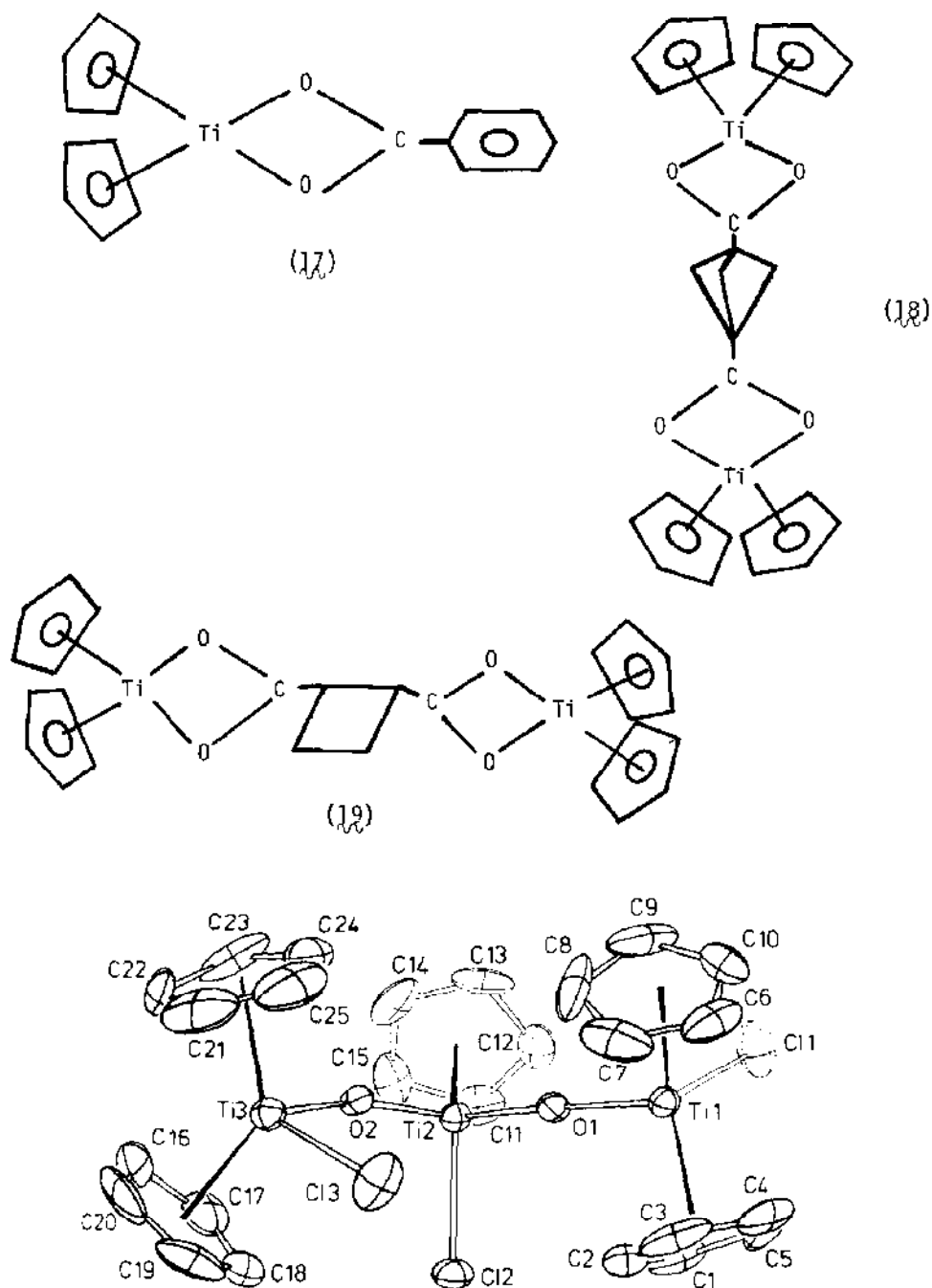
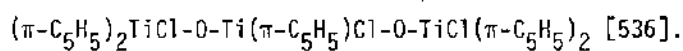


FIGURE 8: Structure of the trinuclear complex



Multani [537]. Reaction of $(\eta^5\text{-MeC}_5\text{H}_4)_2\text{TiCl}_2$ with various thiols (SR) results in the formation of $(\eta^5\text{-MeC}_5\text{H}_4)_2\text{Ti}(\text{SR})_2$ ($\text{R} = \text{Me, Et, Pr, Me}_2\text{CH, Me}_2\text{CHCH}_2$). The dithienyl complex $(\eta^5\text{-C}_5\text{H}_5)_2\text{Ti}(\alpha\text{-thienyl})_2$ has been prepared in 78.5% yield via the treatment of $(\eta^5\text{-C}_5\text{H}_5)_2\text{TiCl}_2$ with α -thienyllithium. Reaction of the dithienyl complex with I_2 , Br_2 or CCl_4 gave $(\eta^5\text{-C}_5\text{H}_5)_2\text{TiX}_2$ ($\text{X} = \text{I, Br, Cl}$), while reaction with RCO_2H gave 63–75% $(\eta^5\text{-C}_5\text{H}_5)_2\text{Ti}(\text{O}_2\text{CR})_2$ ($\text{R} = (\text{O}_2\text{N})_2\text{C}_6\text{H}_3$, C_6F_5 , CF_3 , CCl_3 , CBr_3) [538]. The crystal structure determination of $(\eta^5\text{-C}_5\text{H}_5)_2\text{Ti}(\text{SCH}_3)_2$ reveals the Ti coordination polyhedron to be a distorted tetrahedron formed by the two S atoms of the methanethiolato ligands and the centroids of the Cp rings [539].

Titanocene dichloride reacts with $\text{NaS}_2\text{CNRR}'$ in refluxing CH_2Cl_2 to yield $(\eta^5\text{-C}_5\text{H}_5)_2\text{Ti}(\text{S}_2\text{CNRR}')\text{Cl}$ and $(\eta^5\text{-C}_5\text{H}_5)\text{Ti}(\text{S}_2\text{CNRR}')_3$ ($\text{R} = \text{H, R}' = \text{cyclopentyl}$; $\text{R} = \text{Et, R}' = \text{p-tolyl}$) [540]. A similar reaction between $(\eta^5\text{-C}_5\text{H}_5)\text{TiCl}_3$ and the sodium dithiocarbamate in the appropriate metal/ligand ratio affords $(\eta^5\text{-C}_5\text{H}_5)\text{Ti}(\text{S}_2\text{CNRR}')_n\text{Cl}_{3-n}$ ($\text{R} = \text{Et, R}' = \text{p-MeC}_6\text{H}_4$; $\text{R} = \text{H, R}' = \text{cyclopentyl, cycloheptyl}$; $n = 1\text{--}3$). The physical properties of $(\eta^5\text{-C}_5\text{H}_5)\text{Ti}(\text{S}_2\text{CNRR}')_n\text{Cl}_{3-n}$ ($\text{R} = \text{Et, R}' = \text{p-MeC}_6\text{H}_4$) were interpreted in terms of a monomeric and non-electrolyte nature, in which dithiocarbamate serves as a bidentate ligand [541]. Similar preparative routes were reported by Soni and coworkers [542] for the synthesis of $(\eta^5\text{-MeC}_5\text{H}_4)\text{Ti}(\text{S}_2\text{CNRR}')_3$ and $(\eta^5\text{-C}_5\text{H}_5)\text{Ti}(\text{S}_2\text{CNRR}')_3$ ($\text{R} = \text{R}' = \text{Me, Et, Me}_2\text{CH}$; $\text{R} = \text{Me, R}' = \text{Ph}$). The O,O-diethylphosphonothioyl dithiocarbamate derivatives $(\eta^5\text{-R})_2\text{Ti}[\text{S}_2\text{CNHPS}(\text{OEt})_2]\text{Cl}$ ($\text{R} = \text{C}_5\text{H}_5, \text{MeC}_5\text{H}_4, \text{C}_9\text{H}_7$) have been synthesized and characterized by electrical conductance, magnetic measurements, infrared, nmr and UV spectroscopies [543].

Sulfuration of $(\eta^5\text{-Me}_5\text{C}_5)\text{TiCl}_2$ with Li_2S_2 results in a 55% yield of complex (20); the crystal structure was determined [544]. The chelate complexes (21) ($\text{X} = \text{S, Se}$; $\text{R} = \text{CO}_2\text{Me, CF}_3$; $\text{R}' = \text{H, Me}$) can be prepared by treating complex (20) with $\text{RC}\equiv\text{CR}$. The crystal structure of complex (21) (Figure 9) ($\text{X} = \text{S, R} = \text{CO}_2\text{Me, R}' = \text{Me}$) reveals a conventional bis(methylcyclopentadienyl)titanium moiety chelated by the S atoms of the

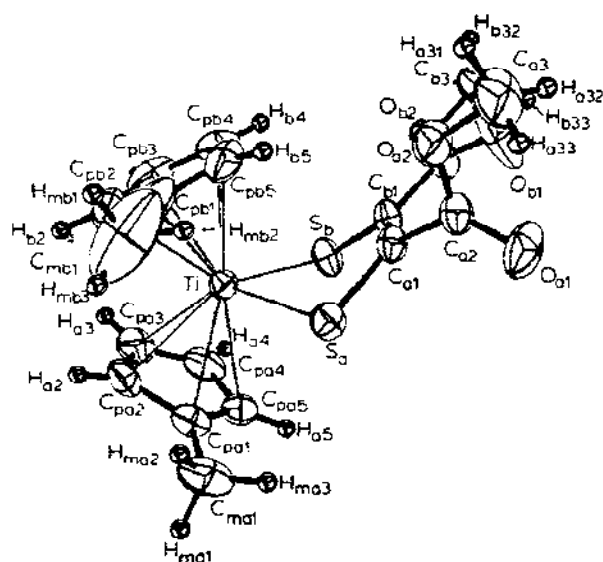
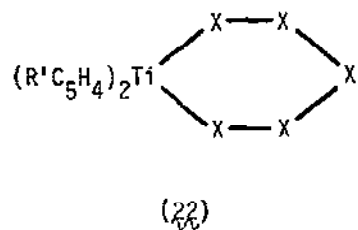
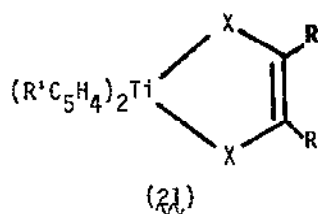
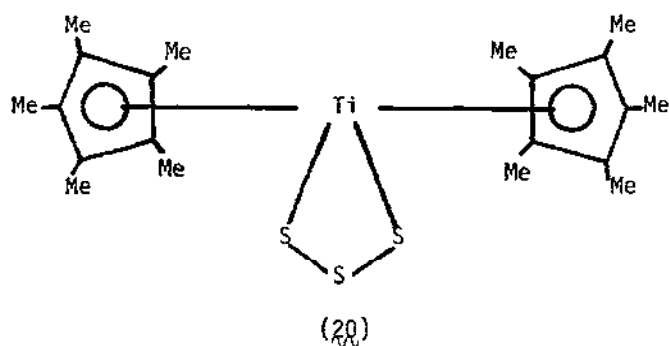
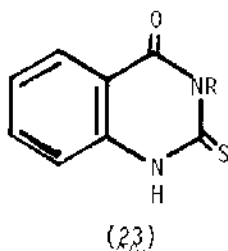


FIGURE 9: ORTEP drawing of the $(\text{CH}_3\text{C}_5\text{H}_4)_2\text{TiS}_2\text{C}_2(\text{CO}_2\text{CH}_3)_2$ molecule with thermal ellipsoids set at the 50% probability level [545].

dithiolene. Complex (21) reacts with a variety of dichloro compounds to yield ligand exchange products [545]. The titanium(IV) complexes Cp_2TiCl_2 and Cp_2TiL_2 ($\text{L} = (23)$; $\text{R} = \text{Me}, \text{Ph}, \text{o-tolC}_6\text{H}_4, \text{Cp}$) were prepared via reflux of



Cp_2TiCl_2 with L in THF. Ligands L serve as N,S bidentate chelating agents [546].

(ii). Reactions

Titanocene dichloride undergoes a variety of reactions. Reaction of Cp_2TiCl_2 with two equivalents of PhMe_2SiLi , or reaction of Cp_2TiCl_2 with one equivalent of PhMe_2SiLi , yields the titanium(III) complex $\text{Cp}_2\text{TiSiMe}_2\text{Ph}$. Highly regio- and stereo-selective silyltitanation by this species was observed with acetylenes and 1,3-dienes [547]. Cp_2TiCl_2 is known to react with α - and β -naphthol in 1:1 and 1:2 molar ratios at 353K in C_6H_6 to yield $\text{Cp}_2\text{Ti}(\text{L})\text{Cl}$ ($\text{L} = \alpha$ - and β -naphthoxy) and Cp_2TiL_2 . The latter complex can also be prepared from the sodium salts of naphthols in aqueous media [548]. In the presence of Et_3N , Cp_2TiCl_2 reacts with HOXPh to yield $\text{Cp}_2\text{Ti}(\text{OXPh})\text{Cl}$ ($\text{X} = \text{CH}_2, \text{CHMe}, \text{CH}_2\text{CH}_2$), which, when reacted with HCl , AcCl or BzCl gave Cp_2TiCl_2 . Reaction of $\text{Cp}_2\text{Ti}(\text{OXPh})\text{Cl}$ with H_2O , MeOH or EtOH produced the corresponding complexes [549]. Diphenyldiazomethane (Ph_2CN_2) reacts with $(\text{CpTiCl}_2)_n$ to yield $(\text{CpTiCl}_2)_2-(\mu\text{-N}_2\text{CPh}_2)$ and then $(\text{CpTiCl}_2)_2(\mu\text{-N}_2\text{CPh}_2)_2$, in which the Ti atoms are bridged by the hydrazonido(2-) ligands [550]. Reaction between $(\text{CpTiCl}_2)_n$ and PhN=NPh has given $(\text{CpTiCl}_2)_2(\mu\text{-NPh})(\mu\text{-N}_2\text{Ph}_2)$ (Figure 10). The x-ray analysis of this

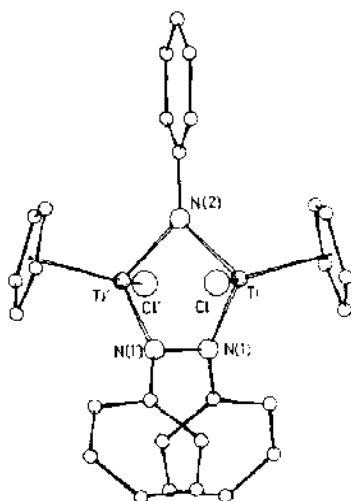


FIGURE 10: The structure of $(\text{Cp}_2\text{TiCl})_2(\mu\text{-NPh})(\mu\text{-N}_2\text{Ph}_2)$, depicting the crystallographic C_2 symmetry of the molecule [550].

complex reveals the presence of bridging hydrazo(2-) and phenylnitrene ligands [550]. The solubility of copolymers of Cp_2MCl_2 ($\text{M} = \text{Ti}, \text{Zr}, \text{Hf}$) with dioximes of seven cyclic diones in 1-methylimidazole was observed to depend on the nature of M and the symmetry of the dioxime, and was independent of the copolymer chain length [551].

Cyclic voltammetry of Cp_2TiX_2 ($\text{X} = \text{Cl}, \text{Br}$) in THF under CO pressure reveals that a chemical reaction with CO accompanies the addition of the first electron to Cp_2TiX_2 . After the transfer of one electron and a decrease in CO pressure, electrolysis gave solutions which exhibited two ESR signals. Electrolysis of the solutions at -1.8V vs SCE produced $\text{Cp}_2\text{Ti}(\text{CO})_2$ in high yield after the transfer of a second electron and absorption of CO. A mechanism involving the generation of anions such as $[\text{Cp}_2\text{Ti}(\text{CO})\text{X}_2]^-$ has been proposed [552]. The use of chemically modified electrodes and the solution electrochemistry of Cp_2TiCl_2 was discussed by Willman [553]. The electrochemical reduction of Cp_2TiCl_2 on a Pt electrode in a propylene carbonate solution (containing LiClO_4) reveals an irreversible first reduction

step and a compound resistant to anodic reoxidation. This compound presumably forms via some chemical reaction which occurs subsequent to the electron transfer process [554].

The dinitrogen reduction reaction in the $(\eta\text{-C}_5\text{H}_5)_2\text{TiCl}_2\text{-Mg}$ system in THF was investigated using ^{13}C and ^1H nmr methods and product characterization. The results were interpreted in terms of the reaction yielding a mixture of compounds in which the Ti atom is bonded to both the $\mu\text{-}(\eta^5\text{-}\eta^5\text{-fulvalene})$ ligand and to the Cp ligands. Dinitrogen undergoes reduction to N^{3-} , which subsequently forms M_3N bridges ($\text{M} = \text{Ti, Mg}$) [555]. Reaction of Cp_2TiCl_2 , $\text{Ti}(\text{OBu})_4$ or TiCl_4 with excess PhMgBr under nitrogen pressure (100 kg-cm^{-2}) gave traces of PhNH_2 after seven hours, but no PhNH_2 forms in the absence of a Ti complex. The analogous reaction of RMgBr ($\text{R} = \text{o- and m-tolyl}$) yields mixtures of isomeric RNH_2 , primarily through an insertion mechanism. Pyrolysis of Cp_2TiR_2 ($\text{R} = \text{m- and p-tolyl}$) under nitrogen pressure results only in the production of mixtures of m- and p- $\text{MeC}_6\text{H}_4\text{NH}_2$; this indicates benzyne intermediate species [556]. The stereochemistries of the reductions of cis- and trans-4-methylcyclohexyl-1-d bromide, under argon, with the 95:5 $\text{Me}_2\text{CHMgBr/Cp}_2\text{TiCl}_2$ system, and of the unlabeled bromides with $(\text{CD}_3)_2\text{CHMgBr/Cp}_2\text{TiCl}_2$ have been determined by ^2H nmr analysis of the resulting cis- and trans-4-methylcyclohexane-1-d [557].

The thermal decomposition of $(\eta^5\text{-C}_5\text{Me}_5)_2\text{TiMe}_2$ in PhMe follows first-order kinetics and yields $(\eta^5\text{-C}_5\text{Me}_5)(\text{C}_5\text{Me}_4\text{CH}_2)\text{TiMe}$ and CH_4 . Labeling studies have shown the decomposition to be intramolecular and CH_4 production to occur by coupling of a Me group with a H from the other TiMe group [558]. Reacting $\text{Cp}_2\text{Ti}(\text{CH}_2\text{Ph})\text{Cl}$ with CCl_4 in C_6D_6 yields Cp_2TiCl_2 , $\text{PhCH}_2\text{CCl}_3$ and $\text{PhCH}_2\text{CH}_2\text{Ph}$ at ambient temperature. The benzyl protons of $\text{Cp}_2\text{Ti}(\text{CH}_2\text{Ph})\text{Cl}$ and $\text{PhCH}_2\text{CCl}_3$ were found to exhibit enhanced CIDNP absorption, the first example of CIDNP enhancement in a thermal reaction [559].

Insertion products, formed via allyl migration, are produced upon reacting $\text{Cp}_2\text{Ti}(\eta^3\text{-allyl})$ or $\text{Cp}_2\text{Ti}(\eta^3\text{-1-methylallyl})$ with CO_2 , PhNCO , PhCH=NPh , Me_2CO

MeCN. Normal insertion was observed with RNC ($R = 2,6\text{-xylyl}$); carbonylation of $\text{Cp}_2\text{Ti}(\eta^3\text{-allyl})$ gave $\text{Cp}_2\text{Ti}(\text{CO})_2$ and $(\text{CH}_2=\text{CHCH}_2)_3\text{COH}$; and allyl elimination occurs for reactions with CS_2 or C_2Ph_2 [560]. Threo- β -methylhomoallyl alcohols have been prepared stereoselectively by the addition reaction of $\text{CpTi}(\text{CH}_2\text{CH}=\text{CHMe})\text{X}$ ($X = \text{Cl, Br, I}$) with aldehydes. For example, reaction of $\text{CpTi}(\text{CH}_2\text{CH}=\text{CHMe})\text{Br}$ with EtCHO in Et_2O yields 92% of a 96:4 mixture of threo-erythro- $\text{H}_2\text{C}=\text{CHCHMeCH}_2\text{OH}$ [561].

The thermally driven metal to ligand electron transfer from Ti(II) to a coordinated nitrogen (L) observed for $(\eta^5\text{-C}_5\text{H}_5)_2\text{Ti(L)}$ ($L = 2,2'\text{-bipyridyl, various substituted 1,10-phenanthrolines}$) also occurs when $L = \text{phthalazine}$. The intramolecular electron transfer leads to the dimerization of phthalazine to produce a binuclear complex $[\text{Cp}_2\text{Ti}(\text{phthalazine})]_2$, whose molecular structure is depicted in Figure 11. The complex has been characterized by crystal structure analysis, ESR and mass spectroscopy, and Fenske-Hall MO calculations [562]. $\text{Cp}_2\text{Ti}(\text{CO})_2$ reacts with DEDM (diethyldiazomalonate) losing

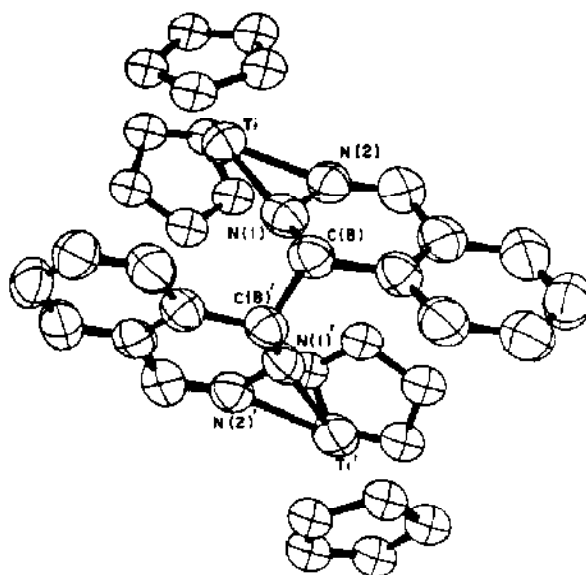


FIGURE 11: Molecular structure of bis[bis(η^5 -cyclopentadienyl)(phthalazine)titanium] [562].

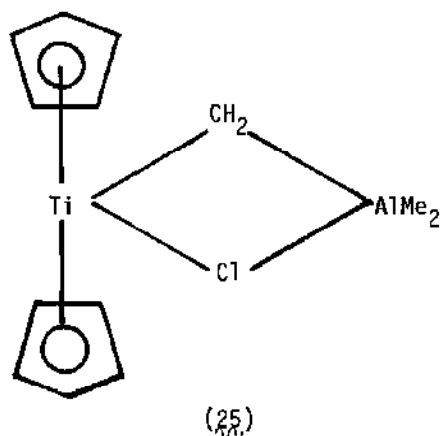
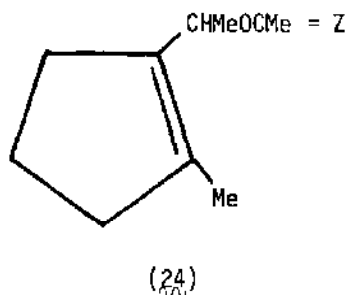
CO and yielding $\text{Cp}_2\text{Ti}(\text{DEDH})$, in which the diazo ligand is $\eta^3\text{-N,N,O}$ -bonded to Ti through both N atoms and one O atom of the ester groups. The complex was spectroscopically and structurally characterized. When the diazoalkane does not contain substituents having donor atoms, the Cp_2Ti unit promotes the reaction of CO with two diazoalkane molecules to produce a carbohydrazido ligand [563]. Reactions between $\text{Cp}_2\text{Ti}(\text{CO})(\text{PEt}_3)$ and either dimethyl maleate or dimethyl fumarate in toluene solution at 273K lead to a single air- and heat-sensitive product, $\text{Cp}_2\text{Ti}(\text{CO})(\eta^2\text{-trans-ileO}_2\text{CCH=CHCO}_2\text{Me})$. Dimethyl maleate is also catalytically isomerized to dimethyl fumarate under these conditions [564].

Acid hydrolysis of $\text{Cp}_2\text{Ti}(\text{OR})_2$ (R = aryl) with HX (X = halo) proceeds in a stepwise fashion to yield $\text{Cp}_2\text{Ti}(\text{OR})\text{X}$ first, and then Cp_2TiX_2 under various conditions. The reaction of $\text{Cp}_2\text{Ti}(\text{OR})\text{X}$ with $\text{R}'\text{Li}$ (R' = aryl) or $\text{R}'\text{OH}/\text{NaNH}_2$, gives $\text{Cp}_2\text{Ti}(\text{OR})\text{R}'$ or $\text{Cp}_2\text{Ti}(\text{OR})(\text{OR}')$, respectively [565]. The reaction of $\text{Cp}(\eta^5\text{-pyrrolyl})\text{TiCl}_2$, $(\eta^5\text{-indenyl})(\eta^5\text{-pyrrolyl})\text{TiCl}_2$ and $\text{Cp}(\eta^5\text{-indenyl})\text{TiCl}_2$ with oxime (8-hydroxyquinoline) in aqueous solution gives rise to the ionic derivatives $[(\eta^5\text{-R})(\eta^5\text{-R}')\text{TiL}]^+\text{Cl}^-$ ($\text{R} = \text{C}_5\text{H}_5$, C_9H_7 , $\text{R}' = \text{C}_4\text{H}_4\text{N}$; $\text{R} = \text{C}_5\text{H}_5$, $\text{R}' = \text{C}_9\text{H}_7$; L = conjugate base of oxime). A number of halide and complex halo anions present in the aqueous solution were isolated as salts of these ionic complexes giving $[(\eta^5\text{-R})(\eta^5\text{-R}')\text{TiL}]^+\text{X}^-$ ($\text{X}^- = \text{Br}^-$, I^- , $\text{ZnCl}_3(\text{H}_2\text{O})^-$, CdCl_4^{2-} , HgCl_3^-), which were shown to be electrolytes by conductivity measurements in nitrobenzene solution. Proton nmr and infrared spectral studies revealed that the ligand L is chelating; thus a tetrahedral coordination about the $\text{Ti}(\text{IV})$ ion was proposed [566]. The $[(\eta^5\text{-R})(\eta^5\text{-R}')\text{TiL}]^+\text{Cl}^-$ complexes react with dithiocarbamate anions in aqueous solution to give $[(\eta^5\text{-R})(\eta^5\text{-R}')\text{TiL}]^+\text{X}^-$ ($\text{X}^- = \text{ile}_2\text{NCS}_2^-$, $\text{Et}_2\text{NCS}_2^-$, $(\text{Me}_2\text{CH})_2\text{NCS}_2^-$) [567].

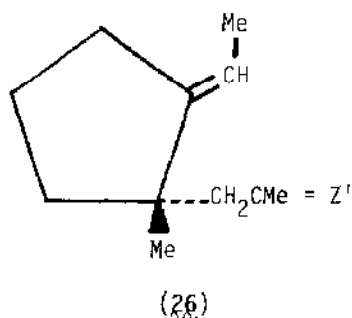
Cyclic voltammetry and coulometry were employed to investigate the oxidative electrochemistry of Cp_2TiX_2 (X = thiolate (SR), ferrocenyl (Fc)). For the $\text{Cp}_2\text{Ti}(\text{SR})_2$ complex in MeCN , three redox waves are observed in the 0.0 to +1.4V range. The first wave was assigned to $\text{Ti}(\text{IV}) \rightleftharpoons \text{Ti}(\text{V})$ and was at least quasi-reversible. The second wave was assigned to a second, one-electron

oxidation of the complex and to the oxidation of the product of the first one-electron oxidation (i.e., $[\text{Cp}_2\text{Ti}(\text{NCMe})(\text{SR})]^+$). This ion supposedly arises by reductive elimination of $\cdot\text{SR}$ from $[\text{Cp}_2\text{Ti}^{\text{V}}(\text{SR})_2]^+$ [568]. Cp_2TiS_5 reacts with Se_2Cl_2 in CS_2 at 273K to form 1,2,3-triselenacyclooctasulfur as the main product [569].

1,5-dienes can be prepared by sequential Ti-mediated methylenation of allyl esters, Claisen rearrangement, and a second methylene transfer reaction. Treating the allyl acetate (24) ($\text{Z} = \text{O}$) with complex (25) in the presence of pyridine gave the corresponding methylene compound, (24) ($\text{Z} = \text{CH}_2$) in 85% yield. The thermal Claisen rearrangement of (24) ($\text{Z} = \text{CH}_2$) in pentane under



argon produced the enone (26) ($Z' = O$) in 50-80% yield. Further methylenation of (26) ($Z' = O$) with (25) gave (26) ($Z' = CH_2$) in 90% yield. Alternatively,

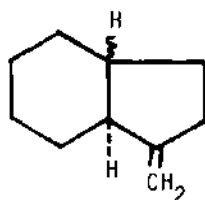


the compound (26) ($Z' = CH_2$) could be prepared directly by treating (24) ($Z = O$) with excess (25) for 12 hrs. at room temperature in the presence of pyridine [570].

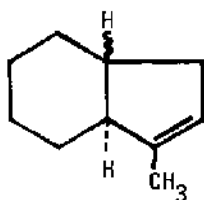
(iii). Catalysis

Cyclopentadienyl titanium compounds are well known for their catalytic role in isomerization and polymerization reactions. Additionally, they are known to catalyse esterification, olefination, and hydrogenation reactions.

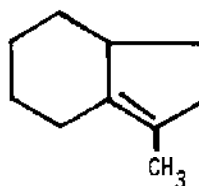
The isomerization of 1-hexene to trans- and cis-2-hexene is catalysed by $(Cp_2TiCl)_2-LiAlH_4$, with maximum activity at a Ti:Al ratio of 1. ESR spectral data are suggestive of the interaction between olefin and catalyst giving two types of active species: a) one responsible for hydrogenation and b) one responsible for isomerization [571]. The cyclization and isomerization of 1,2-divinylcyclohexanes to give hexahydroindenes is catalysed by $Cp_2TiH-AlH_3$. Thus, cis-1,2-divinylcyclohexane gives the cis-indan (27) and in the presence of $\alpha-(\eta^5: \eta^5)$ -fulvalene)di- μ -hydridobis(cyclopentadienyltitanium); compound (27) rearranges to the cis-indene and cis-(28). In the presence of the fulvalene



(27)



(28)



(29)

complex above, cis-1,2-divinylcyclohexane isomerizes at 408K to trans-isomer, at 423K cyclizes to trans-(27), and at 463K to trans-(28). Above 473K, the cis- and trans-(28) compounds isomerize via the hexahydroindene (29) [572]. C_8 - C_{12} cycloalkadienes undergo catalytic isomerization in the presence of a Cp_2TiH -containing catalyst to yield η -cycloalken-1-ylbis(cyclopentadienyl)-titanium(III) ($N = 2-6$) compounds [573].

An investigation of the catalytic activity of $Cp_2TiR X-R'_nAlX'_{3-n}$ ($R = Et$; $X = Cl = X'$; $n = 3$) for ethylene polymerization showed an increase in activity on addition of H_2O to a system containing excess $AlCl_3$. The increased activity was explained in terms of an interaction between the catalytic system and $AlCl_3 \cdot H_2O$ leading to protonation of the active catalytic center (i.e., $[Cp_2TiEtCl \cdot AlCl_3H^+][AlCl_3OH^-]$) which contains a labile Ti-C sigma bond [574]. Similar results were obtained for the catalyst system for which $R = aryl$ or C_1-C_6 alkyl, $R' = C_1-C_{10}$ alkyl or C_2-C_5 alkoxy, X or $X' = Cl, Br$ and $n = 0-3$. Hydrolysis, in this case, supposedly forms an alkoxane of general formula $R^2R^3AlOR^4R^5$ ($R^2, R^3, R^4, R^5 = X', R', OAlR^2R^3$) [575].

The esterification of phthalic anhydride with alcohols over Cp_2TiX_2 or $CpTiX_3$ ($X = halo$) catalysts yields phthalate esters. For example, a mixture of phthalic anhydride (1.5 mole), 2-ethylhexanol (3.45 mole) and Cp_2TiCl_2 (0.98 mole) at 463K for 3 hrs. yields bis(2-ethylhexyl)phthalate [576]. The treatment of $RCH=CHAl(CH_2CHMe_2)_2$ ($R = n-C_5H_{11}, Pr$) with Cp_2TiCl_2 in CH_2Cl_2 yields 1,1-dimetalloalkanes, which when reacted with the ketones $R'COR^2$ ($R' = Me, Ph$;

$R^2 = \text{Me, Et, Ph}$; $R^1 R^2 = (\text{CH}_2)_5$ give 70-82% alkenes $\text{RCH}_2\text{CH}=\text{CR}^1\text{R}^2$ [577] $\text{C}_5\text{-C}_8$ cycloalkenes have been prepared via hydrogenation of benzene or a corresponding dione in the presence of the catalyst $[\text{Cp}_{2-n}(\text{X})_n\text{Ti}(\text{H})_2\text{AlH}(\text{X})]_2$ ($n = 0, 1$; $\text{X} = \text{Cl, Br}$) [578].

b. Other Coordination Complexes of Titanium

(i). Preparation, Characterization and Structure

Reaction of TiEtCl_3 with $\text{Me}_2\text{PCH}_2\text{CH}_2\text{PMe}_2$ affords $\text{Ti}(\text{Me}_2\text{PCH}_2\text{CH}_2\text{PMe}_2)\text{EtCl}_3$ (Figure 12). The crystal structure determination of the complex has been interpreted in terms of a direct bonding interaction between the Ti atom and the $\beta\text{-C-H}$ system [579]. An ESR spectroscopic study of a paramagnetic titanium methylene complex ($\text{TiCH}_2\cdot$), as well as ESR evidence employing isotopically labelled reagents, has demonstrated the facile exchange of the metal-bound CH_2 fragment with the CH_2 group of a terminal olefin (methylene cyclohexane [580]).

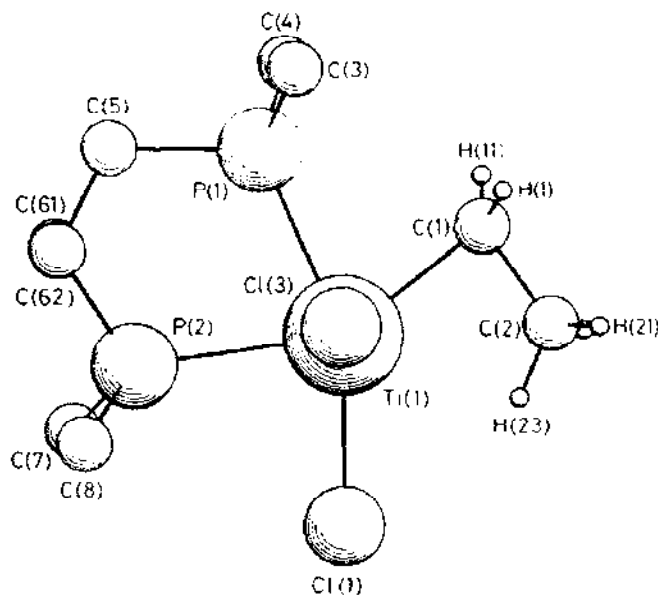


FIGURE 12: Crystal structure of $\text{Ti}(\text{Me}_2\text{PCH}_2\text{CH}_2\text{PMe}_2)\text{EtCl}_3$, showing the plane containing the $\text{P}_2\text{TiC}_2\text{H}(23)$ atoms; the $\text{Cl}(2)$ atom (not shown) is located symmetrically on the $\text{Cl}(3)\text{-Ti}$ axis below the plane.

Studies on complexes of ethylene with Ti, Cr, Fe, Ni, Cu^+ , Ni^{2+} , V, Mn and Co have shown that as the stability of the π complex increased, the olefinic bond weakens and the C-H bond becomes tighter. Furthermore, as the oxidation state of the metal increases, back donation decreases, and the C=C bond becomes less disturbed [581]. The preparation of the allyl titanium(IV) complex $\text{Me}_3\text{Ti}(\text{CH}_2\text{CH}=\text{CH}_2)$ (stabilized as a 1:1 complex with 2,2'-bipyridyl) occurs via reaction of Me_4Ti and $(\text{CH}_2=\text{CHCH}_2)_3\text{B}$ in Et_2O at 223K. TiCl_4 reacts with $\text{CH}_2=\text{CMeCH}_2\text{MgCl}$ to yield $\text{Ti}(\text{CH}_2\text{MeC}=\text{CH}_2)_4$. At 203K, this complex possesses an α -allyl structure, though at higher temperatures a dynamic allyl system is present. Thermal decomposition of $\text{Ti}(\text{CH}_2\text{MeC}=\text{CH}_2)_4$ gives $\text{Ti}(\text{CH}_2\text{MeC}=\text{CH}_2)_2$ [582].

The cyclopropyl-containing bisarene titanium complexes, $(\text{RPh})_2\text{Ti}$ and $[\text{R}(\text{CH}_2)_3\text{Ph}]_2\text{Ti}$ (R = cyclopropyl), have been prepared by low-temperature condensation of the metal with the ligand [583]. An x-ray analysis of $(\eta^6\text{-C}_6\text{H}_6)\text{Ti}(\text{Cl}_2\text{AlCl}_2)_2$, shown in Figure 13, confirms the molecular structure proposed in 1961 by H. Martin and F. Vohwinkel for this complex [584].

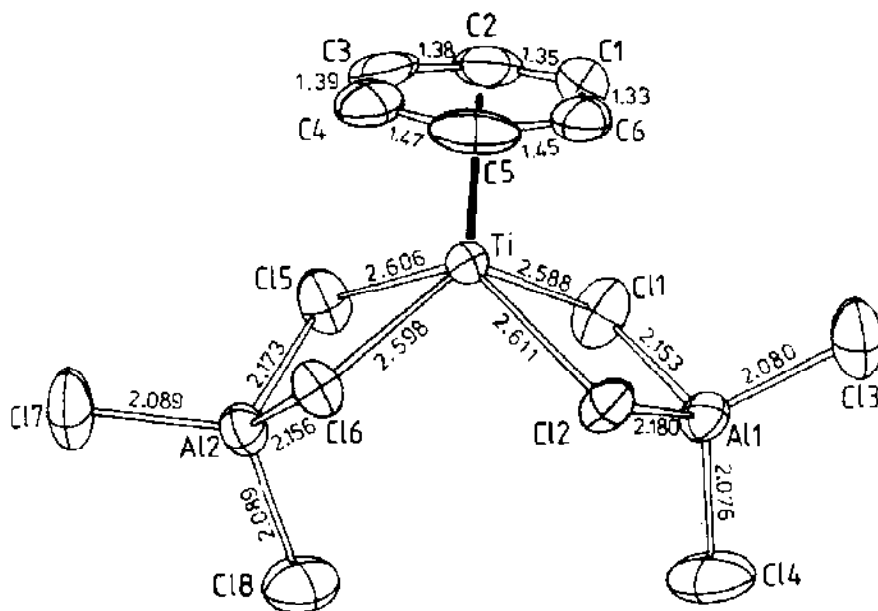


FIGURE 13: Structure of $(\eta^6\text{-C}_6\text{H}_6)\text{Ti}(\text{Cl}_2\text{AlCl}_2)_2$ [579].

The crystal structure of dibenzenetitanium(0) has been determined by Tairova and coworkers [585], and found to possess the prismatic configuration of the sandwich-like structure of $(C_6H_6)_2Cr$. A sandwich structure was also determined crystallographically for ditoluenetitanium [586]. Reaction between $TiCl_2$ and the potassium salt of the 2,4-dimethylpentadienyl anion leads to the formation of $Ti^{II}(2,4-C_7H_{11})_2$, a pyrophoric, volatile, very electron deficient ($14 e^-$) and diamagnetic open sandwich complex. The stability of this complex has been attributed to its low spin nature and large ligand size [587]. Wild and coworkers [588] have synthesized racemic ethylenebis(4m5m6m7-tetrahydro-1-indenyl)titanium dichloride and have determined the molecular structures of this complex, its meso isomer and a binaphthoate complex of its (S,S)-enantiomer.

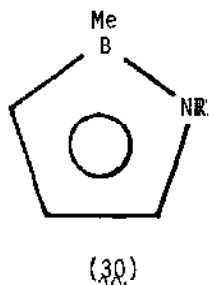
The 1H nmr spectra of $[(\eta^4-C_4H_6)(COT)]Ti$ (C_4H_6 = butadiene; COT = cyclooctatetraene) in toluene- d^8 solvent were recorded as a function of temperature. Direct evidence for a s-cis- η^4 -butadiene conformation was obtained from sub-spectral analysis and iterative computer simulation [589]. Electronic absorption and ESR spectroscopies were employed to examine $(\eta-COT)(\eta^5\text{-fluorenyl})Ti$ in fluid and frozen solutions. The results appear consistent with those of previously studied η^5 -cyclopentadienyl and η^5 -indenyl analogs, though small variations were observed, attributed to the electron-withdrawing effects of the benzo-substituents on the η^5 - C_5 ring [590]. Dominant electronic spectral features in tetrakis(1-norbornyl)titanium(IV) have been assigned to ligand-to-metal charge transfer (LMCT) transitions. Near-UV irradiation of this complex in non-polar solvents yields homolytic cleavage of the Ti-norbornyl bond [591].

The relative stabilities of six alkyl-substituted titanocyclobutanes were investigated. Results indicate that the substituent prefers the β -position in monosubstituted metallacycles. Addition of a second β -substituent (e.g., Me) to the metallacycle results in destabilization [592].

$TiCl_3(MeCH)(ROH)_2$ ($R = Me, Et, Pr, Pr^i, Bu^i$) compounds have been

synthesized from $\text{TiCl}_3(\text{MeCN})$ and ROH , and characterized by infrared spectroscopy and thermogravimetry [593]. No observable EPR signals were observed at room temperature for $\text{TiCl}_3(\text{EtOH})_4$, $\text{TiCl}_3(\text{PrOH})_3$, $\text{TiCl}_3(\text{BuOH})_3$ or $\text{TiCl}_3(2\text{-C}_4\text{H}_9\text{OH})_3$. However, at 77K the (EtOH) and (BuOH) complexes exhibit axial EPR spectra with $g_{\parallel} > g_{\perp}$, while the spectra of the (PrOH) and (2-C₄H₉OH) complexes are single absorption lines. The EPR spectral character for these complexes seem more consistent with a facial (rather than meridional) configuration of Cl ligands [594].

Syntheses have been reported of the $\eta\text{-}1,2\text{-azaboroliny}1$ complex L_2TiBr ($\text{L} =$ (30); $\text{R} = \text{CMe}_3$ [595], trans- $[\text{TiCl}_2(\text{ArCH}=\text{NR})_2]$ ($\text{Ar} = 2\text{-OC}_6\text{H}_4$; $\text{R} = \text{PhCH}_2$, Ph, 4-MeC₆H₄, Et, Pr, Prⁱ, Bu, Bu^{sec}, hexyl, octyl) [596], and the bridging carbene



complex $\{\text{TiCHSiMe}_2\text{NSiMe}_3[\text{N}(\text{SiMe}_3)_2]\}_2$ [597].

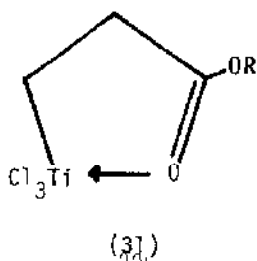
The crystal structure determination of bis[1,2-bis(dimethylphosphino)ethane]tricarbonyltitanium reveals a seven-coordinate, monomeric, phosphine-substituted derivative of $\text{Ti}(\text{CO})_7$. Variable-temperature ^{31}P and ^{13}C nmr studies show the presence of two separable processes, indicative of stereochemical nonrigidity [598].

Konunova and Kudritskaya [599] have discussed the coordination compounds of $\text{Ti}(\text{IV})$, $\text{Zr}(\text{IV})$ and $\text{Hf}(\text{IV})$ with urea. A convenient synthesis of $\text{M}(\text{bpy})_3$ and $\text{M}(\text{phen})_3$ ($\text{bpy} = 2,2\text{-bipyridyl}$; $\text{phen} = 1,10\text{-phenanthroline}$; $\text{M} = \text{Ti, Zr, Nb, Ta, Mo, W, Re, V, Cr}$) has been reported [600]. For titanium, the bpy and phen complexes can be made via sodium amalgam reduction of the titanium chloride. Molecular orbital calculations were reported for $(\text{Cp}_2\text{TiR})_2\text{N}_2$ ($\text{R} = \text{H, p-tolyl}$). The calculated energies of the $a_g \rightarrow b_u$ transition are 1.83 and 1.76eV for the

$R = H$ and $R = p\text{-tolyl}$ complexes, respectively. The N-N bond orders are nearly the same, though the negative charge on the N_2 moiety seems larger for the $R = p\text{-tolyl}$ complex [601]. Resonance Raman spectra of the bridging dinuclear dinitrogen rhenium(I) complex $ClL_4ReN_2TiCl_4(THF)$ ($L = P(CH_3)_2C_6H_5$) were recorded. The Raman lines observed under the conditions employed were associated with the ReN_2Ti linkage vibrations, which are due to the ${}^1E \leftarrow {}^1A_1$ electron transition [602]. $(EtO)_2P(O)CO_2Et$ (tepf) reacts with metal chlorides at elevated temperatures to produce $EtCl$ and $M(\text{depf})_n$ ($\text{depfH} = (EtO)P(O)(OH)CO_2Et$; $M^{n+} = Ti^{3+}, V^{3+}, Cr^{3+}, Fe^{3+}$, etc.). The $M(\text{depf})_n$ are linear, chainlike polymeric species, involving bidentate bridging depf ligands [603].

The coordination complexes trans- $TiCl_4L_2$ ($L = RC_6H_4NHCH=CHC(O)Ph$; $R = H, 4\text{-Me}, 2\text{-Me}, 2\text{-MeO}, 4\text{-MeO}$) have been synthesized and characterized by infrared spectroscopy. The azomethane is oxygen-bonded to Ti and intramolecular hydrogen-bonding within the ligand is observed [604]. The syntheses of the following complexes has also appeared: $TiO(OH)L_2$ ($HL = 3\text{-Br-2HO-5-CH}_3C_6H_2C(CH_3)=NOH$) [605], Ph_2TiL_2 ($LH = \text{salicylaldehyde, acetylacetone, benzoylacetone, dibenzoylmethane, methylsalicylate, benzoylphenylhydroxylamine}$) [606], $Ti(OPh)_{4-x}Cl_x \cdot nL$ ($L = \text{pyridine}$; $n = 1, 2$; $x = 1, 2, 3$), $Ti(OPh)_2Cl_2 \cdot L$ ($L = 2,2'\text{-bipyridyl}$) [607], and $Ti(Ph_3SiO)_4$ [608].

Three titanium homoenolates of alkyl propionates have been prepared via reaction of $TiCl_4$ with 1-alkoxy-1-trimethylsiloxycyclopropane (alkoxy = MeO, EtO, Me_2CHO) to give the dimeric five-membered chelates depicted in structure (31), 2-(alkoxycarbonyl)ethyltrichlorotitanium. The complexes react with bromine and oxygen to yield the respective β -oxygenated propionic esters, while



reaction with aldehydes produces γ -hydroxyesters or γ -chloroesters [609].

The reaction of $\text{Ti}(\text{OPr})_4$ with $(\text{PhCH}_2)_2\text{NOH}$ results in formation of the hydroxylamido complex $\text{Ti}[\text{OH}(\text{CH}_2\text{Ph})_2]_4$. The $\text{Ti}(\text{ONEt}_2)_4$ complex shown in Figure 14 can be prepared from $\text{Ti}(\text{OPr}^i)_4$ and Et_2NOH . The crystal structure of the complex in Figure 14 reveals a coordination number of 8 for Ti with the ligand having O,N-coordination [610]. The preparation and characterization (infrared, nmr, elemental analysis) of $\text{Ti}(\text{OR})_2[\text{R}'\text{C}(\text{S})\text{CHC}(\text{O})\text{R}^2]_2$ ($\text{R} = \text{Pr}^i, \text{Bu}^t$; $\text{R}' = \text{R}^2 =$

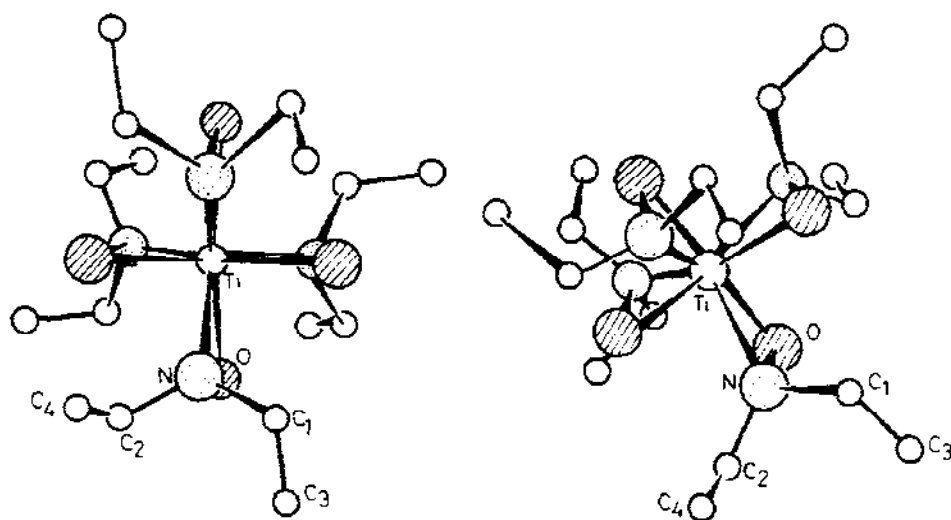


FIGURE 14: Schematic drawing of the structure of $\text{Ti}(\text{ONEt}_2)_4$ [610].

Me ; $\text{R}' = \text{Ph}$, $\text{R}^2 = \text{Me}$) were reported by Kanjolia and coworkers [611].

The x-ray crystal structure of the dimer $[\text{Ti}_2(\text{C}_6\text{H}_{12}\text{NO}_3)_2(\text{C}_3\text{H}_7\text{O})_2]$ in Figure 15 reveals that each half of the dimer contains one Ti atom, a 2,2',2''-nitrolotriethanolate ligand, and a 2-propanolate group. The dimer forms and octahedral coordination is achieved when an oxygen on one arm of the nitrolotriethanolate chelate serves as a bridging group [612].

The preparation and characterization of the complexes $\text{TiO}(\text{HL})_2 \cdot n\text{H}_2\text{O}$ ($\text{H}_2\text{L} = \beta, \delta$ -triketones or β -ketophenols) reveal them to be mononuclear. In addition, they could be used as ligands to prepare homo- and hetero-binuclear complexes [613].

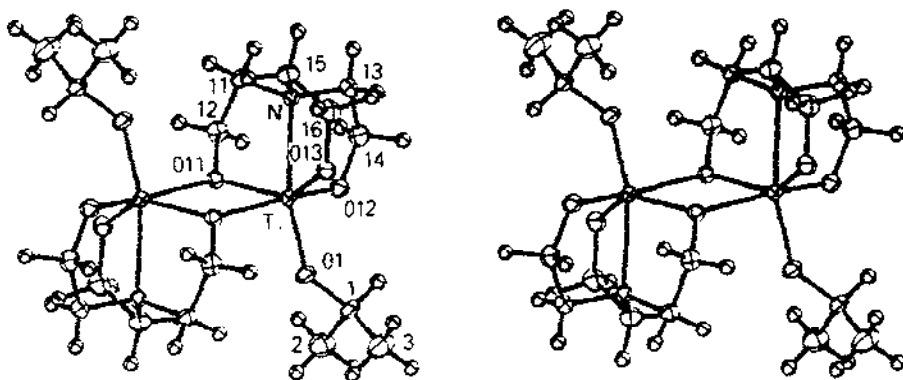


FIGURE 15: Stereodrawing of $\{\text{Ti}[\text{N}(\text{CH}_2\text{CH}_2\text{O})_3][(\text{CH}_3)_2\text{CHO}]\}_2$, for which the hydrogen atoms have been assigned arbitrary radii [612].

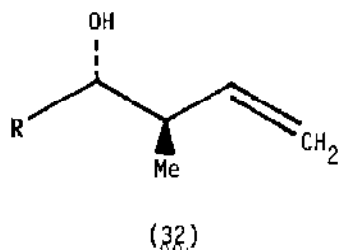
Substituted dithiocarbamate titanium compounds have been synthesized using O,O-diethylphosphonodithiocarbamate [614], N,N-dialkyldithiocarbamates [615, 616], monothiocarbamates [617]. The $(\eta^5\text{-R})_2\text{Ti}[\text{S}_2\text{CNHP}(\text{O})(\text{OEt})_2]\text{Cl}$ ($\text{R} = \text{C}_5\text{H}_5$, MeC_5H_4 , indenyl) compounds were prepared and characterized by infrared and W spectroscopy to reveal a bidentate dithiocarbamate ligand [614]. The treatment of $(\eta^5\text{-C}_{13}\text{H}_9)_2\text{TiCl}_2$ with $\text{NaS}_2\text{CNRR}'$ gave $(\eta^5\text{-C}_{13}\text{H}_9)_2\text{Ti}(\text{S}_2\text{CNRR}')\text{Cl}$ ($\eta^5\text{-C}_{13}\text{H}_9 = \eta^5\text{-fluorenyl}$; $\text{R} = \text{Me, Et, CHMe}_2$; $\text{R}' = \text{Ph, cyclohexyl}$) [616]. A similar procedure was utilized to prepare $(\eta^5\text{-C}_{13}\text{H}_9)_2\text{Ti}(\text{S}_2\text{CNR}_2)$ ($\text{R} = \text{Me, Et, CHMe}_2$) [617]. In all cases, the dithiocarbamate ligand is bidentate. $\text{TiCl}_4(\text{TT})$ and $\text{TiCl}_4(\text{TT})_2$ ($\text{TT} = 1,3,5\text{-trithiane}$) have been prepared and characterized by Wade and Willey [618].

(ii). Reactions

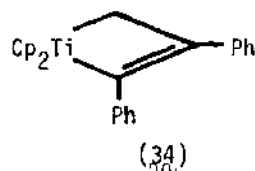
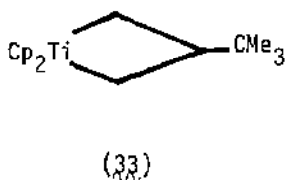
The stereo- and regio-specific addition of $\text{Cp}_2\text{Ti}(\eta^3\text{-CH}_2=\text{CHCH}_2\text{SiMe}_3)$ with aldehydes gives excellent yields of $(\pm)\text{-(R,S)-3-(trimethylsilyl)-4-hydroxy-1-alkenes}$, which undergo deoxysilylation to give either (E)- or (Z)-1,3-dienes

[619]. The highly diastereoselective addition of trans-(RCH=CHCH_2) Ti(OPh)_3 ($\text{R} = \text{Me}, \text{Me}_2\text{CH}, \text{Bu}$) to ketones results in good yields of tertiary homoallylic alcohols which are diastereoisomerically enriched up to 98%. The addition presumably involves a Ti atom coordinated to the CO group of the ketone in a pseudo-1,3-diaxial relation to the vinylic hydrogen atom in the Ti complex

[620]. Stereospecific 1k-addition of $(\text{MeCH=CHCH}_2)\text{Ti(OPh)}_3$ ($\text{R} = \text{CHMe}_2, \text{CHEt}_2, \text{CHMe}_3, \text{PhCH}_2\text{CH}_2, \text{Ph}_2\text{CH}, \text{Ph}, \text{p-tolyl}, \text{p-FC}_6\text{H}_4, \text{p-MeOC}_6\text{H}_4, \text{p-O}_2\text{NC}_6\text{H}_4, \text{p-NCC}_6\text{H}_4$) to aldehydes produced 56-94% β -methyl-homoallylic alcohols (32) [621].



The reaction of the titanacyclobutane (33) with $\text{PhC}\equiv\text{CPh}$ to give the titanacyclobutene (34) is first-order with respect to (33) and zero-order with

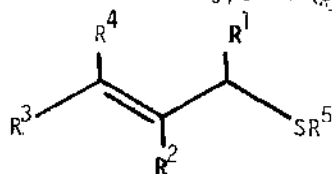


respect to $\text{PhC}\equiv\text{CPh}$. The rate-determining ring-opening of (33) to give $\text{Cp}_2\text{Ti=CH}_2$ and olefin (free or complexed) is followed by rapid trapping by incoming olefin or acetylene. Complex (33) and its analogs are effective catalysts for the olefin metathesis reaction of terminal olefins [622]. Titanacyclobutanes, specifically labelled in the α, β -positions, can be prepared from 1-deuterated terminal olefins [623]. On interaction of these complexes

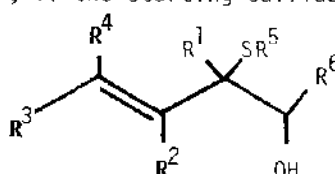
with aluminum alkyls, two processes occur: a) the stereochemistry of the α -center is scrambled by reversible trans-metalation; b) in a slower step, the metallacycle is cleaved to the original olefin with scrambled stereochemistry and $\text{Cp}_2\text{-CH}_2\text{-AlR}_3$. These observations are important in relation to olefin metatheses reactions.

Propylene oxide inserts into metal-chlorine bonds to yield 2-chloroisopropoxy and 2-chloropropoxy compounds. For titanium complexes containing a Cp ligand, the 2-chloroisopropoxy compounds are the major products. Insertion into the metal-oxygen bond is obtained with an electronegative substituent such as the fluoroethoxy ligand ($^t\text{OCH}_2\text{CF}_3$) [624]. A pulsed laser in conjunction with an ion-cyclotron-resonance mass spectrometer was used to generate and study the gas-phase, ion-molecule reaction of Ti^+ with a series of alkanes. This system is dominated by C-H insertions, though some C-C insertion leading to alkane elimination is present. Ti^+ also tends to release multiple sites of unsaturation in the bound hydrocarbon [625].

Upon treating with Me_2TiCl_2 or Me_3Al in the presence of TiCl_4 , a hydrogen atom at the olefinic 4-position of homoallylic alcohols is replaced by a methyl group. Terminal homoallylic alcohols afford E isomers. If the double bond is internal, the carbon chain at the other side of the OH group gives up its original position to the entering methyl group and switches to the other one at the same carbon atom [626]. [(alkylthio)allyl]titanium reagents, prepared by treating the allylic sulfides (35) $\text{R}^1 - \text{R}^4 = \text{H}$; $\text{R}^1 = \text{Me}$, $\text{R}^2 = \text{H}$, Me ; $\text{R}^3 = \text{R}^4 = \text{H}$; $\text{R}^1 = \text{R}^3 = \text{Me}$, $\text{R}^2 = \text{R}^4 = \text{H}$; $\text{R}^5 = \text{Ph}$, Et , Me_3C) with BuLi and $\text{Ti}(\text{OCHMe}_2)_4$, react with R^6CHO ($\text{R}^6 = \text{cyclohexyl}$, Ph , $\text{Me}(\text{CH}_2)_4$, PrCH=CHCHO) to produce erythro-alcohols of the type in (36). However, if the starting sulfides have alkyl

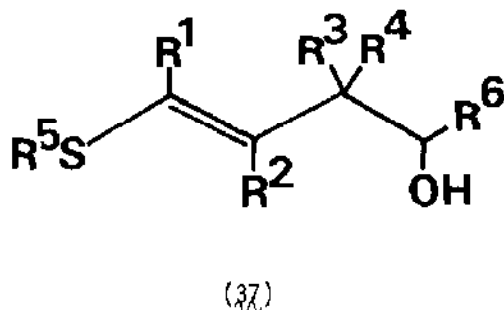


(35)



(36)

substituents at the γ -position of (35) $R^3 = \text{Me}$, $R^4 = \text{H}$, Me , $R^1 = R^2 = \text{H}$), the products are the vinyl sulfide derivatives (37). The erythro-(35) adducts may be transformed into di- and tri-substituted oxiranes and 2-phenylthio-1,3-butadienes with high stereoselectivities [627]. Titanium-induced dicarbonyl



coupling reactions have been described by McMurry [628].

The transesterification of *N*-butyl chloroacetate by sec-butyl-o-titanate in heptane has been shown to be second-order kinetically, first-order in each reagent [629]. The interaction of hydrogen, ethylene, CO and N_2 with superficial titanium-benzyl and titanium hydride compounds was studied by EPR spectroscopy [630].

The thermal decomposition of chelates of 5,5'-methylenedisalicylhydroxamic acid with various metal ions (including Ti(IV) , V(V) , Mo(VI) , Pb(II) , Zn(II) , Ni(II) , Cd(II) , Cu(II) , Fe(III) , Cr(III) and Al(III)) has been studied by thermogravimetric, DTA, infrared spectroscopic and x-ray diffractometric methods. The major steps (dehydration, transformation, and decomposition of the intermediate *N*-hydroxylactams) were proposed to account for the formation of metal oxides as the final products [631]. The first-order kinetics of the thermal decomposition of Ti(acac)_3 (acac = acetylacetonate) to yield acetone, CO and CO_2 were investigated by manometry and mass spectroscopy [632]. The pyrolysis of TiO(OH)L ($\text{HL} = 4,5\text{-dimethyl-2-hydroxyacetophenone oxime}$) was studied by thermogravimetry, and the results were compared with results obtained for ML_2 complexes ($\text{M} = \text{Pd, Cu, Ni, Co}$) [633].

Ugorets and coworkers [634] followed the reaction of Ti(OH)_4 with As_2O_5 in

H_2SO_4 solution by infrared spectroscopy. The reaction proceeds rapidly at first and then slows down. The fast stage was attributed to reaction of H_2AsO_4 with surface OH groups, and the slower part to interior reactions [634]. The hydroxy complex $\text{ScTi}(\text{OH})\text{O}_3 \cdot \text{H}_2\text{O}$ results from reaction of $\text{Sc}(\text{OH})^{2+}$ and H_2TiO_3 in HCl solution at pH 2-4.3. Decomposition of $\text{ScTi}(\text{OH})\text{O}_3 \cdot \text{H}_2\text{O}$ occurs on heating at 673-873K to yield Sc_2O_3 , TiO_2 and H_2O [635]. Reaction between $\text{Ti}(\text{OPr}^i)_4$ and trans-cinnamic acid (HCA) or dihydrocinnamic acid (HDCA) in various stoichiometric ratios produces $\text{Ti}(\text{OPr}^i)_{4-n}(\text{CA})_n$ and $\text{Ti}(\text{OPr}^i)_{4-n}(\text{DCA})_n$ ($n = 1, 3$), respectively. Infrared studies were interpreted [636] in terms of CA and DCA coordinating to Ti through hydroxy oxygen. An alcohol interchange technique was employed to synthesize $\text{Ti}(\text{OBu}^t)_{4-n}(\text{CA})_n$ and $\text{Ti}(\text{OBu}^t)_{4-n}(\text{DCA})_n$ ($n = 1-3$) [636]. The racemization-free transesterification of N-protected (by tert-butoxycarbonyl group) dipeptide methyl esters with Me_2CHOH and PhCH_2OH is catalysed by the titanium(IV) alkoxide complex $\text{Ti}(\text{OCHMe}_2)_4$, giving 79-87% iso-propyl esters and 72-89% benzyl esters, respectively [637]. The synthesis and characterization of $[\text{Ti}(\text{OR})_4](\text{SbCl}_6)_4$, $[\text{Sn}(\text{OR})_4](\text{SbCl}_6)_4$, $[\text{HRO}]\text{X}$ ($\text{X} = \text{BF}_4, \text{ClO}_4$) and $[\text{B}(\text{OR})_4](\text{SbCl}_6)_3$ ($\text{RO} = 1,5\text{-dimethyl-2-phenyl-3H-pyrazol-3-one}$; phenazone) have been reported [638]. These compounds were suggested as intermediates in the acid-catalysed electrophilic substitution of RO. The activation of β -carbon-carbon bonds in the reaction of TiR_4 ($\text{R} = \text{OBu}, \text{Cl}$) with $\text{MeLiCHCH}_2\text{CH}_2\text{CHLiMe}$ in decane at 606-626K to give propylene has been reported by Enikolopyan et al. [639]. Reaction between $\text{TiCl}_{4-n}(\text{OPh})_n$ and L in CCl_4 yields $\text{TiCl}_{4-n}(\text{OPh})_n \cdot 2\text{L}$ ($n = 1-4$; L = acetophenone, benzophenone) [640]. An octahedral structure was proposed for the product, based on infrared spectroscopic and electrical conductivity results.

The effect of chemical exchange of oxygen-containing ligands (lactic, mandelic, sulfosalicylic acids) on relaxation time of solvent (H_2O) protons was studied using complexes of Ti^{3+} and VO^{2+} with ligands as models [641]. Berrie [642] has investigated the intramolecular electron transfer via 3-formylpentane-2,4-dionate in a ruthenium(III)/titanium(III) redox cross reaction.

In the extraction of anionic titanium(IV) chelate compounds with sulfosalicylic acid, pyrocatechol and pyrocatechol-3,5-disulfonic acid, the degree of single stage extraction was observed to depend on a) the size of the organic cation (benzylthiuronium, di- and tri-phenylguanidinium, quinine, Ph_4P^+), and b) the composition of the extracted ion associated [643]. Conductometric, potentiometric and spectroscopic methods were utilized in the determination of the stoichiometry of complexes formed from 1,3-dimethylviolic acid and trivalent titanium, vanadium, chromium, iron and gallium in aqueous solution [644]. The effect of lactic acid, glycerol and glycol on titanium(IV)/gallic acid/sulfosalicylic acid systems at various pH values was compared spectrophotometrically. It was observed that lactic acid forms mixed complexes, whereas glycerol and glycol do not [645]. Ram [646] has presented mechanisms of titanium(III) reductions of keto acid complexes of pentaammine cobalt(III) and catalysis of outer-sphere reactions by N-substituted isonicotinic acid derivatives.

Electron spin resonance spectroscopy was employed to investigate the selective radical oxidation (those in which tervalent carbon is bonded to a substituent of the H1 type, e.g., OH) by titanium(IV) complexes. A lower limit of $\text{ca. } 10^8 \text{ dm}^3\text{-mole}^{-1}\text{-sec}^{-1}$ was estimated for the rate constant of the reaction of a Ti(IV)-EDTA complex with -CHMeOH [647]. The development of a catalytic wave of hydroxylamine was observed in the presence of Ti(IV) with the complexing agents EDTA, nitrilotriacetate, and 1,2-trans-diaminocyclohexane-tetraacetate in a perchlorate supporting electrolyte [648]. The complexing agents result in a shift of the Ti(IV) reduction wave to more positive potentials. In the presence of hydroxylamine, a catalytic substrate wave develops at reduction potentials corresponding to the Ti(IV) complexes; while the complexing agents themselves inhibit the catalytic effect.

Alkylative amination of non-enolizable RCHO by $\text{R'Ti(NR}_2)_3$ yields 15-73% RCHR'NR_2^2 ($\text{R} = (\text{un})\text{substituted Ph, PhCH=CHCH}_2, \text{Me}_3\text{C, 2-furyl}$; $\text{R}' = \text{Me, Bu}$; $\text{NR}_2^2 = \text{NEt}_2, \text{piperidino}$) [649]. A highly diastereo- and regio-selective

hamoaldol reaction between RCHO and the (1-oxyallyl)titanium complexes $(E)\text{-MeCH=CHCH}[\text{Ti}(\text{Et}_2)_3]\text{O}_2\text{CN}(\text{CHMe}_2)_2$ gives 97.0-99.5% (Z)-threo- $\text{RCH}(\text{OH})\text{CHMeCH=CHO}_2\text{CN}(\text{CHMe}_2)_2$ ($\text{R} = \text{Me}_3\text{C}, \text{Me}, \text{Me}_2\text{CH}, \text{Me}_2\text{C=CH}$) [650].

6.11 MISCELLANEOUS

a. Electrochemistry

An investigation of the electrochemical extraction and reextraction of inner-complex anions of Ti(IV) , in the presence of organic cations reveals that in the presence of diphenylguanidinium, Ti(IV) is extracted up to 9% as a complex with 2,7-dichlorochromotropic acid [651]. Employing the standard Ti(IV)/Ti(III) potentials in a non-complexing supporting electrolyte, a polarographic investigation was carried out to shed light on the mechanism and kinetics of electrooxidation of Ti(III) ions on a mercury electrode. The hydrolysis constant determined agrees well with those obtained previously by potentiometry and EPR spectroscopy [652].

Electroreduction of CO to $\text{C}_1 - \text{C}_4$ hydrocarbons in aqueous solutions of pH 6-13 occurs in the presence of a titanium(III)-molybdenum(III)-pyrocatechol catalytic system. The catalytically active species is the carbonyl complex of Mo(III) , and the pyrocatechol complex of Ti(III) serves as an electron relay from the cathode to the active species in the bulk solution [653].

Cyclic voltammograms for $\text{Ti-doped } \alpha\text{-Fe}_2\text{O}_3$ electrodes in 0.1M NaOH show small oxygen reduction and re-oxidation peaks negative of -0.4V vs SHE. For electrodes initially held negative of this potential, the onset of the photocurrent occurs at potentials well positive of the flatband potential of $\alpha\text{-Fe}_2\text{O}_3$. These results were interpreted as due to the penetration of hydrogen into the lattice. Oxygen reduction activity was observed to increase with increasing dopant concentration. The behavior exhibited by this system was interpreted in terms of reaction (7) as the rate-determining step, with titanium donors



mediating charge transfer [654]. Titanium-doped Fe_2O_3 electrodes have been used in the photoelectrolysis of water. The doping of Fe_2O_3 with Ti leads to a shift in the flatband potential of the photoelectrode in the negative direction. The effects of doping and the use of external biased potential on the spectral characteristics of the photolysis current have also been determined [655].

ACKNOWLEDGEMENTS

Our research is generously supported by the Natural Sciences and Engineering Research Council of Canada, and by NATO-81.046 to whom we are very grateful.

REFERENCES

1. To whom correspondence should be addressed.
2. R.C. Fay, Coord. Chem. Rev., 45 (1982) 9-40.
3. J.R. Ufford and N. Serpone, Coord. Chem. Rev., 57 (1984) 301-343.
4. N. Serpone, M.A. Jamieson, F. DiSalvio, P.A. Takats, L. Yeretsian and J.R. Ufford, Coord. Chem. Rev., 58 (1984) 87-167.
5. J.E. Newberry, Annu. Rep. Prog. Chem., Sect. A: Inorg. Chem., 78A (1981) 149-204.
6. J. Whitehead, Kirk-Othmer Encycl. Chem. Technol., 3rd ed., 23 (1983) 131-176, M. Grayson and D. Eckroth, Eds., Wiley, New York, New York.
7. I. Omai, Kagaku Kogyo, 33 (1982) 989-996.
8. S. Chen, Y. Liu, Z. Wang, C. Wang, Q. Yang, X. Jin, X. Xu, G. Li, Y. Tang et al., Fundam. Res. Organomet. Chem., Proc. China-Jpn.-U.S. Trilateral Semin. Organomet. Chem., 1st 1980, (pub. 1982) 117-124.
9. F. Sato, Yuki Gosei Kagaku Kyokaiishi, 40 (1982) 744-751.
10. G.B. Sergeev, V.S. Komarov and A.T. Federova, Vestri. Mosk. Univ., Ser. 2: Khim., 23 (1982) 114-117.
11. K.H. Cho, J.H. Choi and K.W. Choi, Hwahak Kwa Kongop Ui Chinbo, 23 (1983) 500-509.
12. V.A. Perelyaev, D.G. Kellerman and G.P. Shveikin, Osobennosti Elektron. Stroeniya i Svoistva Tverdogaz. Soedin. Titana i Vanadiya, Sverdlovsk, (1982) 13-42.
13. I. Mochida and H. Fujitsu, Kagaku Kogyo, 33 (1982) 898-903.
14. T. Ishii, Mater. Sci. Monogr., 10 (1982) (React. Solids, V 2) 927-932.
15. C. Delmas, J.J. Braconnier, A. Maazaz and P. Hagemmuller, Rev. Chim. Miner., 19 (1982) 343-351.
16. V.A. Ermishkin, E.M. Samoilov and V.G. Sabitov, Zavod. Lab., 48 (1982) 61-62.
17. A.N. Kornilov, N.V. Chelovskaya and G.P. Shveikin, Deposited Doc., (1982) VINITI 987-82, 13pp.
18. E.V. Lysenko and V. Sh. Telyakova, Vestn. Kiev. Politekh. Inst., (Ser): Khim. Mashinostr. Tekhnol., 20 (1983) 43-44.
19. N.D. Mazurenko and G.P. Petrov, Anodnoe Okislenie Met., (1982) 50-53.
20. Yu. G. Zainulin, A.S. Fedukov and S.T. Alyamovskii, Izv. Akad. Nauk SSSR, Neorg. Mater., 19 (1983) 404-407.
21. M.M. Kindrat, Sverkhverd. i Tugoplav. Materialy, Kiev, (1982) 45-49.
22. V.R. Tregulov and R.K. Chuzhko, Poverkhnost, (1982) 101-105.
23. E.A. Zhurakovskii, M.I. Lesnaya and K.S. Proskurka, Izv. Akad. Nauk SSSR, Neorg. Mater., 18 (1982) 1721-1725.
24. J.E. Sundgren, B.O. Johansson and B. Karlsson, Energy Res. Abstr., 8 (1983) Abstr. No. 4734.
25. L. Roux, J. Hanus, J.C. Francois and M. Sigrist, Sol. Energy Mater., 7 (1982) 299-312.
26. A.G. Turchanin and S.A. Babenko, Teplofiz. Vys. Temp., 20 (1982) 887-890.
27. A.I. Kharlamov, A.N. Rafal and V.B. Fedorus, Dopov. Akad. Nauk Ukr. RSR, Ser. B: Geol., Khim. Biol. Nauki, (1983) 47-51.
28. V.V. Volienik, S.S. Kiparisov and K.D. Yasinovskii, Tekhnol. Legk. Splavov, (1982) 41-44.
29. L.P. Mokhracheva, P.V. Gel'd and V.A. Tskhai, Izv. Akad. Nauk SSSR, Neorg. Mater., 19 (1983) 223-227.
30. A.P. Botha and R. Pretorius, Mater. Res. Soc. Symp. Proc., 10 (1982) (Thin Films Interfaces) 129-135.
31. F. D'Heurle, E.A. Irene and C.Y. Ting, Appl. Phys. Lett., 42 (1983) 361-363.
32. G. Venturini, J. Steinmetz and B. Roques, J. Less-Common Met., 87 (1982) 21-30.
33. A. Armigliato, G. Celotti, A. Garulli, S. Guerri, R. Lotti, P. Ostoja, C. Summonte, Appl. Phys. Lett., 41 (1982) 446-448.

34. Y. Saeki, R. Matsuzaki, A. Yajima and M. Akiyama, Bull. Chem. Soc. Japan, 55 (1982) 3193-3196.
35. L. Porte, L. Roux and J. Hanus, Phys. Rev. B: Condens. Matter, 28 (1983) 3214-3224.
36. V.V. Nemoshkalenko, V.P. Krivitskii, M.M. Kindrat and B.P. Mamko, Izv. Akad. Nauk SSSR, Neorg. Mater., 18 (1982) 1596-1597.
37. B. Karlsson, R.P. Shimshock, B.O. Seraphin and J.C. Hayfarth, Phys. Scr., 25, Part 1 (1982) 775-779.
38. R.A. Andrievskii, Yu. F. Khromov and D.E. Svistunov, Zh. Fiz. Khim., 57 (1983) 1641-1644.
39. V.I. Kuchuk, L.L. Molchanova and E.V. Golikova, Deposited Doc., (1981) SPSTL 917 KHP-DB1, 44-52.
40. I. Suni, D. Sigurd, K.T. Ho and M.A. Nicolet, J. Electrochem. Soc., 130 (1983) 1210-1214.
41. M. Morita, Y. Yonehara, Y. Matsuda, H. Mizuno and H. Miura, Denki Kagaku Oyobi Kogyo Butsuri Kagaku, 50 (1982) 755-758.
42. S.V. Gurov, V.N. Troitskii, V.I. Torbov and V.V. Kireiko, Izv. Akad. Nauk SSSR, Neorg. Mater., 18 (1982) 1733-1735.
43. R. Eibler, M. Dorrer and A. Neckel, Theor. Chim. Acta, 63 (1983) 133-141.
44. P. Blaha and K. Schwarz, Int. J. Quantum Chem., 23 (1983) 1535-1552.
45. D.P. Mahapatra and H.C. Padhi, J. Phys. C, 16 (1983) 1433-1436.
46. B. Karlsson and C.G. Ribbing, Energy Res. Abstr., 8 (1983), Abstr. No.4735.
47. L.M. Sheludchenko, Yu. N. Kucherenko and V.G. Aleshin, Metody Rascheta Energ. Strukt. Fiz. Svoistv Krist., Mater. Vses. Konf., 2nd, (1979) Pub. 1982, 111-117.
48. V.V. Nemoshkalenko, Yu. N. Kucherenko, L.M. Sheludchenko and V.Z. Khirinovskii, Metallofizika (Akad. Nauk Ukr. SSR, Otd. Fiz.), 5 (1983) 36-42.
49. W. Carrillo-Cabrera, Acta Chem. Scand., Ser. A, A37 (1983) 93-98.
50. N. Kinomura, F. Muto and M. Koizumi, J. Solid State Chem., 45 (1982) 252-258.
51. N.G. Chernorukov, I.A. Korshunov and M.I. Zhuk, Zh. Neorg. Khim., 27 (1982) 3049-3052.
52. U. Costantino and A. La Ginestra, Thermochim. Acta, 58 (1982) 179-189.
53. M. Inoue, S. Kondo, A. Kishioka and M. Kinoshita, Nippon Kagaku Kaishi, (1982) 1752-1757.
54. P.J. Domaille and W.H. Knoch, Inorg. Chem., 22 (1983) 818-822.
55. C.D. Garner and J.A. Joule, Gov. Rep. Announce. Index (U.S.), 83 (1983) 772.
56. P.C. Ford, A.A. MacDowell and I.H. Hillier, J. Electron Spectrosc. Relat. Phenom., 31 (1983) 75-78.
57. S.A. Malykh, Anodnoe Okislenie Met., (1982) 45-50.
58. A.A. Mazhar, M.M. Hefny, F. El Taib Heakal and M.S. El-Basiouny, Br. Corros. J., 18 (1983) 156-159.
59. V.P. Razygraev, M.V. Lebedeva and A.E. Gorodetskii, Korrosion. Stoikost Titana V Tekhnol. Sredakh Khim. Prom-sti, M., (1982) 48-56.
60. I.V. Riskin, V.B. Torshin, Ya. B. Skuratnik and M.A. Dembrovskii, Mater. Perform., 22 (1983) 9-11.
61. L.V. Kostina, E.G. Kuznetsova, V.M. Novakovskii, E.V. Kasatkin, E.N. Lubnin, E.M. Lazarev and Z.I. Kornilova, Zashch. Met., 19 (1983) 47-54.
62. P.S. Wang, W.E. Moddeman, L.W. Collins and T.N. Wittberg, NTIS Report, MLM-2945; order no. De82017352, 8pp.
63. Y. Yamada and K. Yishida, Jpn. J. Appl. Phys., Part 1, 22 (1983) 36-41.
64. Y. Yamada and K. Yoshida, Jpn. J. Appl. Phys., Part 1, 22 (1983) 759.
65. Y. Yamada, Jpn. J. Appl. Phys., Part 1, 22 (1983) 29-35.
66. A.L. Ivanovskii, V.A. Gubanov, Yu. G. Zainulin, E.Z. Kurmaev, M.P. Butsman and B.I. Zborovskii, Zh. Strukt. Khim., 23 (1982) 42-47.
67. G. Vol'f and V.P. Shirokovskii, Metody Rascheta Energ. Strukt. Fiz. Svoistv Krist., Mater. Vses. Konf., 2nd (1979) Pub. 1982, 191-196.

68. T.C. Devore, High Temp. Sci., 15 (1982) 219-224.
69. C.W. Bauschlicher, Jr. and P.S. Bagus, Chem. Phys. Lett., 101 (1983) 229-234.
70. M. Polak, M. Hefetz, M.H. Mintz and M.P. Dariel, Surf. Sci., 126 (1983) 739-744..
71. S. Banon, C. Chatillon and M. Allibert, High Temp. Sci., 15 (1982) 129-149.
72. S.H. Hong and S. Aasbrink, Acta Crystallogr., Sect. B, B38 (1982) 2570-2576.
73. D.G. Kellerman, V.A. Perelyaev and A.P. Palkin, Zh. Neorg. Khim., 28 (1983) 1645-1649.
74. S.A. Fairhurst, A.D. Inglis, Y. Le Page, J.R. Morton and K.F. Preston, Chem. Phys. Lett., 95 (1983) 444-448.
75. S.P. McAlister and A.D. Inglis, Solid State Commun., 47 (1983) 931-933.
76. F. Climent Montoliu and R. Capellades Font, An. Quim., Ser. B, 79 (1983) 5-8.
77. H.K. Schmidt, R. Capellades and M.I. Vidal, Rev. Tech. Thomson-CSF, 14 (1982) 657-670.
78. D. Miller, S. Mamiche-Afara and M.J. Dignam, Chem. Phys. Lett., 100 (1983) 236-240.
79. A.A. Soliman and H.J.J. Seguin, Thin Solid Films, 100 (1983) 33-42.
80. L.M. Williams, Energy Res. Abstr., 8 (1983), Abstr. No. 5692.
81. C. Blaauw, H.M. Naguib, A. Ahmad and S.M. Ahmed, Sol. Energy Mater., 7 (1982) 331-342.
82. K.J. Hartig, N. Getoff and G. Nauer, Int. J. Hydrogen Energy, 8 (1983) 603-607.
83. S.S. Olevskii, M.S. Sergeev, A.L. Tolstikhina, A.V. Koshchlenko and B.S. Khavin, Izv. Akad. Nauk SSSR, Neorg. Mater., 18 (1982) 1534-1537.
84. J. Joseph and A. Gagnaire, Thin Solid Films, 103 (1983) 257-265.
85. L.D. Arsov, M. Froelicher and A. Hugot Le-Goff, Croat. Chem. Acta, 55 (1982) 277-282.
86. M.B. Svechnikov, Opt.-Mekh. Prom-st., (1983) 39-41.
87. V.G. Devyatov, E.P. Mikhieva and L.M. Usol'tseva, Deposited Doc., (1982) VINITI 1494-82, 14pp.
88. E.A. Strel'tsov, V.P. Pakhomov, R.M. Lazorenko-Manevich and A.I. Kulak, Elektrokhimiya, 19 (1983) 232-235.
89. G.D. Davis, M. Natan and K.A. Anderson, Appl. Surf. Sci., 15 (1983) 321-333.
90. M. Zhao, Tuliao Gongye, 68 (1982) 1-6.
91. V.A. Vasil'evskii, N.D. Betenkov, Yu. V. Egorov and T.A. Denisova, Khim. Tverd. Tela, 5 (1982) 55-65.
92. K. Ooi, T. Kitamura, S. Katoh and K. Sugasaka, Nippon Kagaku Kaishi, (1983) 1-5.
93. G. Draeger, F. Werfel and O. Bruemmer, Phys. Status Solidi B, 113 (1982) K15-K17.
94. S. Nishigaki, Surf. Sci., 125 (1983) 762-770.
95. C. Doremieux-Morin, M. A. Enriquez, J. Sanz and J. Fraissard, J. Colloid Interface Sci., 95 (1983) 502-512.
96. E. Bertel, R. Stockbauer and T.E. Madey, Phys. Rev. B: Condens. Matter, 27 (1983) 1939-1942.
97. K. Sakata, Phys. Status Solidi B, 116 (1983) 145-153.
98. S. Munnix and M. Schmeits, Surf. Sci., 126 (1983) 20-24.
99. R.V. Sushko, A.V. Gette, I.F. Mironyuk and A.A. Chuiko, Zh. Prikl. Khim. (Leningrad), 56 (1983) 1230-1234.
100. G.K. Moiseev, S.K. Popov and L.A. Ovchinnikova, Deposited Doc., (1981) VINITI 5165-81, 23pp.
101. P. Meriaudeau, B. Clerjaud and M. Che, J. Phys. Chem., 87 (1983) 3872-3876.
102. E.A. Strel'tsov, V.P. Pakhomov, R.M. Lazorenko-Manevich and A.I. Kulak, Elektrokhimiya, 19 (1983) 365-368.
103. E.A. Strel'tsov, R.M. Lazorenko-Manevich, V.P. Pakhomov and A.I. Kulak, Elektrokhimiya, 19 (1983) 1148.

104. S.N. Athavale and M.K. Totlani, J. Electrochem. Soc. India, 31 (1982) 119-127.
105. M. Valigi and D. Gazzoli, Stud. Inorg. Chem., 3 (Solid State Chem.) (1983) 197-200.
106. E.G. Ismailov, E.G. Musaev and S.I. Akhundova, Geterog. Katal., Mater. Vses. Konf. Mekh. Katal. Reakts., 3rd, (1981) Pub. 1982, 70-73.
107. E.G. Ismailov and A.M. Musaev, React. Kinet. Catal. Lett., 21 (1982) 181-185.
108. G. Chingas and L. Rowan, Phys. Rev. B: Condens. Matter, 27 (1983) 2636-2639.
109. M. Inomata, K. Mori, A. Miyamoto, T. Ui and Y. Murakami, J. Phys. Chem., 87 (1983) 754-761.
110. K.O. Backhaus, R. Haase, U. Illgen, K. Jancke, J. Richter-Mendau, J. Scheve, I. Schulz and J. Vetter, Ber. Bunsen-Ges. Phys. Chem., 87 (1983) 680-683.
111. A.S. Hare and J.C. Vickerman, J. Chem. Soc., Faraday Trans. 1, 79 (1983) 185-193.
112. L. Burlamacchi, A. Lai and M. Monduzzi, Chem. Phys. Lett., 100 (1983) 549-552.
113. M. Valigi and D. Gazzoli, Mater. Sci. Monogr., 10 (React. Solids, V. 1) (1982) 269-275.
114. L.D. Burke, J.F. Healy and O. Ni Dhubhghaill, Surf. Technol., 16 (1982) 341-347.
115. N.A. Vasyutinskii, Izv. Akad. Nauk SSSR, Neorg. Mater., 19 (1983) 411-415.
116. X.Z. Jiang, T.F. Hayden and J.A. Dumesic, J. Catal., 83 (1983) 168-181.
117. B.H. Chen and J.M. White, NTIS Report, (1982) TR-23; order no. AD-A117892.
118. B.H. Chen, J.M. White, L.R. Brostrom and M.L. Deviney, J. Phys. Chem., 87 (1983) 2423-2425.
119. B.A. Sexton, A.E. Hughes and K. Foger, J. Catalysis, 77 (1982) 85-93.
120. D. Duprez and A. Miloudi, Stud. Surf. Sci. Catal., 17 (Spillover Adsorbed Species) (1983) 163-168.
121. S.J. Decanio, J.B. Miller, J.B. Michel and C. Dybowski, J. Phys. Chem., 87 (1983) 4619-4622.
122. D.E. Resasco and G.L. Haller, J. Catal., 82 (1983) 279-288.
123. S.J. Decanio, T.M. Apple and C.R. Dybowski, J. Phys. Chem., 87 (1983) 194-196.
124. P. Clechet, C. Martelet, R. Olier and J.P. Thomas, J. Electrochem. Soc., 130 (1983) 1795-1796.
125. E. DePauw and J. Marien, Int. J. Mass Spectrom. Ion Phys., 46 (1983) 519-572.
126. A.A. Isirikyan, S.S. Mikhailova, I.A. Polunina and S.N. Tolstaya, Izv. Akad. Nauk SSSR, Ser. Khim., (1983) 20-25.
127. L. Tanaka and J.M. White, NTIS Report, (1982) TR-27; order no. AD-A119742, 23pp.
128. K. Tanaka and J.M. White, J. Catal., 79 (1983) 81-94.
129. R. Schumacher, D.M. Teschner and A.B. Heinzel, Ber. Bunsenges Phys. Chem., 86 (1982) 1153-1156.
130. W. Siripala and M. Tomkiewicz, Phys. Rev. Lett., 50 (1983) 443-446.
131. K. Kobayashi, M. Takata, S. Okamoto, Y. Aikawa, M. Sukigara, Chem. Phys. Lett., 96 (1983) 366-370.
132. J.G. Eon, E. Bordes, A. Vejux and P. Courtine, Mater. Sci. Monogr., 10 (React. Solids, V.2) (1982) 603-609.
133. D.D. Richardson, Radiat. Eff. Lett., 68 (1982) 89-92.
134. S.H. Chien, B.N. Shelimov, D.E. Resasco, E.H. Lee and G.L. Haller, J. Catal., 77 (1982) 301-303.
135. D.E. Resasco and G.L. Haller, Stud. Surf. Sci. Catal., 11 (1982) 105-112.
136. P. Meriaudeau, J.F. Dutel, M. Dufaux and C. Naccache, Stud. Surf. Sci. Catal., 11 (Met.-Support Met.-Addit. Eff. Catal.) (1982) 95-104.
137. R. Burch and A.R. Flambard, J. Catal., 78 (1982) 389-405.

138. S. Takasaki, K. Takahashi, H. Suzuki, Y. Sato, A. Ueno and Y. Kotera, Chem. Lett., (1983) 265-268.
139. T.M. Dukhovnaya, D.V. Sokol'skii and K. K. Dzhardamalieva, Zh. Fiz. Khim., 56 (1982) 2999-3002.
140. P. Turlier, J.A. Dalmon and G.A. Martin, Stud. Surf. Sci. Catal., 11 (Met.-support Met.-addit. Eff. Catal.), (1982) 203-210.
141. S.D. Worley, G.A. Mattson and R. Caudill, J. Phys. Chem., 87 (1983) 1671-1673.
142. P. Meriaudeau, H. Ellestad and C. Naccache, J. Mol. Catal., 17 (1982) 219-223.
143. J.C. Conesa, M.T. Sanz, J. Soria and G. Munera, J. Mol. Catal., 17 (1982) 231-240.
144. M.A. Vannice, C.C. Twu and S.H. Moon, J. Catal., 79 (1983) 70-80.
145. J. Hu, Z. Hong, Y. Song and H. Wang, Stud. Surf. Sci. Catal., 17 (Spillover Adsorbed Species) (1983) 53-62.
146. M. Vannice and C.C. Twu, J. Catal., 82 (1983) 213-222.
147. H. Yoshioka, S. Naito and K. Tamaru, Chem. Lett., (1983) 981-984.
148. J.P. Reymond, B. Pommier and S.J. Teichner, Stud. Surf. Sci. Catal., 11 (Met.-support Met.-addit. Eff. Catal.), 337-348.
149. C.K. Vance and C.H. Bartholomew, Appl. Catal., 7 (1983) 169-177.
150. I. Mochida, K. Suetsugu, H. Fujitsu and K. Takeshita, Chem. Lett., (1983) 177-180.
151. H. Wang, M. Xie, Z. Wei, Z. Hong, X. Wang, Z. Hu, Y. Chen and Z. Guo, China-Jpn.-U.S. Symp. Heterog. Catal. Relat. Energy Probl., B09C (1982) 5pp.
152. Y. Chen, Z. Wei, Y. Chen, H. Lin, Z. Hong, H. Liu, Y. Dong, C. Yu and W. Li, J. Mol. Catal., 21 (1983) 275-289.
153. A. Kato, S. Matsuda and T. Kamo, Ind. Eng. Chem. Prod. Res. Dev., 22 (1983) 406-410.
154. S. Okazaki and T. Okuyama, Bull. Chem. Soc. Japan, 56 (1983) 2159-2160.
155. I. Mochida, K. Suetsugu, H. Fujitsu, K. Takeshita, K. Tsuji, Y. Sagara and A. Ohyoshi, J. Catal., 77 (1982) 519-526.
156. I. Mochida, K. Suetsugu, H. Fujitsu and K. Takeshita, J. Phys. Chem., 87 (1983) 1524-1529.
157. R. Ohnishi, T. Morikawa, Y. Hiraga and K. Tanabe, Z. Phys. Chem. (Wiesbaden), 130 (1982) 205-209.
158. S. Xia and Z. Liu, Fenzi Kexue Yu Huaxue Yanjiu, 3 (1983) 103-105.
159. R.P. Groff and W.H. Manogue, J. Catal., 79 (1983) 462-465.
160. V.I. Krupenskii, Khim. Drev., (1983) 90-93.
161. A.A. Efremov, Yu. D. Pankrat'ev, A.A. Davydov and G.K. Boreskov, React. Kinet. Catal. Lett., 20 (1982) 87-91.
162. J. Santos and J.A. Dumesic, Stud. Surf. Sci. Catal., 11 (Met.-support Met.-addit. Eff. Catal.), (1982) 43-51.
163. K. Kosaka and S. Okazaki, Nippon Kagaku Kaishi, (1982) 1443-1448.
164. J. Cui, D. Li and E. Min, China-Jpn.-U.S. Symp. Heterog. Catal. Relat. Energy Probl., A02C (1982), 5pp.
165. J.W. Schultze and C. Bartels, J. Electroanal. Chem. Interfacial Electrochem., 150 (1983) 583-592.
166. D. Duonghong, W. Erbs, L. Shuben and M. Graetzel, Chem. Phys. Lett., 95 (1983) 266-268.
167. M.R. Balasubramanian and K.S. De, Indian J. Chem., Sect. A, 22A (1983) 654-656.
168. T.M. Apple and C. Dybowski, Surf. Sci., 121 (1982) 243-248.
169. A. Miloudi and D. Duprez, React. Kinet. Catal. Lett., 22 (1983) 181-184.
170. C.Y. Hsiao, C.L. Lee and D.F. Ollis, J. Catal., 82 (1983) 418-423.
171. V. Jeyanthi, Indian J. Chem., Sect. A, 21A (1982) 447-448.
172. S. Kodama, M. Yabuta and Y. Kubokawa, Chem. Lett., (1982) 1671-1674.
173. V. Augugliaro, A. Lauricella, L. Rizzuti, M. Schiavello and A. Sclafani, Int. J. Hydrogen Energy, 7 (1982) 845-849.
174. V. Augugliaro, F. D'Alba, L. Rizzuti, M. Schiavello and A. Sclafani, Int. J. Hydrogen Energy, 7 (1982) 851-855.

175. R.W. Matthews, Aust. J. Chem., 36 (1983) 191-197.
176. K. Chandrasekaran and J.K. Thomas, Chem. Phys. Lett., 99 (1983) 7-10.
177. E. Borgarello, J. Desilvestro, M. Graetzel and E. Pelizzetti, Helv. Chim. Acta, 66 (1983) 1827-1834.
178. I.S. Kolomnikov, T.V. Lysyak, E.A. Konash, A.V. Rudnev, E.P. Kalyazin and Yu. Ya. Kharitonov, Zh. Neorg. Khim., 28 (1983) 528-529.
179. Y. Matsumoto, H. Nagai and E. Sato, J. Phys. Chem., 86 (1982) 4664-4668.
180. P.R. Harvey, R. Rudham and S. Ward, J. Chem. Soc., Faraday Trans. 1, 79 (1983) 1381-1390.
181. J.M. Herrmann, M.N. Mozzanega and P. Pichat, J. Photochem., 22 (1983) 333-343.
182. J. Lacoste, R. Arnaud and J. Lemaire, C.R. Seances Acad. Sci., Ser. 2, 295 (1982) 1087-1092.
183. M.A. Fox and C.C. Chen, Tetrahedron Lett., 24 (1983) 547-550.
184. Y. Oosawa, Chem. Lett., (1983) 577-580.
185. E. Borgarello and E. Pelizzetti, Chim. Ind. (Milan), 65 (1983) 474-478.
186. C.G. Stevens, N.J. Wessman, J.E. Bowman and W.J. Ramsey, Chem. Phys. Lett., 91 (1982) 335-338.
187. K. Hauffe, Chem.-Ztg., 107 (1983) 190-196.
188. G. Blondeel, A. Harriman, G. Porter, D. Urwin and J. Kiwi, J. Phys. Chem., 87 (1983) 2629-2636.
189. G. Blondeel, A. Harriman and D. Williams, Sol. Energy Mater., 9 (1983) 217-227.
190. A. Harriman, G. Porter and P.C. Walters, Sol. Energy R&D Eur. Community, Ser. D, 2 (Photochem., Photoelectrochem. Photobiol. Processes), (1983) 46-50.
191. T. Li, H. Tang, K. Qi and W. Gu, Cuihua Xuebao, 4 (1983) 159-162.
192. Y. Chen, Z. Wei and Y. Chen, Cuihua Xuebao, 4 (1983) 125-130.
193. D. Duprez and A. Maloudi, Stud. Surf. Sci. Catal., 11 (Met.-support Met.-addit. Eff. Catal.), (1982) 179-184.
194. S. Teratani, C. Sungbom, K. Tanaka and Y. Takagi, China-Jpn.-U.S. Symp. Heterog. Catal. Relat. Energy Probl., A22J (1982), 5pp.
195. X. Wen, Y. Han, L. Yang and J. Li, Taiuangneng Xuebao, 4 (1983) 330-332.
196. J. Disdier, J.M. Herrmann and P. Pichat, J. Chem. Soc., Faraday Trans. 1, 79 (1983) 651-660.
197. A.M. Miles, NASA (Contract Rep.) Cr, (1982) NASA-Cr-169887, NAS1.26: 169887, 21pp. (available NTIS).
198. M.R. St. John, A.J. Furgala and A.F. Sammells, J. Phys. Chem., 87 (1983) 801-805.
199. H. Yoneyama, Y. Takao, H. Tamura and A.J. Bard, J. Phys. Chem., 87 (1983) 1417-1422.
200. M. Schiavello, L. Rizzuti, A. Sciafani, I. Majo, V. Augugliaro and P.L. Yue, Adv. Hydrogen Energy, 3 (Hydrogen Energy Prog., V. 2), (1982) 821-826.
201. P.V. Kamat and M.A. Fox, J. Phys. Chem., 87 (1983) 59-63.
202. I. Balberg, P. Braun and F.P. Viehboeck, Sol. Energy Mater., 7 (1982) 183-202.
203. C. Gutierrez and P. Salvador, J. Electroanal. Chem., Interfacial Electrochem., 138 (1982) 457-463.
204. L.M. Williams, Diss. Abstr. Int. B, 44 (1983) 246-247.
205. A. Praet, F. Vanden Kerchove, W.P. Gomes and F. Cardon, Sol. Energy Mater., 7 (1983) 481-490.
206. T. Hepel, M. Hepel and R.A. Osteryoung, J. Electrochem. Soc., 129 (1982) 2132-2141.
207. F.T. Liou, C.Y. Yang and S.N. Levine, J. Electrochem. Soc., 130 (1983) 893-895.
208. K.H. Yoon and S.O. Yoon, Yo Op Hoe Chi, 20 (1983) 31-36.
209. J.P. Frayret, A. Caprani, F. Charru and G. Momplot, Electrochimica Acta, 27 (1982) 1525-1528.
210. S.K. Kovach and A.T. Vas'ko, Elektrokhimiya, 19 (1983) 252-256.
211. M. Handschuh, W. Lorenz, C. Aegerter and T. Katterle, J. Electroanal. Chem. Interfacial Electrochem., 144 (1983) 99-104.

212. E.P. Mikheeva, V.G. Devyatov and V.M. Kolchanova, Kinet. Katal., 24 (1983) 418-421.
213. Y. Fujimura, K. Nakamae and I. Sakai, Kobunshi Ronbunshu, 39 (1982) 777-782.
214. Y. Nakato, A. Tsumura and H. Tsubomura, J. Phys. Chem., 87 (1983) 2402-2405.
215. H. Misawa, T. Kanno, H. Sakuragi and K. Tokumaru, Denki Kagaku Oyobi Kogyo Butsuri Kagaku, 51 (1983) 81-82.
216. J. Kiwi, J. Phys. Chem., 87 (1983) 2274-2276.
217. T. Sakata, T. Kawai and K. Hashimoto, Denki Kagaku Oyobi Kogyo Butsuri Kagaku, 51 (1983) 79-80.
218. M. Gissler and A.J. Mc Evoy, J. Electroanal. Chem. Interfacial Electrochem., 142 (1982) 375-380.
219. L.A. Mirkind, V.V. Gorodetskii and I.L. Gorodetskaya, Elektrokhimiya, 19 (1983) 1183-1187.
220. G.N. Trusov, V. Busse-Macukas, E. Ya. Kryuchkova and M.F. Fandeeva, Deposited Doc., (1982) VINITI, 1054-82, 12pp.
221. Yu. E. Roginskaya, B. Sh. Galyamov, I.D. Belova, R.R. Shifrina, V.B. Kozhevnikov and V.I. Bystrov, Elektrokhimiya, 18 (1982) 1327-1334.
222. V.I. Andreev and V.E. Kazarinov, Itogi Nauki Tekh., Ser.: Elektrokhim., 19 (1983) 47-82.
223. L.A. Mirkind, V.E. Kazarinov, V.N. Andreev and G.L. Al'bertinskii, Elektrokhimiya, 19 (1983) 1144-1147.
224. L.A. Mirkind, G.L. Al'bertinskii and A.G. Kornienko, Elektrokhimiya, 19 (1983) 122-126.
225. V.I. Ignat'ev and I.A. Parshikov, Deposited Doc., (1982) VINITI, 2369-82, 11pp.
226. C. Cominellis and E. Plattner, Oberflaeche-Surf., 23 (1982) 315-318.
227. J. Sanchez, M. Koudelka and J. Augustynski, J. Electroanal. Chem. Interfacial Electrochem., 140 (1982) 161-166.
228. J.F. Houlihan, R.J. Pollock and C.P. Madacs, Electrochim. Acta, 28 (1983) 585-590.
229. T. Kobayashi, H. Yoneyama and H. Tamura, J. Electrochem. Soc., 130 (1983) 1706-1711.
230. P. Pichat, M.N. Mozzanega, J. Disdier and J. M. Herrmann, Nouv. J. Chim., 6 (1982) 559-564.
231. E.A. Strel'tsov, A.I. Kulak, D.V. Sviridov and V.P. Pakhomov, Elektrokhimiya, 19 (1983) 546-548.
232. E.A. Strel'tsov, V.V. Sviridov, A.I. Kulak and V.P. Pakhomov, Elektrokhimiya, 19 (1983) 998-1000.
233. E.A. Strel'tsov, Deposited Doc., (1981) VINITI, 575-82, 716-20.
234. H. Hada, Y. Yonezawa and Y. Momoki, Bull. Chem. Soc. Japan, 55 (1982) 3633-3634.
235. E.A. Strel'tsov, V.V. Sviridov, A.I. Kulak and V.P. Pakhomov, Elektrokhimiya, 19 (1983) 1000-1002.
236. Y. Nakato and H. Tsubomura, Isr. J. Chem., 22 (1982) 180-183.
237. S. Meguro, O. Takagi, B. Ise and S. Toshima, Kinzoku Hyomen Gijutsu, 33 (1982) 278-284.
238. S.K. Kovach, A.T. Vas'do and Yu. S. Krasnov, Ukr. Khim. Zh. (Russ. Ed.), 49 (1983) 608-611.
239. M.V.C. Sastri and G. Nagasubramanian, Int. J. Hydrogen Energy, 7 (1982) 873-876.
240. E. Ya. Kryuchkova and G.N. Trusov, Zashch. Met., 19 (1983) 442-444.
241. K.H. Hough, Bull. Inst. Chem., Acad. Sin., 29 (1982) 19-23.
242. D.M. Shub, M.F. Reznik, V.V. Shalaginov, E.N. Lubnin, N.V. Kozlova and V.W. Lomova, Elektrokhimiya, 19 (1983) 502-508.
243. E.I. Vasilevskaya, V.V. Sviridov, N.I. Kuntsevich and A.I. Kulak, Dokl. Akad. Nauk BSSR, 26 (1982) 918-920.
244. D.W. DeBerry and A. Viehbeck, J. Electrochem. Soc., 130 (1983) 249-251.

245. M.A. Fox, J.R. Hohman and P.V. Kamat, Can. J. Chem., 61 (1983) 888-893.
246. G.M. Zverev, O.E. Sidoryuk and L.A. Skvortsov, Kvantovaya Elektron. (Moscow), 8 (1981) 2274-2276.
247. T. Ohzuko and T. Hirai, Electrochim. Acta, 27 (1982) 1263-1266.
248. V.V. Sviridov, N.I. Kuntsevich, G.A. Sokolik and N.N. Tarasik, Vestsi Akad. Navuk BSSR, Ser. Khim. Navuk, (1982) 3-9.
249. V.V. Sviridov, N.I. Kuntsevich and G.A. Sokolik, Vestsi Akad. Navuk BSSR, Ser. Khim. Navuk, (1982) 56-64.
250. V.V. Sviridov, N.I. Kuntsevich, G.A. Sokolik and I.N. Evtukhovich, Vestsi Akad. Navuk BSSR, Ser. Khim. Navuk, (1983) 30-35.
251. Yu. V. Nechipurenko, G.A. Pagaisha, A.G. Sokolov and G.A. Branitskii, Zh. Nauchn. Prikl. Fotogr. Kinematogr., 28 (1983) 181-184.
252. J.C. Marinace and R.C. McGibbon, J. Electrochem. Soc., 129 (1982) 2389-2390.
253. P.S. Wang, T.N. Wittberg and R.G. Keil, Proc. Int. Pyrotech. Semin., 8th, (1982) 693-708.
254. V.I. Zarko, L.N. Ganyuk and G.M. Kozub, Dopov. Akad. Nauk Ukr. RSR, Ser. B: Geol., Khim. Biol. Nauki, (1983) 48-50.
255. H. Melder, B. Zrnic, D. Sevdic, P. Lulic and J. Sirola, Nafta (Zagreb), 34 (1983) 33-38.
256. D.J. Coates, J.W. Evans, S.S. Pollack and S. Sidney, Fuel, 61 (1982) 1245-1248.
257. J. Wu, Kogai to Taisaku, 19 (1983) 483-490.
258. K.W. Blazey, J.M. Cabrera and K.A. Mueller, Solid State Commun., 45 (1983) 903-906.
259. B. Odekirk, Diss. Abstr. Int. B, 43 (1983) 2612.
260. P. Salvador and C. Gutierrez, Surf. Sci., 124 (1983) 398-406.
261. D.H.M.W. Thewissen, K. Timmer, M. Eeuwhorst-Reinten, A.H.A. Tinnemans and A. Mackor, Stud. Inorg. Chem., 3 (Solid State Chem.) (1983) 243-246; D.H.M.W. Thewissen, K. Timmer, M. Eeuwhorst and A.H.A. Tinnemans, Isr. J. Chem., 22 (1982) 173-176.
262. K. Domen, S. Naito, T. Onishi and K. Tamaru, Chem. Phys. Lett., 92 (1982) 433-434.
263. J.M. Lehn, J.P. Sauvage, R. Ziessel and L. Hilaire, Sol. Energy R&D Eur. Community, Ser. D, 2 (Photochem. Photoelectrochem. Photobiol. Processes) (1983) 117-120.
264. R.U.E. 'T Lam, L.G.J. De Haart and A.W. Wiersma, Stud. Inorg. Chem., 3 (Solid State Chem.) (1983) 255-258.
265. P. Salvador, V.M. Fernandez and C. Gutierrez, Sol. Energy Mater., 7 (1982) 323-329.
266. D.E. Aspnes and A. Heller, J. Phys. Chem., 87 (1983) 4919-4929.
267. A.H.A. Tinnemans, T.P.M. Koster, D.H.M.W. Thewissen, C.W. De Kreuk and A. Mackor, J. Electroanal. Chem. Interfacial Electrochem., 145 (1983) 449-456.
268. M. Ulman, A.H.A. Tinnemans, A. Mackor, B. Aurian-Blajeni and M. Halmann, Int. J. Sol. Energy, 1 (1982) 213-222.
269. A.H.A. Tinnemans, T.P.M. Koster, D.H.M.W. Thewissen and A. Mackor, Sol. Energy R&D Eur. Community, Ser. D, 2 (Photochem. Photoelectrochem. Photobiol. Processes) (1983) 86-91.
270. D.W. Murphy, M. Greenblatt, S.M. Zahurak, R.J. Cava, J. Waszczak, G.W. Hull Jr. and R.S. Hutton, Rev. Chim. Miner., 19 (1982) 441-449.
271. M. Watanabe and Y. Sekikawa, J. Solid State Chem., 44 (1982) 337-342.
272. A. Maazaz and C. Delmas, C.R. Seances Acad. Sci., Ser. 2, 295 (1982) 759-760.
273. H. Izawa, S. Kikkawa and M. Koizumi, J. Phys. Chem., 86 (1982) 5023-5026.
274. A. Anichini, P. Porta, M. Valigi and I.L. Botto, J. Solid State Chem., 49 (1983) 309-317.
275. T. Ohsaka and Y. Fujiki, Solid State Commun., 44 (1982) 1325-1327.
276. D. Groult and B. Raveau, Mater. Res. Bull., 18 (1983) 141-146.
277. B.M. Gatehouse and I.E. Grey, J. Solid State Chem., 46 (1983) 151-155.

278. G.V. Bazuev, Oksidnye Bronzy, (1982) 104-121.
279. M.A. Abdullaev, D. Kh. Amirkhanova, N. Matern, H. Oppermann, W. Reichelt, E.I. Terukov and P.P. Khokhlachev, Izv. Akad. Nauk SSSR, Neorg. Mater., 19 (1983) 1676-1681.
280. A.A. Shchepetkin, R.G. Zakharov, V.I. Ponomarev and E.G. Rasskazova, Zh. Neorg. Khim., 27 (1982) 3179-3182.
281. M. Drogenik and D. Hanzel, Mater. Res. Bull., 17 (1982) 1457-1460.
282. Y. Tamaura, T. Kanzaki and T. Katsura, Ferrites, Proc. ICF, 3rd, 1980, (1982) 15-19.
283. G. Chattopadhyay and H. Kleykamp, Z. Metallkd., 74 (1983) 182-187.
284. V.V. Shalaginov, N.V. Kozlova, V.N. Lomova and D.M. Shub, Zh. Neorg. Khim., 28 (1983) 2196-2200.
285. K.S. De, J. Ghose and M.R. Balasubramanian, Indian J. Chem., Sect. A, 22A (1983) 599-600.
286. T. Horiuchi, T. Sakata and T. Kurose, Josai Shika Daigaku Kiyo, 11 (1982) 451-456.
287. N.G. Eror and U. Balachandran, J. Solid State Chem., 45 (1982) 276-279.
288. J. Gautron, P. Lemasson, B. Poumellec and J.F. Marucco, Sol. Energy Mater., 9 (1983) 101-111.
289. B.G. Shabalin, Mineral. Zh., 4 (1982) 54-61.
290. H. Shibahara, Bull. Kyoto Univ. Educ., Ser. B, 62 (1983) 15-25.
291. B.V. Rozentuller, K.N. Spiridonov and O.V. Krylov, Mekhanizm Katalit. Reaktsii. Materialy 3 Vses. Konf., Novosibirsk, Ch. T (1982) 120-123.
292. D. Theis, H. Venghaus and G. Ebbinghaus, Siemens Forsch.-Entwicklungsber., 11 (1982) 265-270.
293. I. Lindner and S. Kemmler-Sack, Naturwissenschaften, 69 (1982) 445-446.
294. M.R. Nunes and F.M.A. Da Costa, Stud. Inorg. Chem., 3 (Solid State Chem.) (1983) 817-820.
295. K.G. Eror and U. Balachandran, Spectrochim. Acta, Part A, 39A (1983) 261-263.
296. G.V. Bazuev, O.V. Makarova and G.P. Shveikin, Izv. Akad. Nauk SSSR, Neorg. Mater., 19 (1983) 108-112.
297. E.B. Panasenko, R.G. Begunova and N.F. Sklokina, Fiz.-Khim. Issled. Soedin., Met. Ikh Splavov, (1981) 65-74.
298. E.B. Panasenko, R.G. Bagunova and M.P. Shul'gina, Khimiya i Khim. Tekhnol. i Metallurgiya Redk. Elementov, Apatity, (1982) 37-43.
299. G.V. Bazuev and G.P. Shveikin, Kokl. Akad. Nauk SSSR, 266 (1982) 1396-1399 [chem.].
300. E.B. Panasenko, R.G. Begunova and N.F. Sklokina, Fiz.-Khim. Osn. Redkomet. Syr'ya, (1983) 64-70.
301. D. Bahadur and O. Parkash, J. Solid State Chem., 46 (1983) 197-203.
302. O.V. Sidorova, N.V. Porotnikov and K.I. Petrov, Zh. Neorg. Khim., 27 (1982) 1959-1962.
303. N.V. Porotnikov, O.V. Sidorova and L.N. Margolin, Zh. Neorg. Khim., 28 (1983) 299-302.
304. M. Gernan and L.M. Kovba, Zh. Neorg. Khim., 28 (1983) 1034-1036.
305. T. Kala, Phys. Status Solidi A, 73 (1982) 573-578.
306. H. Kodama and A. Watanabe, J. Solid State Chem., 44 (1982) 169-173.
307. D.J. Smith and J.L. Hutchison, J. Microsc. (Oxford), 129 (1983) 285-293.
308. N.P. Smolyaninov, I.G. Sidortsov and O.V. Sidortsova, Zh. Neorg. Khim., 27 (1982) 2662-2668.
309. R. Kozlowski, R.F. Pettifer and J.M. Thomas, Springer Ser. Chem. Phys., 27 (EXAFS Near Edge Struct.) (1983) 313-315.
310. G.C. Bond and P. Konig, J. Catal., 77 (1982) 309-322.
311. D. Kh. Sembaev, B.V. Suvorov, L.I. Saurambaeva and F.A. Ivanovskaya, Geterog. Katal., Mater. Vses. Konf. Mekh. Katal. Reakts., 3rd, 1981, (1982) 58-61.
312. M. Galantowicz, M. Gasior, B. Grzybowska and J. Sloczynski, Przem. Chem., 62 (1983) 87-89.
313. O.M. Il'inich and A.A. Ivanov, Kinet. Katal., 24 (1983) 613-617.

314. I.M. Chmyr, N.R. Bukeikhanov and B.V. Suvorov, Izv. Akad. Nauk Kas. SSR, Ser. Khim., (1983) 43-46.
315. T. Shikada, H. Ogawa, K. Fujimoto and H. Tominaga, Nippon Kagaku Kaishi, (1983) 141-146.
316. K. Fujimoto and T. Shikada, Chem. Lett., (1983) 515-518.
317. I.M. Pearson, H. Ryu, U.C. Wong and K. Nobe, Ind. Eng. Chem. Prod. Res. Dev., 22 (1983) 381-382.
318. S. Morikawa, K. Takahashi, H. Yoshida, O. Harasaki and S. Kurita, Nenryo Kyokaishi, 61 (1982) 1024-1030.
319. Y. Nakagawa, T. Ono, H. Miyata and Y. Kubokawa, Bull. Univ. Osaka Prefect. Ser. A, 31 (1982) 69-73.
320. K. Mori, A. Miyamoto and Y. Murakami, Z. Phys. Chem. (Wiesbaden), 131 (1982) 251-254.
321. H. Miyata, Y. Nakagawa, T. Ono and Y. Kubokawa, Chem. Lett., (1983) 1141-1144.
322. R. Haase, U. Illgen, G. Ohlmann, J. Richter-Mendau, J. Scheve and I. Schulz, Stud. Surf. Sci. Catal., 16 (Prep. Catal. 3) (1983) 213-224.
323. G. Kreysa, G. Breidenbach and K.J. Mueller, Ber. Bunsenges. Phys. Chem., 87 (1983) 66-71.
324. H.P. Dhar, D.W. Howell and J. O'Mara Bockris, J. Electrochem. Soc., 129 (1982) 2178-2183.
325. Ya. A. Yaraliev, Azerb. Khim. Zh., (1982) 72-76.
326. S.A. Malykh, Deposited Doc., (1981) VINITI 575-82, 781-5.
327. L.E. Tsygankova, V.I. Vigdorovich, T.V. Korneeva and E. Ose, Elektrokhimiya, 19 (1983) 109-112.
328. Yu. S. Ruskoĭ, V.A. Grinberg and T.I. Kuznetsova, Zashch. Met., 18 (1982) 748-752.
329. I.V. Riskin, L.M. Lukatskii and V.A. Timonin, Korrozion. Stoikost Titana v Tekhnol. Sredakh Khim. Prom-sti, M., (1982) 56-64.
330. N.V. Korovin, N.V. Kuleshov, Yu.I. Shishkov, V.K. Luzhin, Yu.M. Vol'kovich Yu.F. Zav'yalov and R.N. Shchelokov, Zh. Prikl. Khim. (Leningrad), 56 (1983) 1902-1905.
331. G. Bewer, Schriftenr. Gdmb., 37 (Elektrolyse Nichteisenmet.) (1982) 429-436.
332. D.H. Bradhurst, P.M. Heuer and G.Z.A. Stolarski, Int. J. Hydrogen Energy, 8 (1983) 85-90.
333. I. Richy, M. Rumeau and S. Sakho, Inf. Chim., 231 (1982) 223-225.
334. X.R. Xiao and H. Ti Tien, J. Electrochem. Soc., 130 (1983) 55-59.
335. D. Woehrle, R. Bannehr, B. Schumann, G. Meyer and N. Jaeger, J. Mol. Catal., 21 (1983) 255-263.
336. E.V. Krivtsova, L.L. Kuz'min and G.V. Makhaeva, Izv. Vyssh. Uchebn. Zaved. Khim. Khim. Tekhnol., 25 (1982) 1101-1103.
337. J. Van Zee and R.E. White, J. Electrochem. Soc., 130 (1983) 2003-2012.
338. L.D. Burke, J.F. Healy and O.J. Murphy, J. Appl. Electrochem., 13 (1983) 459-468.
339. L.D. Burke, M.E. Lyons and M. McCarthy, Adv. Hydrogen Energy, 3 (Hydrogen Energy Prog. 4, V. 1) (1982) 267-278.
340. A. Bandi, I. Vartires, A. Mihelis and C. Hainarosie, J. Electroanal. Chem. Interfacial Electrochem., 157 (1983) 241-250.
341. Y. Huang, H. Ye and Y. Zhang, Shanghai Jiaotong Daxue Xuebao, (1982) 25-34.
342. V.V. Shalaginov, D.M. Shub, N.V. Kozlova, E.H. Lubnin and N.V. Kul'kova, Zh. Prikl. Khim. (Leningrad), 56 (1983) 1302-1305.
343. V.V. Shalaginov, D.M. Shub, N.V. Kozlova and V.N. Lomova, Elektrokhimiya, 19 (1983) 537-541.
344. M. Saeki and M. Onoda, Bull. Chem. Soc. Japan, 55 (1982) 3144-3146.
345. J. Von Boehm and H.M. Isomaki, J. Phys. C, 15 (1982) L733-L737.
346. R.P. Beyer, J. Chem. Eng. Data, 28 (1983) 347-348.
347. A.A. Balchin, J. Mater. Sci. Lett., 2 (1983) 457-462.
348. M. Onoda and M. Saeki, Acta Crystallogr., Sect. B, Struct. Sci., B39 (1983) 34-39.

349. H. Boller and H. Blaha, J. Solid State Chem., 45 (1982) 119-126.
350. A.N. Fitch, C. Riekel, R.C.T. Slade and B.E.F. Fender, Solid State Commun., 44 (1982) 1075-1077.
351. Y. Matsuda, M. Morita and K. Ohta, Denki Kagaku Oyobi Kogyo Butsuri Kagaku, 51 (1983) 291-292.
352. R. Kanno, Y. Takeda, M. Imura and O. Yamamoto, J. Appl. Electrochem., 12 (1982) 681-685.
353. K. Endo, H. Inara, K. Watanabe and S. Gonda, J. Solid State Chem., 44 (1982) 268-272.
354. S. Jandl, J. Deslandes and M. Banville, Infrared Phys., 22 (1982) 327-329.
355. O. Gorochoy, A. Katty, N. Le Nagard, C. Levy-Clement and R.M. Schleich, Mater. Res. Bull., 18 (1983) 111-118.
356. T. Jacobsen, K. West and S. Atlung, Electrochim. Acta, 27 (1982) 1007-1011.
357. H.A. Hallak and P.A. Lee, Solid State Commun., 47 (1983) 503-505.
358. A. Kitani, K. Kato, H. Nishihara, S. Yamanaka and K. Sasaki, Denki Kagaku Oyobi Kogyo Butsuri Kagaku, 51 (1983) 391-395.
359. E.J. Fraser and S. Phang, J. Power Sources, 10 (1983) 23-31.
360. K. Cedzynska, A.J. Parker and P. Singh, J. Power Sources, 10 (1983) 13-21.
361. J.R. Dahn, Diss. Abstr. Int. B, 43(12, Pt. 1) (1983) 4041.
362. J.R. Dahn and R.R. Haering, Can. J. Phys., 61 (1983) 1093-1098.
363. R. Osorio and L.M. Falicov, J. Chem. Phys., 77 (1982) 6218-6222.
364. R.O. De Cerqueira, Energy Res. Abstr., 7 (1982) Abstr. No. 61596.
365. S. Kikkawa and M. Kotzumi, Nippon Kagaku Kaishi, (1983) 306-308.
366. H.J.M. Bouwmeester, E.J.P. Dekker, K.D. Bronsema, R.J. Raange and G.A. Wiegers, Rev. Chim. Miner., 19 (1982) 333-342.
367. P. Colombet and L. Frichet, Solid State Commun., 45 (1983) 317-322.
368. Y. Tazuke and T. Endo, J. Magn. Magn. Mater., 31-34 (1983) 1175-1176.
369. M. Schaeferli, J. Brunner, H.P. Vaterlaus and F. Levy, J. Phys. C, 16 (1983) 1527-1536.
370. H.P. Vaterlaus, F. Levy and H. Berger, J. Phys. C, 16 (1983) 1517-1526.
371. H. Nozaki, M. Saeki and M. Onoda, J. Solid State Chem., 46 (1983) 132-137.
372. M. Plischke, K.K. Bardhan, R. Leonelli and J.C. Irwin, Can. J. Phys., 61 (1983) 397-404.
373. G.A. Scholz and R.F. Frindt, Can. J. Phys., 61 (1983) 965-970.
374. K. Ohshima and S.C. Moss, Acta Crystallogr., Sect. A, Found. Crystallogr., A39 (1983) 298-305.
375. M. Schaeferli and J. Brunner, Solid State Commun., 45 (1983) 305-307.
376. N.N. Vershinin, Yu.I. Malov, S.E. Nadkhina and E.A. Ukshe, Elektrokhimiya, 19 (1983) 567-569.
377. R.D. Raub, Energy Res. Abstr., 7 (1982) Abstr. No. 61075.
378. S. Anzai, M. Nakada, S. Ohta, K. Tominaga and A. Fujii, J. Magn. Magn. Mater., 31-34 (1983) 1467-1468.
379. M. Saeki and M. Onoda, Chem. Lett., (1982) 1329-1330.
380. K. Klepp and H. Boller, J. Solid State Chem., 48 (1983) 388-395.
381. W.H. Goodman, Diss. Abstr. Int. B, 44 (1983) 793.
382. G.I. Kadyrova and E.A. Ivanova, Khimiya i Khim. Tekhnol. i Metallurgiya Redk. Elementov, Apatity, (1982) 29-33.
383. V.I. Ivanenko, G.I. Kadyrova and V.I. Kravtsov, Deposited Doc., (1981) SPSTL KHP-D81, 142-8.
384. M.R. Udupa, Thermochim. Acta, 57 (1982) 377-381.
385. E.A. Podozerskaya and E.A. Obolenskaya, Fiz.-Khim. Osn. Redkomet. Svy'ya, (1983) 86-89.
386. E.K. Sikorskaya, L.I. Biryuk, Ya.G. Goreschchemko and M.I. Andreeva, Ukr. Khim. Zh. (Russ. Ed.), 48 (1982) 1022-1024.
387. G.K. Maksimova and D.L. Motov, Zh. Prikl. Khim. (Leningrad), 56 (1983) 1460-1462.
388. A.I. Nikolaev, N.I. Kasikova, O.A. Zalkind and A.G. Babkin, Zh. Neorg. Khim., 28 (1983) 2338-2341.

389. P.D. Townsend, K. Ahmed, P.J. Chandler, S.W.S. McKeever and H.J. Whitlow, Radiat. Eff., 72 (1983) 245-257.
390. T.N. Rezhukhina, T.I. Gorshkova and A.A. Tsvetkov, Zh. Fiz. Khim., 57 (1983) 1651-1656.
391. V.I. Shapoval, V.I. Taranenko, V.V. Nerubashchenko and L.L. Kaidanovich, Ukr. Khim. Zh. (Russ. Ed.), 48 (1982) 926-929.
392. R. Schmidt, W. Hiller and G. Pausewang, Z. Naturforsch., B: Anorg. Chem., Org. Chem., 388 (1983) 849-851.
393. Yu.N. Moskvich, A.M. Polyakov, G.I. Dotsenko and M.L. Afanas'ev, Zh. Neorg. Khim., 27 (1982) 1972-1976.
394. R.L. Lichti, J. Chem. Phys., 78 (1983) 7323-7329.
395. P. Choudhury, B. Ghosh, G.S. Raghuvanshi and H.D. Bist, J. Raman Spectrosc., 14 (1983) 99-101.
396. M. Bose, K. Roy and A. Ghoshray, J. Phys. C, 16 (1983) 645-650.
397. P. Choudhury, B. Ghosh, O.P. Lamba and H.D. Bist, J. Phys. C, 16 (1983) 1609-1613.
398. R. Domesle and R. Hoppe, Z. Anorg. Allg. Chem., 495 (1982) 27-38.
399. M. Yokoyama, T. Oota and I. Yamai, Kenkyu Shisetsu Nenpo, 9 (1982) 39-43.
400. L. Ciavatta and A. Pirozzi, Polyhedron, 2 (1983) 769-774.
401. J. Slivnik, A. Rahten, J. Macek, S. Milicev and B. Sedej, Vestn. Slov. Kem. Drus., 30 (1983) 313-323.
402. A.P. Kajwadkar and L.K. Sharma, Indian J. Pure Appl. Phys., 21 (1983) 193-194.
403. T.C. Devore, High Temp. Sci., 15 (1982) 263-273.
404. J.J. Verbist, Stud. Inorg. Chem., 3 (Solid State Chem.) (1983) 535-538.
405. T.C. Devore and T.N. Gallaher, High Temp. Sci., 16 (1983) 83-88.
406. Q. Yang, G. Liu, B. Fang, W. Wang and L. Sha, Xiyou Jinshu, 1 (1982) 38-44.
407. I. Pollini, Solid State Commun., 47 (1983) 403-408.
408. G. Vlaic, J.C.J. Bart, W. Cavigiolo and A. Michalowicz, Springer Ser. Chem. Phys., 27 (EXAFS Neardge Struct.) (1983) 307-309.
409. D.J. Kushner, T.A. Landry, M.C. Tyrrell and H.A. Akers, Anal. Biochem., 133 (1983) 116-119.
410. L. Benco and R. Boca, Proc. Conf. Coord. Chem., 9th, (1983) 15-20.
411. S. Mohan and K.G. Ravi Kumar, Indian J. Pure Appl. Phys., 20 (1982) 741-742.
412. C. Mousty-Desbuquoit, J. Riga and J.J. Verbist, J. Chem. Phys., 79 (1983) 26-32.
413. C. Detellier and M.J. McGlinchey, J. Magn. Reson., 50 (1982) 50-63.
414. N. Kh. Tumanova, N.M. Sarnavskii, L.V. Bogdanovich, V.N. Bel'dii and G.N. Novitskaya, Ukr. Khim. Zh. (Russ. Ed.), 49 (1983) 264-267.
415. S. Troyanov and G.N. Mazo, Zh. Neorg. Khim., 28 (1983) 1617-1619.
416. T. Riis, I.M. Dahl and O.H. Ellestad, J. Mol. Catal., 18 (1983) 203-214.
417. V.L. Solozhenko, Ya. A. Kalashnikov and V.V. Mishin, Vestn. Mosk. Univ., Ser. 2: Khim., 24 (1983) 183-185.
418. A. Justnes, E. Rytter and A.F. Andresen, Polyhedron, 1 (1982) 393-396.
419. M. Drillon, G. Pourroy, J.C. Bernier and R. Georges, Stud. Inorg. Chem., 3 (Solid State Chem.) (1983) 585-588.
420. Ts.B. Konunova and S.A. Kudritskaya, SPSTL Deposited Doc., (1981) SPSTL 783 KHP-D81, 6pp.
421. Ts.B. Konunova and S.A. Kudritskaya, Zh. Neorg. Khim., 28 (1983) 788-780.
422. Ts.B. Konunova, A. Yu. Tsivadze, A.N. Smirnov and S.A. Kudritskaya, Deposited Doc., (1981) SPSTL 780 KHP-D81, 12pp.
423. Ts.B. Konunova, A. Yu. Tsivadze, A.N. Smirnov and S.A. Kudritskaya, Zh. Neorg. Khim., 28 (1983) 910-914.
424. Ts.B. Konunova, A. Yu. Tsivadze, A.N. Smirnov and S.A. Kudritskaya, Deposited Doc., SPSTL (1981) 781 KHP-D81, 11pp.
425. Ts.B. Konunova, A. Yu. Tsivadze, A.N. Smirnov and S.A. Kudritskaya, Deposited Doc., (1981) SPSTL 782 KHP-D81, 6pp.
426. Ts.B. Konunova and S.A. Kudritskaya, Deposited Doc., (1981) SPSTL 784 KHP-D81, 9pp.

427. E.V. Polyakova, V.M. Vinogradov and R.V. Vizgert, Izv. Vyssh. Uchebn. Zaved., Khim. Khim. Tekhnol., 25 (1982) 1436-1440.
428. M.C. Martinez, M.T. Pereira, M.R. Bermejo and M. Gayoso, Acta Cient. Compostelana, 18 (1981) 15-26.
429. I.E. Uflyand, Yu.I. Ryabukhin, V.N. Askalepov and V.P. Kurbatov, Koord. Khim., 8 (1982) 1283.
430. B.P. Hajela and S.C. Jain, Indian J. Chem., Sect. A, 21A (1982) 530-532.
431. H.W. Roesky, M. Kuhn and J.W. Bats, Chem. Ber., 115 (1982) 3025-3031.
432. D.S. Aspandiyarova and S.S. Uskova, Izv. Akad. Nauk Kaz. SSR, Ser. Khim., (1982) 76-78.
433. R.V. Vizgert, E.V. Polyakova and V.M. Vinogradov, Zh. Obshch. Khim., 52 (1982) 2548-2551.
434. K. Kudaka, K. Izumi and K. Sasaki, Am. Ceram. Soc. Bull., 61 (1982) 1236.
435. J.C.J. Bart, I.W. Bassi, M. Calcaterra, E. Albizzati, U. Giannini and S. Parodi, Z. Anorg. Allg. Chem., 496 (1983) 205-216.
436. I. Kulawik and B. Brozek, Zesz. Nauk. Uniw. Jagiellon., Pr. Chem., 27 (1982) 51-67.
437. G.A. Skorobogatov, B.P. Dymov, B.E. Dzevitskii, S.W. Busov and V.A. Bryukvin, Zh. Obshch. Khim., 53 (1983) 9-14.
438. D.S. Haas, S.J. Dyke, Proc. Int. Pyrotech. Semin., 8th, (1982) 1011-1027.
439. J.B. Kinney and R.H. Staley, J. Phys. Chem., 87 (1983) 3735-3740.
440. G.V. Malykhina, A.K. Molodkin, V.V. Kurilkin, Yu.E. Bogatov and V.I. Moskalenko, Deposited Doc., (1982) VINITI 3814-Pt.2-82, 144-7.
441. S.I. Saratovskikh, E.V. Kiseleva, O.N. Babkina, F.S. D'yachkovskii, V.I. Ponomarev and L.O. Atovmyan, Kinet. Katal., 24 (1983) 207-210.
442. A.A. Baulin, Yu.K. Maksyutin, T.I. Burmistrova, V.M. Shepel, V.P. Nekhoroshev and S.S. Ivanchev, React. Kinet. Catal. Lett., 21 (1982)
443. H.M. Walborsky and H.H. Wuest, J. Am. Chem. Soc., 104 (1982) 5807-5808.
444. G.W. Petrova and O.N. Efimov, Elektrokhimiya, 19 (1983) 978.
445. A. Clerici and O. Porta, Tetrahedron Lett., 23 (1983) 3517-3520.
446. A. Clerici and O. Porta, Tetrahedron, 39 (1983) 1239-1246.
447. K.S. Minsker, A.M. El'yashevich, V.M. Yanborisov and Yu.A. Sangalov, Vysokomol. Soedin., Ser. A, 24 (1982) 2597-2600.
448. F. Sato, T. Akiyama, K. Iida and M. Sato, Synthesis, (1982) 1025-1026.
449. Y. Ito, H. Kato, H. Imai and T. Saegusa, J. Am. Chem. Soc., 104 (1982) 6449-6450.
450. S. Hara, H. Dojo and A. Suzuki, Chem. Lett., (1983) 285-286.
451. M.R. Saidi, Heterocycles, 19 (1982) 1473-1475.
452. U.B. Jensen, Diss. Abstr., Int. B, 43 (1982) 1093.
453. O.S. Roshchupkina, A.P. Lisitskaya and N.D. Golubeva, Kinet. Katal., 23 (1982) 1208-1214.
454. C.R. Marsh, Eur. Pat. Appl. EP 48,627.
455. R. Kh. Kudashev, N.M. Vlasova, Yu. B. Monakov, K.S. Minsker and S.R. Rafikov, Prom-st. Sint. Kauch., (1982) 4-8.
456. L.A. Kazaryan, E.H. Kropacheva, Kinet. Katal., 23 (1982) 491-493.
457. V.V. Frolova, A.S. Estrin, L.G. Andrianova, A.V. Fursenko and V.A. Grechanovskii, Prom-st. Sint. Kauch., (1982) 7-9.
458. K. Soga, S.I. Chen and R. Ohnishi, Polym. Bull. (Berlin), 8 (1982) 473-478.
459. R.A. Epstein and R. Mink, Eur. Pat. Appl. EP 43,185.
460. R.A. Epstein and R. Mink, Eur. Pat. Appl. EP 44,445.
461. L.F. Kovrizhko, M.M. Gostev, I.M. Cherkashina and Yu.B. Monakov, Kauch. Rezina, (1982) 15-16.
462. A. Siove and M. Fontanille, Eur. Polym. J., 17 (1981) 1175-1183.
463. D.K. Jenkins, Polymer, 23 (1982) 1971-1976.
464. P. Galli, P. Barbe, G. Guidetti, R. Zannetti, A. Martorana, A. Marigo, M. Bergozza and A. Fichera, Eur. Polym. J., 19 (1983) 19-24.
465. G.B. Sergeev and V.S. Komarov, Vysokomol. Soedin., Ser. B, 24 (1982) 313-315.
466. J.C.W. Chien, J.C. Wu and C.I. Kuo, J. Polym. Sci., Polym. Chem. Ed., 20 (1982) 2019-2032.

467. J.C.W. Chien, J.C. Wu and C.I. Kuo, J. Polym. Sci., Polym. Chem. Ed., 21 (1983) 737-750.
468. J.C.W. Chien, J.C. Wu and C.I. Kuo, J. Polym. Sci., Polym. Chem. Ed., 21 (1983) 725-736.
469. G.N. Mazo and S.I. Troyanov, Zh. Neorg. Khim., 28 (1983) 2704-2706.
470. J. Anglada, P.J. Bruna S.D. Peyerimhoff and R.J. Buenker, Theochem, 10 (1983) 299-308.
471. A. Fujimori and N. Tsuda, J. Less-Common Met., 88 (1982) 269-272.
472. Z.I. Kudabaev, A.F. Shevakin, O.T. Malyuchkov, G.V. Shcherbedinskii, G.V. Kost and L.N. Padurets, Izv. Akad. Nauk SSSR, Neorg. Mater., 19 (1983) 744-747.
473. Z.I. Kudabaev, A.F. Shevakin and G.V. Shcherbedinskii, Nov. Metody Strukt. Issled. Met. i Splavov Materialy Seminara, M., (1982) 104-108.
474. C. Korn, Phys. Rev. B: Condens. Matter, 28 (1983) 95-111.
475. N. Salibi and R.M. Cotts, Phys. Rev. B: Condens. Matter, 27 (1983) 2625-2627.
476. R. Goering and G. Scheler, Exp. Tech. Phys., 30 (1982) 491-497.
477. P. Millenbach and M. Givon, J. Less-Common Met., 87 (1982) 179-184.
478. P. Millenbach and M. Givon, J. Less-Common Met., 92 (1983) 339-342.
479. M.L. Lieberman, R.S. Carlson, C.T. Rittenhouse and J.W. Fronabarger, Proc. Int. Pyrotech. Semin., 8th, (1982) 869-884.
480. S.A. Sheffield and A.C. Schwarz, Proc. Int. Pyrotech. Semin., 8th, (1982) 972-990.
481. V.A. Lavrenko, V. Zh. Shemet and S.K. Dolukhanyan, Khim. Tekhnol. (Kiev), (1982) 62-63.
482. A.J. Maeland and G.G. Libowitz, J. Less-Common Met., 89 (1983) 197-200.
483. S.K. Dolukhanyan, R.A. Karimyan, A.G. Akopyan and A.G. Merzhanov, Zh. Neorg. Khim., 28 (1983) 1101-1105.
484. C.W. Park and J.Y. Lee, J. Less-Common Met., 91 (1983) 189-201.
485. S.M. Shapiro, F. Reidinger and J.F. Lynch, J. Phys. F, 12 (1982) 1869-1876.
486. M. Gupta, J. Less-Common Met., 88 (1982) 221-230.
487. D.A. Papaconstantopoulos and A.C. Switendick, J. Less-Common Met., 88 (1982) 273-281.
488. W. Baden, P.C. Schmidt and A. Weiss, J. Less-Common Met., 88 (1982) 171-179.
489. R. Hempelmann, D. Richter and A. Heidemann, J. Less-Common Met., 88 (1982) 343-351.
490. R. Hempelmann, E. Wicke, G. Hilscher and G. Wiesinger, Ber. Bunsenges. Phys. Chem., 87 (1983) 48-55.
491. S. Hayashi, K. Hayamizu and O. Yamamoto, J. Chem. Phys., 78 (1983) 5096-5102.
492. E. Debowska, Phys. Status Solidi B, 117 (1983) 699-706.
493. R.C. Bowman Jr., A.J. Maeland and W.K. Rhim, Phys. Rev. B: Condens. Matter, 26 (1982) 6362-6378.
494. R.C. Bowman Jr., A.J. Maeland, W.K. Rhim and J.F. Lynch, NATO Conf. Ser., 6, 6 (Electron. Struct. Prop. Hydrogen Met.) (1983) 479-484.
495. R.C. Bowman Jr., J.F. Lynch and J.R. Johnson, Mater. Lett., 1 (1982) 122-126.
496. J.F. Lynch, J.R. Johnson and R.C. Bowman Jr., NATO Conf. Ser., 6, 6 (Electron. Struct. Prop. Hydrogen Met.) (1983) 437-442.
497. J.R. Johnson, J.J. Reilly, F. Reidinger, L.M. Corliss and J.M. Hastings, J. Less-Common Met., 88 (1982) 107-114.
498. R.C. Bowman Jr., B.D. Craft, A. Attalla and J.R. Johnson, Int. J. Hydrogen Energy, 8 (1983) 801-808.
499. B.M. Bulichev, E.V. Evdokimova, A.I. Sizov and G.L. Soloveichik, J. Organomet. Chem., 239 (1982) 313-320.
500. T.I. Arsen'eva and N.N. Vyshinskii, Fiz. Khim. Metody Analiza, Gor'kii, (1981) 41-44.
501. L.E. Manzer, Inorg. Synth., 21 (1982) 84-86.
502. D.F.R. Gilson and G. Gomez, J. Organomet. Chem., 240 (1982) 41-47.

503. J. Tirouflet, J. Besancon, B. Gautheron, F. Gomez and D. Fraisse, J. Organomet. Chem., 234 (1982) 143-150.
504. D.B. Jacobson, G.D. Byrd and B.S. Freiser, J. Am. Chem. Soc., 104 (1982) 2320-2321.
505. H. Koepf and N. Klouras, Chem. Scr., 19 (1982) 122-123.
506. J.J. Singh, G. Singh, N. Kumar, R.K. Sharma and R.K. Multani, Indian J. Chem., Sect. A, 21A (1982) 631-634.
507. Y. Dong, S. Wu, R. Zhang and S. Chen, Kexue Tongbao, 27 (1982) 1436-1440.
508. J.C. Leblanc, C. Moise, A. Maisonnat, R. Poilblanc, C. Charrier and F. Mathey, J. Organomet. Chem., 231 (1982) C43-C48.
509. M.C. Boehm, Inorg. Chim. Acta, 62 (1982) 171-182.
510. J.S. Merola, R.A. Gentile, G.B. Ansell, M. Modrick and S. Zentz, Organometallics, 1 (1982) 1731-1733.
511. F. Bottonley and F. Grein, Inorg. Chem., 21 (1982) 4170-4178.
512. C.E. Carraher Jr., R.A. Schwarz, J.A. Schroeder, M. Schwarz and H.M. Molloy, Org. Coat. Plast. Chem., 43 (1980) 798-803.
513. S.A. Cohen, P.R. Auburn and J.L. Bercaw, J. Am. Chem. Soc., 105 (1983) 1136-1143.
514. A.R. Dias, M.S. Salema and J.A.M. Simoes, Organometallics, 1 (1982) 971-973.
515. S. Chen, Y. Liu and J. Wang, Sci. Sin. (Eng. Ed.), 25 (1982) 341-348.
516. C.R. Lucas, J. Organomet. Chem., 235 (1982) 281-291.
517. B. Demerseman, P.H. Dixneuf, J. Douglade and R. Mercier, Inorg. Chem., 21 (1982) 3942-3947.
518. D.A. Straus and R.H. Grubbs, J. Am. Chem. Soc., 104 (1982) 5499-5500.
519. M.M. Franci and W.J. Hehre, Organometallics, 2 (1983) 457-459.
520. W.P. Leung and C.L. Raston, J. Organomet. Chem., 240 (1982) C1-C4.
521. V.B. Shur, E.G. Berkovich, M.E. Vol'pin, B. Lorenz and M. Wahren, J. Organomet. Chem., 228 (1982) C36-C38.
522. D. Walther, G. Kreisel and R. Kimmse, Z. Anorg. Allg. Chem., 487 (1982) 149-160.
523. B.H. Edwards, R.D. Rogers, D.J. Sikora, J.L. Atwood and M.D. Rausch, J. Am. Chem. Soc., 105 (1983) 416-426.
524. Q. Yang, X. Jin, X. Xu, G. Li, Q. Yang and S. Chen, Sci. Sin. (Engl. Ed.), 25 (1982) 356-366.
525. M.K. Rastogi, Curr. Sci., 51 (1982) 924-925.
526. J. Wang, Q. Liu and S. Chen, Kexue Tongbao, 27 (1982) 767.
527. S. Chen and Y. Liu, Huaxue Xuebao, 40 (1982) 913-925.
528. G. Li and D. Zhang, Huaxue Xuebao, 40 (1982) 1177-1181.
529. Z. Xie and S. Chen, Gaodeng Xuexiao Xuebao, 3 (1982) 489-494.
530. K. Doeppert, R. Sanchez-Delgado, H.P. Klein and U. Thewalt, J. Organomet. Chem., 233 (1982) 205-213.
531. D.M. Hoffman, N.D. Chesler and R.C. Fay, Organometallics, 2 (1983) 48-52.
532. D.M. Hoffman, Diss. Abstr. Int. B, 43 (1983) 2203.
533. H.P. Klein and U. Thewalt, J. Organomet. Chem., 232 (1982) 41-46.
534. R.S. Arora, S.C. Hari, R.K. Multani, J. Inst. Chem. (India), 54 (1982) 143-145.
535. A.W. Clauss, S.R. Wilson, R.M. Buchanan, C.G. Pierpont and D.H. Hendrickson, Inorg. Chem., 22 (1983) 628-636.
536. H.P. Klein, U. Thewalt, K. Doeppert and R. Sanchez-Delgado, J. Organomet. Chem., 236 (1982) 189-195.
537. R.S. Arora and R.K. Multani, J. Inst. Chem. (India), 53 (1981) 297-298.
538. Yu.A. Ol'dekop, V.A. Knizhnikov, Zh. Obshch. Khim., 52 (1982) 1571-1575.
539. M.A.A.F. de C.T. Carrondo and G.A. Jeffrey, Acta Crystallogr., Sect. C, C39 (1983) 42-44.
540. S. Kumar and N.K. Kaushik, Acta Chim. Acad. Sci. Hung., 109 (1982) 13-20.
541. S. Kumar and N.K. Kaushik, J. Inorg. Nucl. Chem., 43 (1981) 2679-2681.
542. P. Soni, K. Chandra, R. Sharma and B.S. Gang, J. Indian Chem. Soc., 59 (1982) 913-915.
543. G.S. Sodhi and N.K. Kaushik, Acta Chim. Acad. Sci. Hung., 111 (1982) 207-212.

544. P.H. Bird, J. McCall, A. Shaver and U. Siriwardane, Angew. Chem., 94 (1982) 375-376.
545. C.M. Bolinger and T.B. Rauchfuss, Inorg. Chem., 21 (1982) 3947-3954.
546. S.K. Sengupta and K. Nizamuddin, Indian J. Chem., Sect. A, 21A (1982) 426-427.
547. K. Tamao, M. Akita, R. Kanatani, N. Ishida and M. Kumada, J. Organomet. Chem., 226 (1982) C9-C13.
548. A.K. Sharma and N.K. Kaushik, Synth. React. Inorg. Met.-Org. Chem., 12 (1982) 827-834.
549. S. Wu and Y. Zhou, Lanzhou Daxue Xuebao, Ziran Kexueban, 18 (1982) 57-C3.
550. S. Gambarotta, C. Floriani, A. Chiesi-Villa and C. Guastini, J. Chem. Soc., Chem. Commun., (1982) 1015-1017.
551. C.E. Carraher Jr. and L.P. Torre, Macromol. Solutions: Solvent-Prop. Relat. Polym., [Pap. Symp.], 1981, (1982) 61-69.
552. N. El Murr and A. Chaloyard, J. Organomet. Chem., 231 (1982) 1-4.
553. K.W. Willman, Diss. Abstr. Int. B, 42 (12, Pt. 1) (1982) 4782.
554. K. Ohashi and T. Tonegawa, Mem. Fac. Eng., Osaka City Univ., 22 (1981) 107-113.
555. P. Sobota and Z. Janas, J. Organomet. Chem., 243 (1983) 35-44.
556. Sh.A. Mamedov, I.L. Nizker, V.S. Akhmedov and E.G. Gumbatov, Sb. Tr. Inst. Neftekhim. Protsessov im. Yu. G. Mamedaliev, Akad. Nauk Az. SSR, 13 (1982) 112-118.
557. J.A. Rillatt and W. Kitching, Organometallics, 1 (1982) 1089-1093.
558. C. McDade, J.C. Green and J.E. Bercaw, Organometallics, 1 (1982) 1629-1634.
559. D.J. Cardin, J.M. Kelly, G.A. Lawless and R.J. Trautman, J. Chem. Soc., Chem. Commun., (1982) 228-229.
560. E. Klei, J.H. Teuben, H.J. DeLiefde Meijer, E.J. Kwak and A.P. Bruins, J. Organomet. Chem., 224 (1982) 327-339.
561. F. Sato, K. Iida, S. Iijima, H. Moriya and M. Sato, J. Chem. Soc., Chem. Commun., (1981) 1140-1141.
562. D.R. Corbin, G.D. Stucky, W.S. Willis and E.G. Sherry, J. Am. Chem. Soc., 104 (1982) 4298-4299.
563. S. Gambarotta, C. Floriani, A. Chiesi-Villa and C. Guastini, J. Am. Chem. Soc., 104 (1982) 1918-1924.
564. I.H. Williams, D. Spangler, D.A. Femac, G.M. Maggiora and R.L. Schowen, J. Am. Chem. Soc., 105 (1983) 31-40.
565. Y. Liu and S. Chen, Gaodeng Xuexiao Huaxue Xuebao, 3 (1982) 495-501.
566. G.S. Sodhi, A.K. Sharma and N.K. Kaushik, J. Organomet. Chem., 238 (1982) 177-183.
567. G.S. Sodhi, A.K. Sharma and N.K. Kaushik, Synth. React. Inorg. Met.-Org. Chem., 12 (1982) 947-957.
568. A.R. Dias, W. Vining, W. Coco and R. Rosen, Organometallics, 2 (1983) 68-79.
569. R. Laitinen, N. Rautenberg, J. Steidel and R. Steudel, Z. Anorg. Allg. Chem., 486 (1982) 116-128.
570. J.W. Stevenson and T.A. Bryson, Tetrahedron Lett., 23 (1982) 3143-3146.
571. E.V. Evdokimova, G.L. Soloveichik and B.M. Bulychov, Kinet. Katal., 23 (1982) 1109-1113.
572. K. Mach, P. Sedmera, L. Petrusova, H. Antropiusova, V. Hanus and F. Turecek, Tetrahedron Lett., 23 (1982) 1105-1108.
573. K. Mach, L. Petrusova, H. Antropiusova, A. Dosedlova and P. Sedmera, Chem. Zvesti, 36 (1982) 191-200.
574. E.A. Fushman, A.N. Shupik, L.F. Borisova, V.E. L'vovskii and F.S. D'yachdovskii, Dokl. Akad. Nauk SSSR, 264 (1982) 651-655.
575. J. Cihlar, J. Mejstrik, O. Hamrik and M. Kunz, Czech. CS 197,023 (Patent).
576. Sekisui Chemical Co., Jpn. Kokai Tokkyo Koho JP 82,106,641 (patent).
577. T. Yoshida, Chem. Lett., (1982) 429-432.
578. B.M. Bulychov and E.V. Evdokimova, Otkrytiya, Izobret., Prom. Obraztsy, Tovarnye Znaki, (1982) 94-95.
579. Z. Dawoodi, J. Chem. Soc., Chem. Commun., (1982) 802-803.

580. P.J. Krusic and F.R. Tebbe, Inorg. Chem., 21 (1982) 2900-2902.
581. H. Boegel and G. Rasch, Z. Chem., 22 (1982) 191-192.
582. M. Panse and K.H. Thiele, Z. Anorg. Allg. Chem., 485 (1982) 7-14.
583. S.P. Kolesnikov, S.L. Povarov and A. Ya. Shteinshneider, Izv. Akad. Nauk SSSR, Ser. Khim., (1982) 415-418.
584. U. Thewalt and F. Stollmaier, J. Organomet. Chem., 228 (1982) 149-152.
585. G.G. Tairova, E.F. Kvashina, O.N. Krasochka, G.A. Kichigina, Yu.A. Shvetsov, E.M. Lisetskii, L.O. Atovmyan and Yu.G. Borod'ko, Nouv. J. Chim., 5 (1981) 603-604.
586. G.G. Tairova, O.N. Krasochka, V.I. Ponomarev, E.F. Kvashina, Yu.A. Shvetsov, E.M. Lisetskii, D.P. Kiryukhin, L.O. Atovmyan and Yu.G. Borod'ko, Transition Met. Chem. (Weinheim Ger.) 7 (1982) 189-192.
587. J.Z. Liu and R.D. Ernst, J. Am. Chem. Soc., 104 (1982) 3737-3739.
588. F.R. Wild, L. Zsolnai, G. Huttner and H.H. Brintzinger, J. Organomet. Chem., 232 (1982) 233-247.
589. R. Benn and G. Schroth, J. Organomet. Chem., 228 (1982) 71-85.
590. E. Samuel, G. Labauze and D. Vivien, J. Chem. Soc., Dalton Trans., (1981) 2353-2356.
591. H.B. Abrahamson, M.E. Martin, J. Organomet. Chem., 238 (1982) C58-C62.
592. D.A. Straus and R.H. Grubbs, Organometallics, 1 (1982) 1658-1661.
593. M. Kohutova and M. Zikmund, Proc. Conf. Coord. Chem., 9th, (1983) 169-174.
594. G. Plesch, Inorg. Chim. Acta, 72 (1983) 117-118.
595. G. Schmid, S. Amirkhalili, U. Hoehner, D. Kamphann and R. Boese, Chem. Ber., 115 (1982) 3830-3841.
596. M.D. Boveda Fontan, J. Romero and A. Sousa, Acta Cient. Compostelana, 18 (1981) 155-162.
597. R.P. Planalp, R.A. Anderson and A. Zalkin, Organometallics, 2 (1983) 16-20.
598. P.J. Dmaille, R.L. Harlow and S.S. Ureford, Organometallics, 1 (1982) 935-938.
599. Ts.B. Konunova and S.A. Kudritskaya, Koordinats. Soedin. Perekhod. Elementov. Vopr. Khimii i Khim. Tekhnol., Kishinev, (1983) 35-41.
600. J. Quirk and G. Wilkinson, Polyhedron, 1 (1982) 209-211.
601. V.N. Borshch and A.F. Shestakov, Zh. Fiz. Khim., 56 (1982) 1546-1547.
602. L.M. Kachapina, V.N. Borshch, G.A. Kichigina, V.D. Makhaev and A.P. Borisov, Nouv. J. Chim., 6 (1982) 253-258.
603. C.M. Mikulski, P. Sanford, N. Harris, R. Rabin and R.M. Karayannis, J. Coord. Chem., 12 (1983) 187-195.
604. I.E. Uflyand, V.P. Kurbatov and E.S. Kukharicheva, Deposited Doc., (1981) SPSTL 706, KHP-281, 8pp.
605. K. Lal and S.R. Malhotra, An. Quim., Ser. B, 79 (1983) 56-58.
606. S.K. Pandit, S. Gopinathan and C. Gopinathan, Indian J. Chem., Sect. A, 21A (1982) 78-80.
607. X. Yu and G. Xie, Kexue Tongbao, 27 (1982) 1241-1242.
608. Yu.V. Makarov and G.V. Polyakova, Otkrytiya Izobret., Prom. Obraztsy, Tovarnye Znaki, (1982) 93.
609. E. Nakamura and I. Kuwajima, J. Am. Chem. Soc., 105 (1983) 651-652.
610. K. Wieghardt, I. Tolksdorf, J. Weiss and W. Swiridoff, Z. Anorg. Allg. Chem., 490 (1982) 182-190.
611. R.K. Kanjolia, C.K. Narula and V.D. Gupta, Curr. Sci., 51 (1982) 983-986.
612. R.L. Harlow, Acta Crystallogr., Sect. C, Cryst. Struct. Commun., C39 (1983) 1344-1346.
613. U. Casellato, S. Tamburini, P.A. Vigato, A. DeStefani, M. Vidali and D.E. Fenton, Inorg. Chim. Acta, 69 (1983) 45-51.
614. G.S. Sodhi and N.K. Kaushik, Acta Chim. Acad. Sci. Hung., 108 (1981) 389-394.
615. A.K. Sharma and N.K. Kaushik, J. Inorg. Nucl. Chem., 43 (1981) 3024-3027.
616. A.K. Sharma and N.K. Kaushik, Synth. React. Inorg. Met.-Org. Chem., 11 (1981) 685-693.

617. V.D. Gupta and V.K. Gupta, Indian J. Chem., Sect. A, 22A (1983) 250-252.
618. S.R. Wade and G.R. Willey, Inorg. Chim. Acta, 72 (1983) 201-204.
619. F. Sato, Y. Suzuki and M. Sato, Tetrahedron Lett., 23 (1982) 4589-4592.
620. D. Seebach and L. Widler, Helv. Chim. Acta, 65 (1982) 1972-1981.
621. L. Widler, Helv. Chim. Acta, 65 (1982) 1085-1089.
622. J.B. Lee, K.C. Ott and R.H. Grubbs, J. Am. Chem. Soc., 104 (1982) 7491-7496.
623. K.C. Ott, J.B. Lee and R.H. Grubbs, J. Am. Chem. Soc., 104 (1982) 2942-2944.
624. R. Choukroun, Inorg. Chim. Acta, 58 (1982) 121-122.
625. G.D. Byrd, R.C. Burnier and B.S. Freiser, J. Am. Chem. Soc., 104 (1982) 3565-3569.
626. K. Fujita, E. Moret and M. Schlosser, Chem. Lett., (1982) 1819-1822.
627. Y. Ikeda, K. Furuta, N. Meguriya, M. Ikeda and H. Yamamoto, J. Am. Chem. Soc., 104 (1982) 7663-7665.
628. J.E. McMurtry, Acc. Chem. Res., 16 (1983) 405-411.
629. A. Uri and A. Tuulmets, Org. React. (Tartu), 18 (1981) 179-185.
630. V.A. Poluboyarov, G.A. Nesterov, V.A. Zakharov and V.F. Anufrienko, Mekhanizm Katalit. Reaktsii. Materialy 3 Vses. Konf. Novosibirsk, (Ch. 2) (1982) 175-178.
631. L.F. Capitan-Vallvey, D. Gazquez and F. Salinas, Thermochim. Acta, 56 (1982) 15-23.
632. L.M. Dyagileva, E.I. Tsyganova, V.P. Mar'in and Yu.A. Aleksandrov, Zh. Obshch. Khim., 52 (1982) 2024-2026.
633. M. Mittal, K. Lal and S.P. Gupta, J. Indian Chem. Soc., 60 (1983) 188-189.
634. M.Z. Ugorets, B.S. Baipisova, A.Z. Beilina and F. Kh. Iskakbekova, Zh. Prikl. Khim. (Leningrad), 56 (1983) 1629-1631.
635. A.V. Zagorodnyuk, L.V. Sadkovskaya, R.L. Magunov and A.P. Zhirnova, Ukr. Khim. Zh. (Russ. Ed.), 49 (1983) 462-464.
636. B. Singh, A.K. Narula, R.N. Kapoor and P.N. Kapoor, Indian J. Chem. Soc., 22A (1983) 156-158.
637. H. Rehwinkel and W. Steglich, Synthesis, (1982) 826-827.
638. E. Akguen, Chem.-ZTG., 106 (1982) 371-373.
639. N.S. Enikolopyan, P.E. Matkovskii, L.N. Russiyan, A.T. Papoyan, D.B. Furman and F.S. D'yachkovskii, Dokl. Akad. Nauk SSSR, 266 (1982) 1142-1144 [Chem].
640. K.C. Malhotra, N. Sharma and S.C. Chaudhry, Proc. Indian Natl. Sci. Acad., Part A, 48 (1982) 244-247.
641. A.N. Glebov, Yu.I. Sal'nikov, A.V. Sakharov, Z.A. Saprydova and E.L. Gogolashvili, Zh. Neorg. Khim., 28 (1983) 1443-1447.
642. B.H. Berrie, Diss. Abstr. Int. B, 44 (1983) 490.
643. A. Janson, G. Rudzitis and L. Karklina, Deposited Doc., (1981) VINITI 4031-81, 18pp.
644. J. de D. Lopez Gonzalez, C. Valenzuela Calahorra and M.A. Romera Molina, An. Quim., Ser. B, 78 (1982) 372-376.
645. P. Murugaiyan, C.K. Pillai and C. Venkateswarly, Indian J. Chem., Sect. A, 21A (1982) 851-852.
646. M.S. Ram, Diss. Abstr. Int. B, 44 (1983) 1113.
647. B.C. Gilbert, R.O.C. Norman, P.S. Williams and J.N. Winter, J. Chem. Soc., Perkins Trans. 2, (1982) 1439-1445.
648. R.S. Zabrarova and N.I. Babashkina, Deposited Doc., (1981) SPSTL 474 KHP-082, 8pp.
649. D. Seebach and M. Schiess, Helv. Chim. Acta, 65 (1982) 2598-25602.
650. R. Hanks and D. Hoppe, Angew. Chem., 94 (1982) 378-379.
651. A. Jansone, B. Purins and G. Rudzitis, Latv. Psr Zinat. Akad. Vestis, Kim. Ser., (1982) 426-431.
652. Ya.I. Tur'yana and L.M. Maluka, Zh. Obshch. Khim., 53 (1983) 260-265.
653. G.N. Petrova, O.N. Efimov and V.V. Strelets, Izv. Akad. Nauk SSSR, Ser. Khim., (1983) 2042-2047.
654. N.S. McAlpine and R.A. Fredlein, Aust. J. Chem., 36 (1983) 11-17.
655. V.M. Arutyunyan, A.G. Sarkisyan, G.R. Panosyan and G.E. Shakhnazaryan, Izv. Akad. Nauk Arm. SSR, Fiz., 18 (1983) 39-47.